AD-A021 473

AXIAL-CENTRIFUGAL COMPRESSOR PROGRAM, EVALUATION OF AUSFORMED BEARINGS

Eric N. Bamberger, et al

General Electric Company

Prepared for:

Army Air Mobility Research and Development Laboratory

February 1976
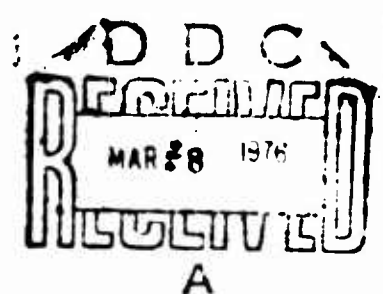
070150

AXIAL-CENTRIFUGAL COMPRESSOR PROGRAM, EVALUATION OF AUSFORMED BEARINGS

General Electric Company
Aircraft Engine Group
Cincinnati, Ohio 45215

DDC

MAR 8 1976

A

February 1976

Final Report for Period 1 August 1972 - 15 June 1975

Approved for public release;
distribution unlimited.

Prepared for

EUSTIS DIRECTORATE

U. S. ARMY AIR MOBILITY RESEARCH AND DEVELOPMENT LABORATORY

Fort Eustis, Va. 23604

EUSTIS DIRECTORATE POSITION STATEMENT

The work documented in this report was performed as an addendum to a contract for research and development of an axial-centrifugal compressor. The impetus was a compressor test rig bearing failure that highlighted the extent to which bearing technology is being pushed. It is recognized that the instant effort featured far too few bearings to provide a sample size sufficient to demonstrate completely the bearing qualifications; however, the trend of the test is considered to be valid and sets the stage for additional efforts to provide the confidence required to incorporate 35mm ausformed bearings into advanced aircraft engines.

Robert A. Langworthy, of the Propulsion Technical Area, Technology Applications Division, served as Project Engineer for this effort.

2(a)

REPORT DOCUMENTATION PAGE		READ INSTRUCTIONS BEFORE COMPLETING FORM
1. REPORT NUMBER USAAMRDL-TR-75-55	2. GOVT ACCESSION NO.	3. RECIPIENT'S CATALOG NUMBER
4. TITLE (and Subtitle) AXIAL-CENTRIFUGAL COMPRESSOR PROGRAM, EVALUATION OF AUSFORMED BEARINGS		5. TYPE OF REPORT & PERIOD COVERED Final 1 August 1972-15 June 1975
		6. PERFORMING ORG. REPORT NUMBER R75AEG473
7. AUTHOR(s) Eric N. Bamberger John C. Clark Terrence E. Russell Donald A. Smeaton		8. CONTRACT OR GRANT NUMBER(s) DAAJ02-71-C-0050
9. PERFORMING ORGANIZATION NAME AND ADDRESS General Electric Company Aircraft Engine Group Cincinnati, Ohio 45215		10. PROGRAM ELEMENT, PROJECT, TASK AREA & WORK UNIT NUMBERS 62207A 1G162207AA71 02 004 EK
11. CONTROLLING OFFICE NAME AND ADDRESS Eustis Directorate, U.S. Army Air Mobility Research & Development Laboratory, Fort Eustis, Virginia 23604		12. REPORT DATE February 1976
		13. NUMBER OF PAGES 119
14. MONITORING AGENCY NAME & ADDRESS(If different from Controlling Office)		15. SECURITY CLASS. (of this report) Unclassified
		15a. DECLASSIFICATION/DOWNGRADING SCHEDULE

16. DISTRIBUTION STATEMENT (of this Report)

Approved for public release; distribution unlimited.

17. DISTRIBUTION STATEMENT (of the abstract entered in Block 20, if different from Report)

18. SUPPLEMENTARY NOTES

19. KEY WORDS (Continue on reverse side if necessary and identify by block number)

Bearings	Ausforging
Tool Steel	High-Energy Rate Forging
Thermomechanical Working	
Ausforming	

20. ABSTRACT (Continue on reverse side if necessary and identify by block number)

A development program was performed to manufacture, test, and evaluate 35mm diameter ball bearings, utilizing thermomechanically processed rings and balls. The program was subdivided into three main elements:

    Manufacture of Test Bearings
    Test Facility Design and Construction
    Bearing Life Testing

DD FORM
1 JAN 73 1473   EDITION OF 1 NOV 65 IS OBSOLETE

All three tasks were completed successfully and are detailed in this report.

35-mm-bore angular contact ball bearings, typical of those used in advanced Army propulsion systems were produced using high-energy-rate forging techniques to form the inner and outer rings, and forward extrusion to produce the ball stock. These bearings were tested in specially designed turbine-driven high-speed test facility, at a speed of 65,000 rpm, at an axial load of 500 lb. and at a temperature of 160°F-180°'. The initial bearing configuration planned for this test series was found to be inadequate for the above test conditions. A series of iterations was therefore introduced which resulted in a viable test bearing.

The results of the fatigue life tests performed on the bearings having Consumable Vacuum Melt (CVM) M-50 ausformed components show an approximate sevenfold improvement in the B_{10} life of the bearings when compared to the results of tests performed on bearings utilizing standard processed rings and balls. The bearing configuration and the test conditions for the ausformed and standard bearings were identical.

These results are in good agreement with previous work performed on small-diameter bearings having thermomechanically processed components. The results again show the capability of the ausforming process to improve fatigue life, even in a bearing with a marginal design at the expected operating conditions.

FOREWORD

TABLE OF CONTENTS

Preceding page blank

TABLE OF CONTENTS (Continued)

LIST OF ILLUSTRATIONS

LIST OF TABLES

INTRODUCTION AND BACKGROUND

The rapid developments in aircraft propulsion system technology over the past 25 years have placed unprecedented demands on the materials and processes areas. While most of the emphasis of this work has been on materials for turbine disks and buckets, compressor blades, combustors, etc., a lesser (but nevertheless important) effort has been the improvement of materials used for rolling-element bearings. In the past, this has resulted in replacement of the conventional bearing steels (such as 52100) with high-speed tool steels (such as M-1, M-50) or, in special applications, with materials such as AISI 440C. For that matter, improved melting and processing techniques have upgraded the performance of the 52100 type of steels and have, in an equally evolutionary fashion, increased the life and reliability of the tool steels. During the mid '60s, it became apparent that the need for further improvements in bearing performance and reliability would accelerate, and that new processes to upgrade the properties of existing bearing materials would be a major technological challenge.

The reasons for the increased demands on engine bearings can be traced to several factors, among which are: longer life requirements, higher loads and speeds, and overall system cost. Current military and commercial aircraft engines are designed to operate without overhaul for time periods far in excess of the operational lives of the earlier generations of engines. Current and future versions of military engines have thrust ratings two to three times greater than earlier models. In part, this is achieved by increasing engine rotational speeds and component system loading. Both of these factors reflect in higher stresses on the main shaft bearings.

Initially, a major concern was the effect of ultrahigh-speed operation on bearing life. Analysis[1] had shown that because of the high centrifugal loads imposed by the rolling elements on the outer races, life of the component system would be significantly reduced. Recent work, however, has shown that in the case of relatively large bore diameter bearings (120mm) eminently successful operation can be achieved with essentially state-of-the-art bearings at speeds up to and including 3×10^6 DN.[2] (DN is the product of bearing bore diameter in mm and inner ring rotational speed in rpm.) It should be cautioned, however, that there is some question as to the direct extrapolation of the large diameter bearing test results to small high-speed bearings such as those of interest in the present report.

Nevertheless, the high-speed operational problems are now viewed as somewhat less of a technical barrier, and consequently many of the high-risk

11

options under consideration such as hollow rolling elements, ceramic balls, etc., are no longer considered to be essential to achieve reliable bearing operation at speeds up to and including 3 X 10^6 DN.

The second major concern, dealing with bearing reliability, has become increasingly more important in view of the exponential increases in systems cost and complexity. Premature bearing distress, and the potential secondary damage as a result thereof, simply cannot be tolerated.

For many years, General Electric[3] and other major aircraft engine procedures[4] have evaluated and investigated new materials with the aim of improving bearing fatigue life. This comprehensive search has not yielded a material sufficiently superior to the widely used M-50 tool steel to warrant its introduction into critical engine applications. Consequently, an alternative approach was initiated, aimed at improving the rolling element fatigue life characteristics of M-50. One of the more promising approaches to accomplishing this task was the incorporation of a thermomechanical metal working process (ausforming) into the production cycle of M-50 bearings.

The generic term "ausforming" describes a thermomechanical processing technique which, in the present case, consists of the deformation of a high-speed tool steel using various metal working procedures while the material is in the metastable austenitic condition. In the present case forging was the primary technique and thus the term ausforging is used interchangeably with ausforming.

The process of ausforming was first discussed in 1954 by Lips and Van Zuilen,[5] who reported the significant improvements in both strength and ductility which had been obtained by warm-working metastable austenite prior to its transformation to martensite. Schmatz and Zackay,[6] of the Ford Scientific Laboratories, substantiated the original work by Lips and Van Zuilen, showing similar remarkable strength increases in several steels. Since then, the thermomechanical processing of certain steels in the metastable austenitic temperature range has been, and is being, studied extensively by laboratories inside and outside of the United States.[7,8]

General Electric first recognized the advantages of ausforming in a program aimed at improving the strength-to-weight ratio of solid rocket cases.[9] In this work, a shear-spinning method was developed by which scaled-down rocket cases were formed while the material was in the metastable austenitic condition. The excellent results achieved in this program in improving the mechanical properties of three tool steels encouraged General Electric to seek other uses for this process. It was recognized that one of the most promising applications would be for rolling-element bearings. To establish the feasibility of using ausforming as a means of improving the rolling contact fatigue characterisitics of bearing steels, a program sponsored by the U.S. Navy was initiated in 1962. This program consisted of studying various deformation processes, effects of percentage of

deformation, and associated metallurgical considerations on the rolling contact fatigue life of M-50, a typical bearing steel. Fatigue testing was performed on the General Electric-developed rolling-contact fatigue tester (RC rig), which has been shown to be a reliable indicator in terms of predicting full-scale bearing test results. The results of the program, presented in a Navy report[10] and an ASME paper,[11] were again highly encouraging. A summary of the results, graphically illustrated in Figure 1, showed that the rolling contact fatigue life of the M-50 increased by a factor of six to eight. In conjunction with the testing phase, a comprehensive metallurgical study was conducted to determine the basic mechanisms effecting the property improvements.

The choice of consumable vacuum-melted (CVM) M-50 material in the above program was based on the consideration that this 4 Cr, 4 Mo, 1V, 0.8C, iron-base tool steel is the structural material predominantly used for critical bearing applications in high-performance jet engines. It was and still is the first choice for this application; therefore, any significant improvement in its properties would represent a sizable advance in bearing materials technology. Additionally, a large body of data was available on this material which could be used to compare the improvements achieved by ausforming.

It was also fortuitous that M-50 had the required transformation characteristics for ausforming. This is illustrated best by comparing the two time-temperature-transformation curves shown in Figure 2. The upper curve presents the transformation kinetics of AISI 52100, another commonly used bearing steel. The phase changes in this steel occur rapidly upon quenching from the austenitic range; consequently, there is not sufficient time to effect any type of deformation in the austenite prior to its transformation to martensite. The lower curve illustrates the transformation characteristics of an AISI M type tool steel. This material is ideally suited for ausforming, as it has a sizable region where the austenite is isothermally stable. Sufficient time is available to thermomechanically process the material as illustrated by the arrow. Based on these considerations, M-50 was used in the initial (as well as subsequent) studies and also was chosen as the material investigated in the program discussed herein.

The encouraging results of the initial ausformed bearing studies led to a second program which was designed to demonstrate that actual bearing components could be produced by ausforming, and to establish the validity of the fatigue life improvements by performing tests using actual bearing hardware. In this latter program[12] small size bearings were manufactured having ausformed inner rings and balls. The test results of the ausformed bearings confirmed the highly encouraging data shown by the earlier rolling contact fatigue tests. Additionally, work performed by NASA[13] also showed the significant fatigue life improvement possible by the use of ausforming.
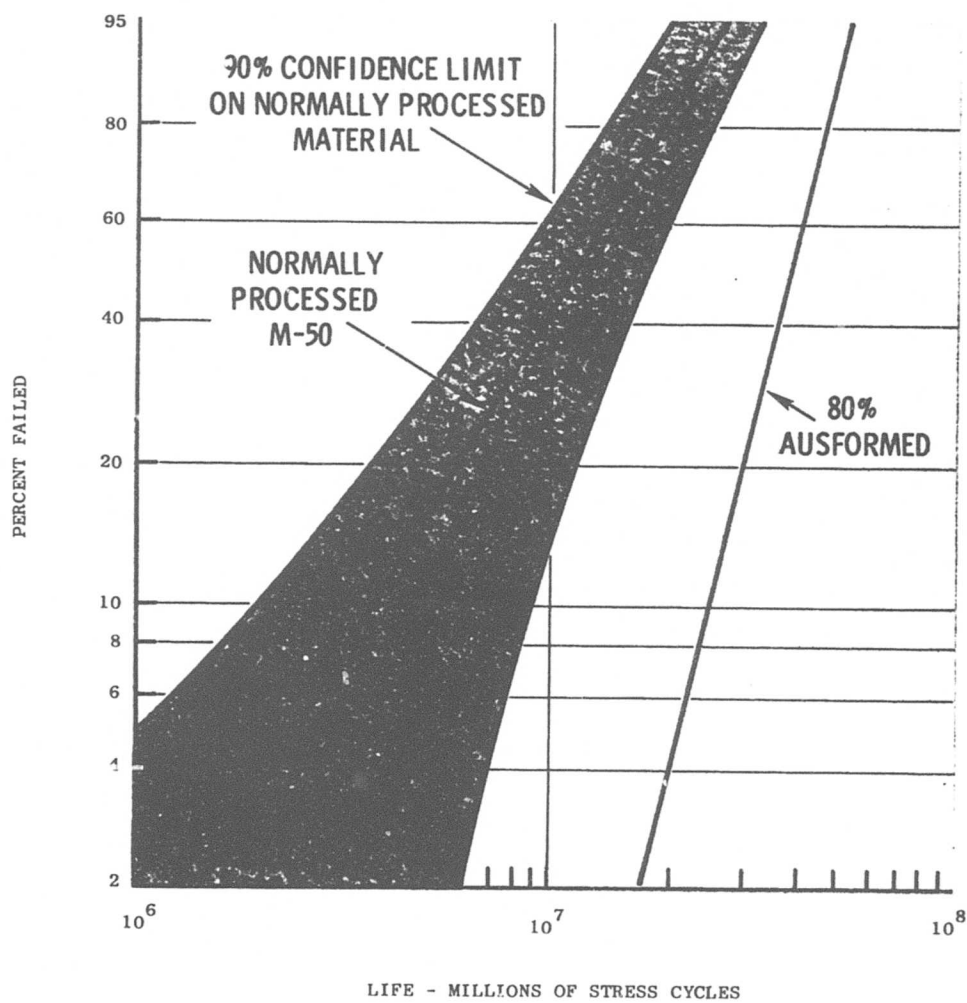
Figure 1. Effect of Ausforming on Rolling Contact
Fatigue Life of AISI M-50 (Reference 11)

14
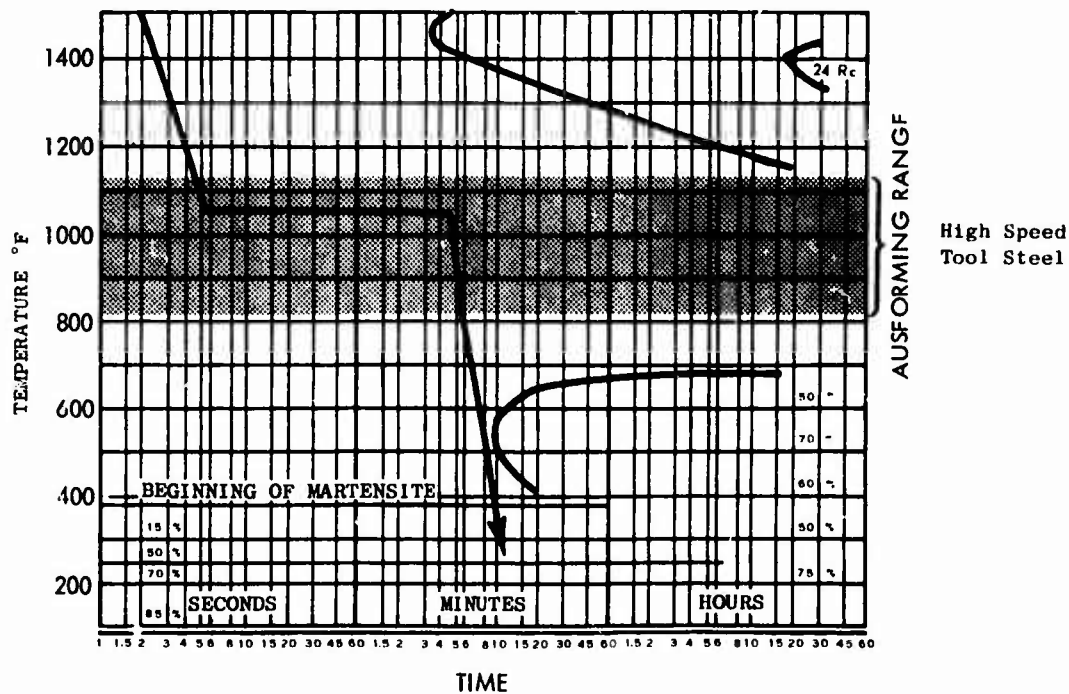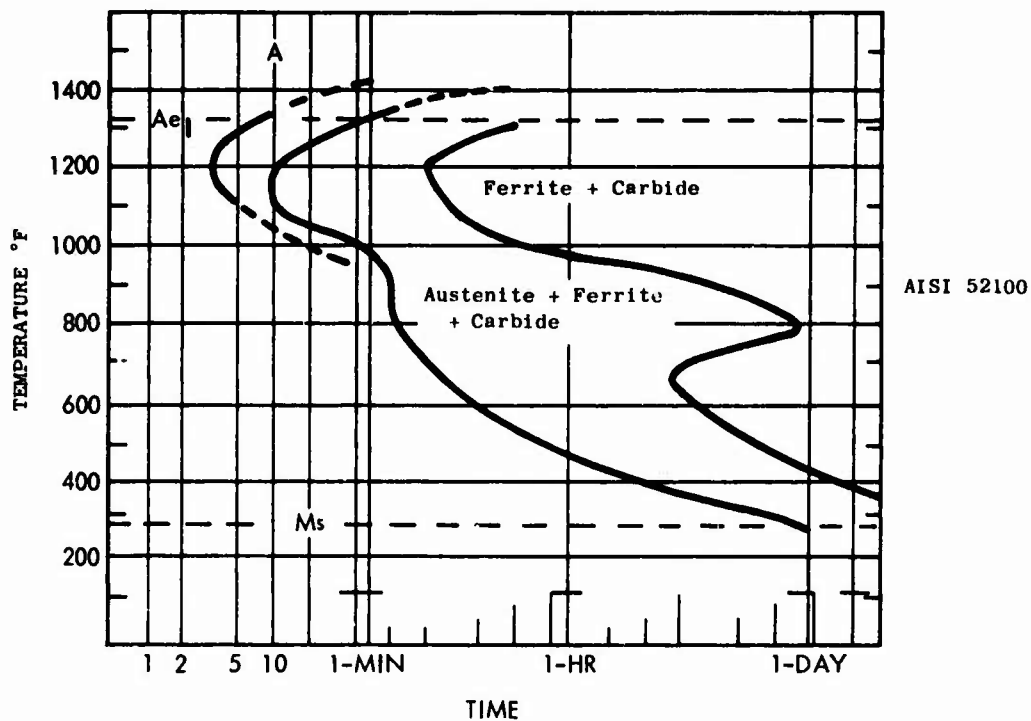
Figure 2. Isothermal Transformation Diagrams for AISI
52100 and a Typical M-Type High-Speed Tool Steel

The work reported in the current report was undertaken principally to substantiate the initial good results obtained on small-diameter ausformed bearings. There were, however, several other objectives:

o Producing and testing a bearing having all ausformed components. The earlier tests had only thermomechanically formed inner races and balls.

o To produce these components utilizing the most current processing technique, i.e., high-energy-rate forging. This procedure had been developed primarily for large-diameter parts.[14,15]

o To establish a production sequence and capability for the relatively small diameter bearings (35-75mm) common to advanced U.S. Army propulsion systems.

TECHNICAL PROGRAM

The objective of the program described herein was the manufacture and testing of 35mm bore bearings having all components (except the cage) made by thermomechanical processing. As envisioned initially, the program did not include any bearing design activity other than the normal life calculations. The bearing design was dictated by the terms of the contract, and was similar to the bearing used on the General Electric ATACC (Advanced Technology Axial-Centrifugal Compressor) Program.

During the initial bearing tester checkout runs, as well as some of the early baseline tests, i.e., tests performed on bearings using standard machined and heat-treated components, it became apparent that because of the severe test conditions of the bearing test program, the existent bearing design was not adequate.

This realization posed two challenges. The most immediate and undoubtedly the most pressing of these was the need to "fix" the existing design in order to make it viable for the current program. This task was made difficult by the fact that at this point in time, because of the concurrent paths of forging development, bearing manufacture, tester checkout and baseline testing, all of the ausformed components had been produced. Consequently, the major dimensional envelopes of the bearing rings, i.e., bore, inner OD, outer ID, inner width, etc., were frozen. Changing these dimensions would have required redoing all of the metal-working tasks, which was not an acceptable option because of time and funding considerations.

As a result, the design corrections had to be made without significantly affecting the print dimensions of the bearing. A discussion of the original design in the context of the planned test program is presented in the following section. Additionally, and for the record, the individual design modifications and iterations are cited, including those made to the bearing test facility.

The second challenge was to perform an in-depth analytical parametric study to determine the correct bearing design for a typical, small, high-speed application, and to generate sufficient design data to cover the size ranges most common to current and advanced Army aircraft propulsion systems. While this latter study was not a requirement of the basic contract, it was felt that its inclusion would greatly enhance the overall value of the work performed. Consequently, the results of the design optimization study will be summarized in a later section of this report and presented in detail in Appendix A to this report.

Lastly, since the role of elastohydrodynamic (EHD) lubrication becomes an extremely important and critical consideration in the operation of high-speed bearings, Appendix B has been added, wherein this subject is discussed relative to the small-bore bearings of interest in this report.

ATACC VEHICLE BEARING DESIGN

The basic bearing utilized in this program is the thrust bearing from the General Electric ATACC vehicle. This bearing was originally designed by the bearing vendor to loads, speeds and operating conditions as specified by the General Electric Company. The following were the original design conditions.

Shaft Speed	61,000 RPM
Shaft Materials	AM355
Bearing Load	100 lb
Oil-In-Temp	90°F

The resulting bearing design is shown in Figure 3. The critical geometry features are tabulated on the figure. These are free-state, or dimensions as the parts are received.

Following a failure of this bearing on the ATACC vehicle, which appeared to be due to loss of internal clearance, the design was reviewed; it was found that the clearance was inadequate for operation at the quoted conditions and that actual loads were in the 200-250 pound range. The following changes were consequently instituted:

	Old Design	New Design
Contact Angle	15 ± 1.5°	30 ± 2.0°
Internal Radial Clearance	0.0004-0.0007 in.	0.0017-0.0022 in.
End Play	0.004 in. max	0.0074 in. max
Inner Race Curvatures	0.525	0.52
Outer Race Curvatures	0.515	0.52

Following this design change the bearings operated successfully in the ATACC vehicle.

Development Test Bearing Design

The above modified bearing was the design specified for the ausformed bearing development program. It was selected by the Army and the contractor, since bearings were in existence for baseline testing. Based on standard practice, the fatigue test loads were increased to produce fatigue failures

18
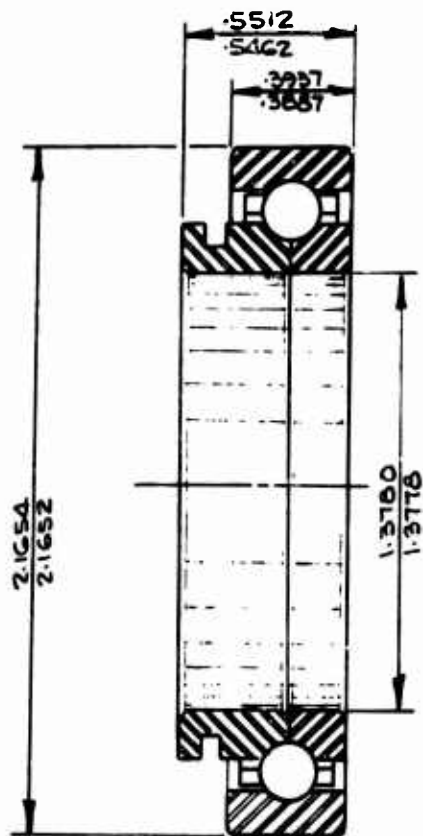
Contact Angle	15 ± 1.5°
Internal Radial Clearance	.0004-.0007"
End Play	.004" Max.
Inner Race Curvature Ratio	.525
Outer Race Curvature Ratio	.515
Number of Balls	18
Ball Diameter	3/16"
Cage Clearance at Land Riding Surface.	.012-.018"
Cage Clearance at Non-Riding Surface	.024-.050"
Ball Pocket Clearance	.008-.017"

Figure 3. Original ATACC Vehicle Bearing Design

in a reasonable test time. This is the normal approach of various engine manufacturers as well as most bearing vendors. The following were the selected test conditions:

Thrust Load	500 lb
Shaft Speed	65,000 RPM
Oil-In-Temp	160°F-180°F

During early checkout of the rig, and because of the limited number of baseline test bearings available, off-the-shelf bearings (Split-Ball Bearing PN HDB-007) with the same external dimensional envelopes were procured and utilized. Rig checkout went smoothly using these bearings. All emergency shutdown instrumentation for unattended running was checked out and performed satisfactorily.

Upon initiation of the baseline testing, early nonfatigue type failures were encountered. These failures were indicative of boundary lubrication, cage inadequacies and oil-supply problems. This situation was reviewed with cognizant Army project personnel, and it was decided that continuing the program at that point would have resulted in the generation of data not relevant to the main objective of the program, which was the evaluation of the relative fatigue life of standard versus thermomechanically processed bearings. Consequently, it was decided to attempt to modify, within overall bearing envelope dimensions, the bearings and the test apparatus in order to achieve a viable test program. The specific changes and the reasons for these are briefly discussed in the next sections.

Lubrication Technique and Housing Modifications

In the original proposal, under-race cooling was proposed as the lubrication method. This was based on experience with the high-speed NASA test program[15] wherein the use of jet lubrication was found to be necessary at DN's above 2.2-2.4 million due to the inability to maintain thermal equilibrium in the bearings. In the referenced program, it was found that inner-race temperatures increased at a higher rate than those of the outer races, thereby reducing the internal clearances.

In the present case, since the DN was in a marginal area (2.28×10^6) and since the lubrication scheme for the ATACC vehicle test bearings was via jet lubrication, it was decided by the contractor and the Army to utilize a similar single jet cooling and lubrication scheme.

Early test results indicated the existence of an axial temperature gradient. In addition, testing experience in the General Electric Lynn laboratories indicated that a heavyweight housing could prevent proper thermal matchup in small-diameter bearings. It was, therefore, decided to incorporate dual jets (from both sides) on each test bearing and to simulate aircraft weight

20

housings for the bearing mounts. A discussion of the rig modification is presented in a later section of this report. Following this, a checkout test was once again performed using the slave, off-the-shelf, bearings. The results were good from a thermal standpoint, but fatigue failures occurred after only 8.5 hours on both test bearings. Figure 4 shows a comparison of the baseline test bearing and the slave bearings. Noting the greater cage clearances of the slave bearings, it was decided to chamfer the inner races and retainers as shown in Figure 5 prior to running additional baseline tests.

Bearing Modification, Chamfer Inner Race and Retainer Corners

The purpose of chamfering the corners is to ease the flow path of the lubricant. This is done on the General Electric T700 engine main thrust bearing, which is the third bearing shown on Figure 4. Following this change and coupled with the previous successful slave bearing test, testing was reinitiated on the baseline bearings. The rig was shut down after only 0.7 hour, and upon disassembly it was noted that one of the bearings had failed, although failure was in a surface fatigue mode and not the expected and desired subsurface initiated fatigue of a properly lubricated high-speed bearing.

Also observed was significant wear in the ball pockets of the cage. This indicated that the balls and cage were "fighting" each other. The phenomenon is not expected in ball bearings under pure thrust load, where normally stable cage operation occurs with very little cage/ball interplay. It should be noted that the slave bearings, operating under the same speed, loads, and temperatures, did not suffer from cage wear and surface fatigue failures. Noting this, the possibility of a relationship between the cage wear and the surface fatigue was investigated.

Surface fatigue occurs when operating in a marginal elastohydrodynamic (EHD) lubrication regime. For a detail discussion on EHD, see Appendix B. This normally occurs at high operating temperatures and low speeds, and would not be predicted in the current test series as the test conditions would be expected to provide full film (EHD) lubrication. Review of other General Electric experience revealed that surface fatigue can also be generated when there is sufficient cage interference to disturb the normal ball motion. This interference with the ball apparently causes sliding in the contacts, sufficient to effect a break through of the oil film resulting in asperity contact and terminating in surface initiated fatigue. Therefore, the next series of modifications to the test bearings was aimed at eliminating this cage interference. The continuing success with the Split-Ball slave bearing provided further evidence that the problem was indeed geometry related. The slave bearing balls were 33 percent greater in diameter than those used in the test bearings. Unfortunately a change of this magnitude could not be made since the thermomechanically processed bearing components were well beyond the stage where a major dimensional change was feasible.

21

.019
.066
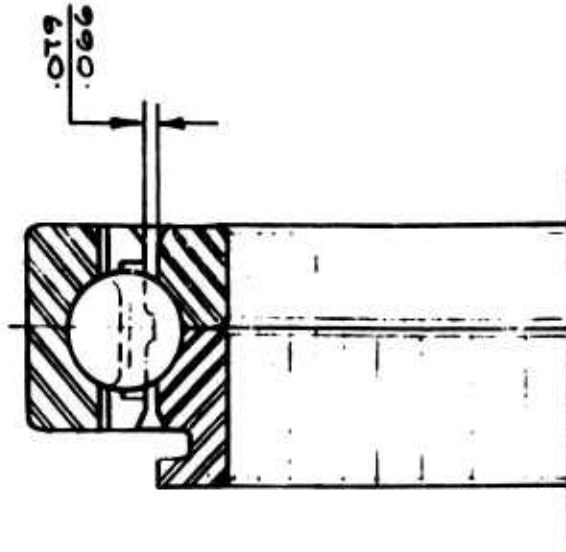
46mm
16 Balls
.3125 Dia.

T700
GAS GENERATOR
THRUST BEARING.

.100

.013
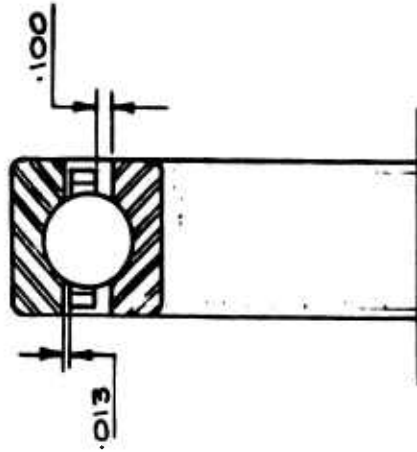
35mm
19 Balls
.250 Dia.

SLAVE BEARING.

.050
.024
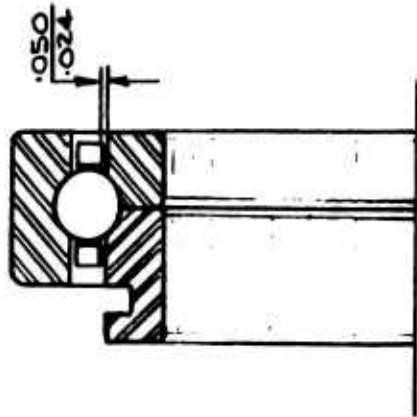
35mm
18 Balls
.1875 Dia.

ATACC
THRUST BEARING.

Figure 4. Comparative Envelope Dimensions for Three Bearing Types

22

.025
.015 CHAMFER
45° BASIC
2 PLACES

.05
.03 CHAMFER
45° BASIC
2 PLACES

35 mm
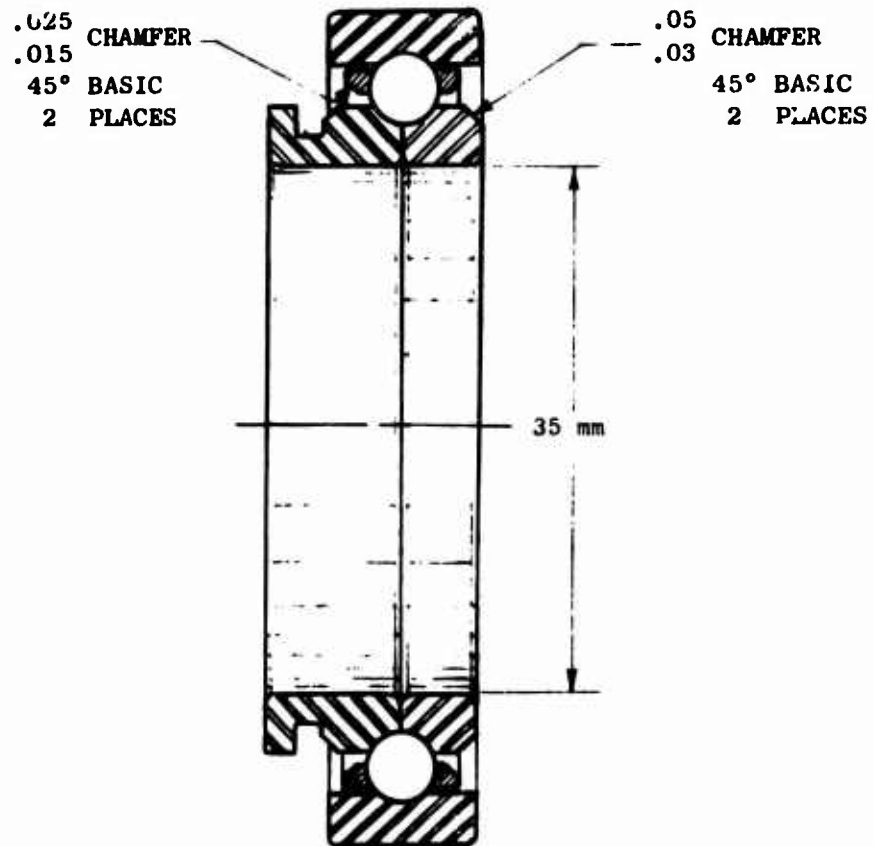
Figure 5. Test Bearing With Modified Cage and Races To
Improve Lubricant Penetration

Shaft Rework and Modified Start Procedure

The significant number of teardowns and buildups had caused scoring on the test shaft. When fits and clearances are extremely critical as in small high-speed bearings, any raised metal can cause problems. The rig shaft was reworked, chromium plated and reground to size, with care to limit taper across the axial bearing seat. Taper was controlled by requiring diameter inspections at various axial locations.

A break-in cycle was defined as shown below for the first run of a new bearing.

Speed - RPM	Time - Minutes
10,000	5
20,000	5
30,000	10
40,000	10
50,000	10
60,000	10
65,000	10

Restarts were operated at 30,000 RPM for 15 minutes before accelerating back to full speed. The shaft rework and break-in start did not correct the problems of cage wear; however, the step start was retained throughout the remainder of the program.

Bearing Modification, Rework Cages To Remove Retention Tangs

A stack-up of parts in the bearing was requested of the bearing vendor. This investigation revealed that within the print tolerance range, the ball retention tang could contact the ball while in operation. Since the tangs are functional for assembly purposes only, they were removed by machining the cages. This would not be a viable solution in a full-scale vehicle, although for the test program it was feasible since the test rig assembly could be accomplished without the retention tangs. Unfortunately, a short run of one-half hour at a reduced speed (55,000 RPM) again showed cage wear, and the tang correction was considered ineffective.

Bearing Modification, New Cages, Oversize Ball Pockets

Cage interference is occasionally caused by low ball pocket clearance. If the ball pocket clearance is less than the land riding cage clearance, the cage can become ball rather than land guided. In the present case, the land riding clearance was 0.012-0.018 inch and the ball pocket clearance 0.008-0.017 inch. Consequently, a modified cage was obtained with the pocket clearance increased to 0.020-0.026 inch, and again run at 55,000 RPM for 7.8 hours. Teardown once again revealed cage distress. It should be

24

noted that standard practice in these modification tests consisted of using one slave bearing and one baseline bearing. The continued good performance of the slave bearing provided assurance of proper rig operation.

Bearing and Rig Modification, Under-Race Cooling

Failing to obtain proper operation on the baseline bearings, it was decided to rework a bearing and utilize under-race cooling. Testing with this configuration showed a very definite improvement with only slight cage distress. Since this test was run with an existing baseline bearing, it utilized an outer-land riding cage. It was felt that one additional iteration to inner land riding cages was desired based on the NASA 3.0 million DN bearing tests.[2]

Bearing Modification, Inner Land Riding Cages, Additional Under-Race Cooling Slots

Inner land riding cages were procured from the vendor and assembled into bearings at General Electric. In addition, the number of cooling slots at the split inner-race interface was increased from 4 to 8 to insure symmetrical cooling of the races. Testing with this configuration resulted in the desired subsurface fatigue failures in the raceway along with only minor cage wear.

Table 1 tabulates the history of the test points through the changes outlined above. It will be noted by reviewing this table that the slave bearing operates without cage distress throughout the development. The key difference is felt to be the larger ball diameter in this bearing. The effects of ball diameter are discussed in detail in Appendix A. However, the final test results with under-race cooling and inner land riding cages, assured that the current design was adequate for the planned test program, albeit with a very limited margin. The endurance program was initiated at these test conditions, and the results are given in a later section of this report.

PARAMETRIC DESIGN STUDY - SUMMARY

As a result of the problems categorized in the previous section, a design study was conducted to determine the deficiencies in the basic design and to provide guidelines for a bearing design in future programs of this type.

In conducting a parametric study for an engine design, a mission cycle would be defined, and the study would involve a wide variation in operating conditions. For the present it was elected to conduct the study as a single-point investigation, with check on bearing operation at the specified test conditions. The basic conditions selected were those approximating the normal operational characteristics of the ATACC Vehicle. These are:

25

TABLE 1

SUMMARY OF BEARING AND TEST RIG MODIFICATIONS

Test #	Brg. Type	Speed (rpm)	Load (lb)	Total Time (hr)	Remarks
1	S	65,000	500	15.0	Rig checkout
2	S	65,000	500	15.0	Rig checkout
3	C	65,000	500	0.8	Surface fatigue - balls
4	C	65,000	500	0.8	Suspended - No damage
5	C	65,000	500	18.6	Surface fatigue
6	C	65,000	500	18.6	Suspended - Split line damage
7	C	65,000	500	8.0	Surface fatigue
8	C	65,000	500	8.0	Suspended - No damage
9	C	65,000	500	2.0	Suspended - High torque
10	C	65,000	500	2.0	Suspended - High torque
11	S	65,000	500	2.7	Rig C/O, suspended
12	S	65,000	500	2.7	Rig C/O, outer race fatigue spall

- Rig Modification, install dual oil jets, reduce mass of bearing housing

Test #	Brg. Type	Speed (rpm)	Load (lb)	Total Time (hr)	Remarks
13	S	65,000	500	8.5	Outer race fatigue
14	S	65,000	500	8.5	Outer and inner race fatigue

- Bearing Modification, chamfer inner race and retainer corners

Test #	Brg. Type	Speed (rpm)	Load (lb)	Total Time (hr)	Remarks
15	C	65,000	500	0.7	Cage distress
16	C	65,000	500	0.7	Suspended

- Bearing and Rig Modifications, change fit-up, regrind shaft, incorporate run-in procedure

Test #	Brg. Type	Speed (rpm)	Load (lb)	Total Time (hr)	Remarks
17	C	65,000	500	14.6	Ball and cage damage
18	C	65,000	500	14.6	Suspended
19	C	65,000	500	9.5	Cage damage
20	C	65,000	500	9.5	Cage damage

- Bearing Modification, rework cages to remove retention tangs

Test #	Brg. Type	Speed (rpm)	Load (lb)	Total Time (hr)	Remarks
21	C	55,000	500	0.5	Cage distress
22	C	55,000	500	0.5	Cage distress
23	S	65,000	500	15.2	Rig C/O, outer race spall
24	S	65,000	500	15.2	Rig C/O, outer race spall

S - Slave Bearing, Split Ball P/N HDB-007
C - Control Bearing, M-50, nonausformed

TABLE 1

SUMMARY OF BEARING AND TEST RIG MODIFICATIONS

(Continued)

Test #	Brg. Type	Speed (rpm)	Load (lb)	Total Time (hr)	Remarks
- Bearing Modification, new cages, oversize ball pockets					
25	C	55,000	500	7.8	Cage wear
26	S	55,000	500	7.8	Suspended
- Bearing and Rig Modification, introduces under-race cooling					
27	C	65,000	500	13.6	Slight cage distress
28	S	65,000	500	13.6	Suspended
- Bearing Modifications, inner land riding cages, additional under-race cooling slots					
29	C	65,000	500	28.0	Small I/R fatigue
30	S	65,000	500	28.0	Suspended

S - Slave Bearing, Split Ball P/N HDB-007
C - Control Bearing, M-50, nonausformed

27

```
Thrust Load      =  250 lb
Shaft Speed      =  65,000 RPM
Oil Temperature  =  160°F-180°F
```

The development bearing test conditions were the same except that load was increased to 500 lb, to produce more rapid failures.

Simple expressions can be used to relate contact angle, radial clearance and end clearance.

$$P_d = 2BD(1 - Cos \ \alpha)$$

$$P_E = 2BD \ Sin \ \alpha$$

where P_d = internal radial clearance

P_E = end play (clearance)

B = total curvature = $(f_i + f_o - 1)$

D = ball diameter

α = contact angle

f_i = inner-race curvature

f_o = outer-race curvature

From the preceding equations, it can be seen that both clearances are linear functions of ball diameter and total curvature. The end play of a bearing in an engine or test vehicle utilizing centrifugal stages is more critical than a purely axial stage machine. The axial clearances must be capable of taking the full axial play of the main thrust bearings. The effect that these clearances have on engine performance is greater on a centrifugal stage than on an axial stage, and it must be limited. The end play can be reduced by introduction of a modification to the split races as shown in Figure 6. The end play in the bearing is then given by the following equation:

$$P_E = 2BD(Sin\alpha)-W_s$$

W_s is defined as the shim thickness. The bearing deemed to be the best compromise has the following dimensions:

```
Ball Diameter         =  .3125 in.

Inner-Race Curvature  =  .56

Outer-Race Curvature  =  .51

Pitch Diameter        =  1.9095 in.

Contact Angle         =  28°-32°
```
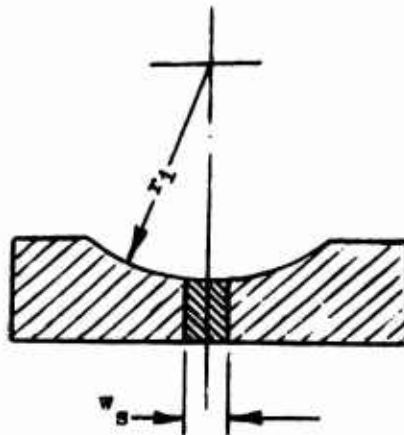
(a) Inner rings of split inner ring
ball bearing showing shim for
grinding.
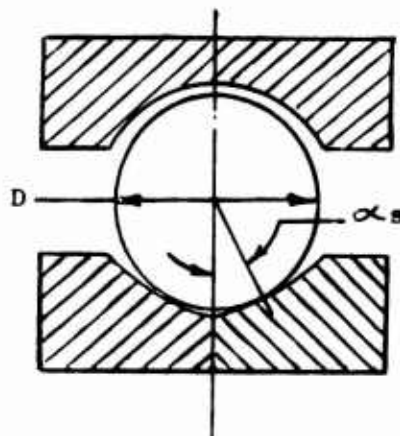
(b) Split inner ring ball bearing
assembly showing shim angle.

Figure 6. Modification of Inner Race To Reduce End Play (Clearance)

The shim angle and shim thickness have not been defined since they will depend on the actual application and fit-up. As stated in the introduction to this section, the study is single point and does not consider a mission cycle. The exact values could change depending on a full investigation. However, for any high-speed application, it is imperative that ball diameters and clearances be thoroughly investigated.

The results of the parametric design study are discussed in detail in Appendix A. The pertinent conclusions in relation to the baseline bearing design are:

- Ball diameter should be increased.

- Total curvature should be increased.

- The manufactured contact angle would remain the same, but the operating angles are increased significantly by the ball diameter and curvature change.

- Jet lubrication was not successful on the present design at the test conditions, but could be utilized for a redesign with the above changes. This is verified by the successful operation of the slave bearings.

BEARING MANUFACTURE

Material

The raw material for the ausformed bearings was double vacuum melted (vacuum induction melted-vacuum arc remelted) AISI M-50. Both inner and outer rings as well as the original set of balls were made from one heat. Due to the need to redo the balls (discussed later) a second heat was utilized for the latter.

Ausforging Facilities

A controlled-energy-flow forming technique (CEFF) was utilized for the ausforming. This high-velocity metal-working procedure has been a production process for a number of years.[16]

The equipment used is shown schematically in Figure 7 and illustrated in Figure 8. The CEFF equipment uses the counter-blow concept, but employs two independent cylinders to accomplish this action. Nitrogen is pressurized at maximum energy to 1400 psi. Provision is made to operate the machine with dissimilar pressures in the two cylinders. This allows the balancing of the system to provide equal momentum at impact, which, in turn, provides efficient and rapid transfer of energy to the tooling and to the work piece. A trigger system, with a hydromechanical lock for the
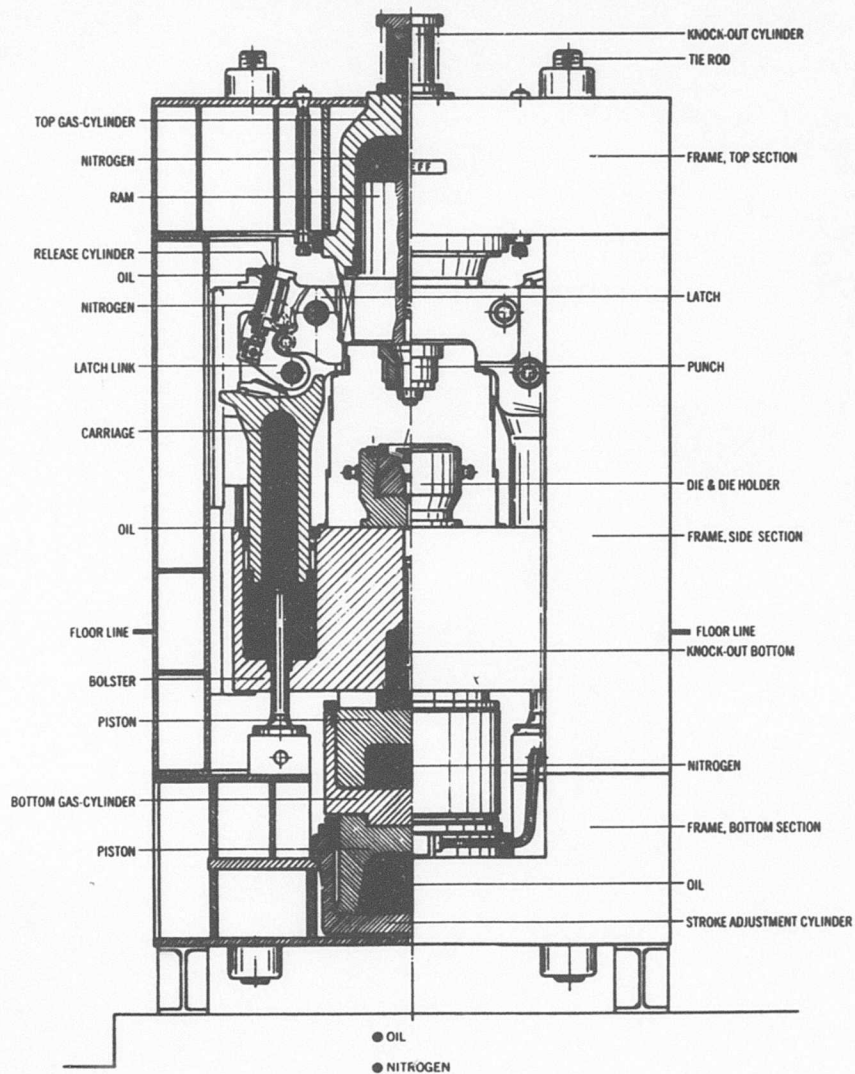
Ready for Impact

Figure 7. Schematic of High-Energy-Rate Forging Equipment (CEFF)
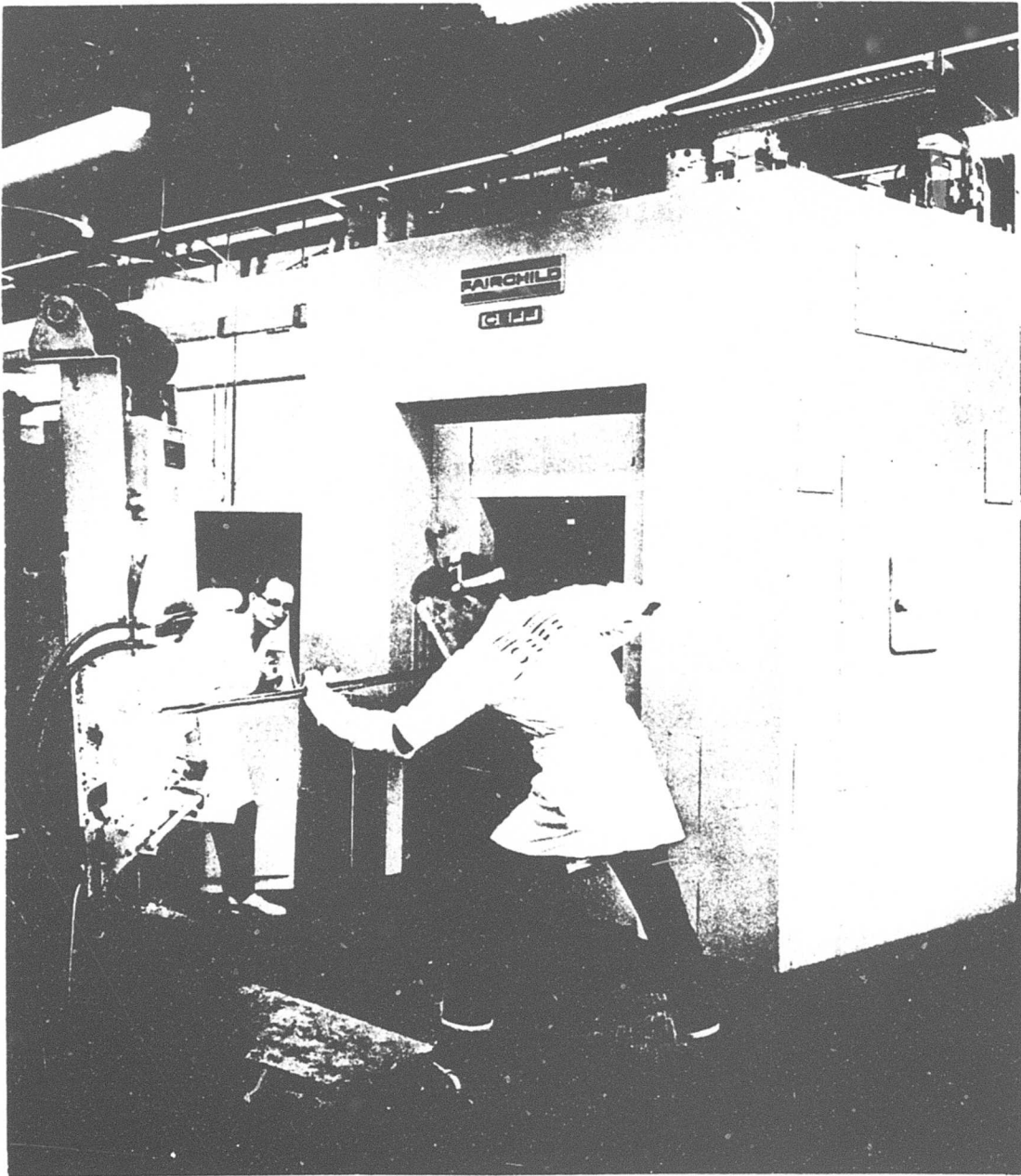
31

Figure 8. CEFF Machine in Operation - Operator Is Shown
Removing Forging Blank From Furnace Preparatory
to Placing it Into Die

32

upper ram and lower bolster, synchronizes the simultaneous release of both parts of the tool. After firing, the latch system separates the tools to their starting positions in conjunction with ancillary pressure cylinders. The energy can be established by regulating the cylinder pressure and by adjusting the forging stroke. The combinations of stroke and cylinder pressures that may be used to obtain equivalent pressures are given in the theoretical curves in Figure 9.

The planned forging technique for each component was as follows:

Outer Ring   -   Backward Extrusion

Inner Ring   -   Forward Extrusion

Ball Blanks   -   Forward Extrusion

Ring Ausforming

Both inner and outer ring forgings were made using the high-energy-rate forging process discussed in the previous section. One of the major concerns in ausforming the inner rings was to maintain an optimum macro grain-flow condition in the raceway region. Die design and preform volume therefore became a significant consideration. The final forging drawing for subject part is shown in Figure 10. The actual inner ring is indicated on this drawing, to show its relative position to the as-forged blank.

To achieve the desired dimensions as shown on the forging drawing, starting preforms having a .780 inch O.D. and heights of either 1.76 inches or 2.09 inches were used. The two different heights were necessary in order to achieve proper grain-flow for the puller groove half and the plain half inner rings. As can be seen on the bearing drawing (Figure 5), the puller groove half has a greater width than the plain side.

A number of forging trials were required for the inner rings, mainly to assure a near net configuration in the raceway area. The final forgings had less than .006 inch of excess material in the raceway area. Table 2 shows the major dimensions.

The ausforging cycle for the inner rings was as follows:

Preheat 1400°F, 30 min.

Austenitize 2075°F, 30-40 min. (endothermic atmosphere)

Rapid Air Cool to 1400°F

Stabilize at 1400°F - 5 min.

Forge

Direct Oil Quench to 150°F

33
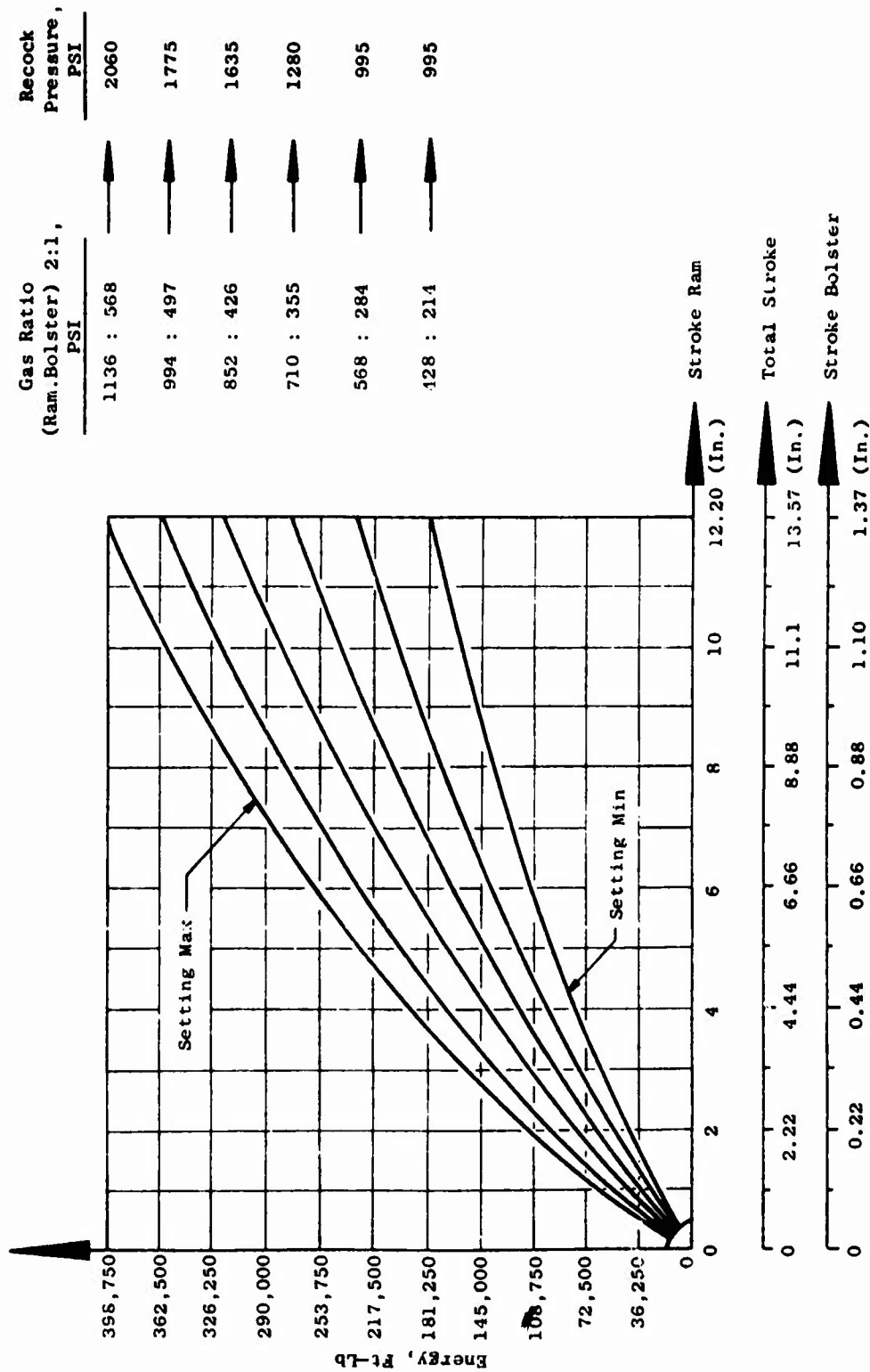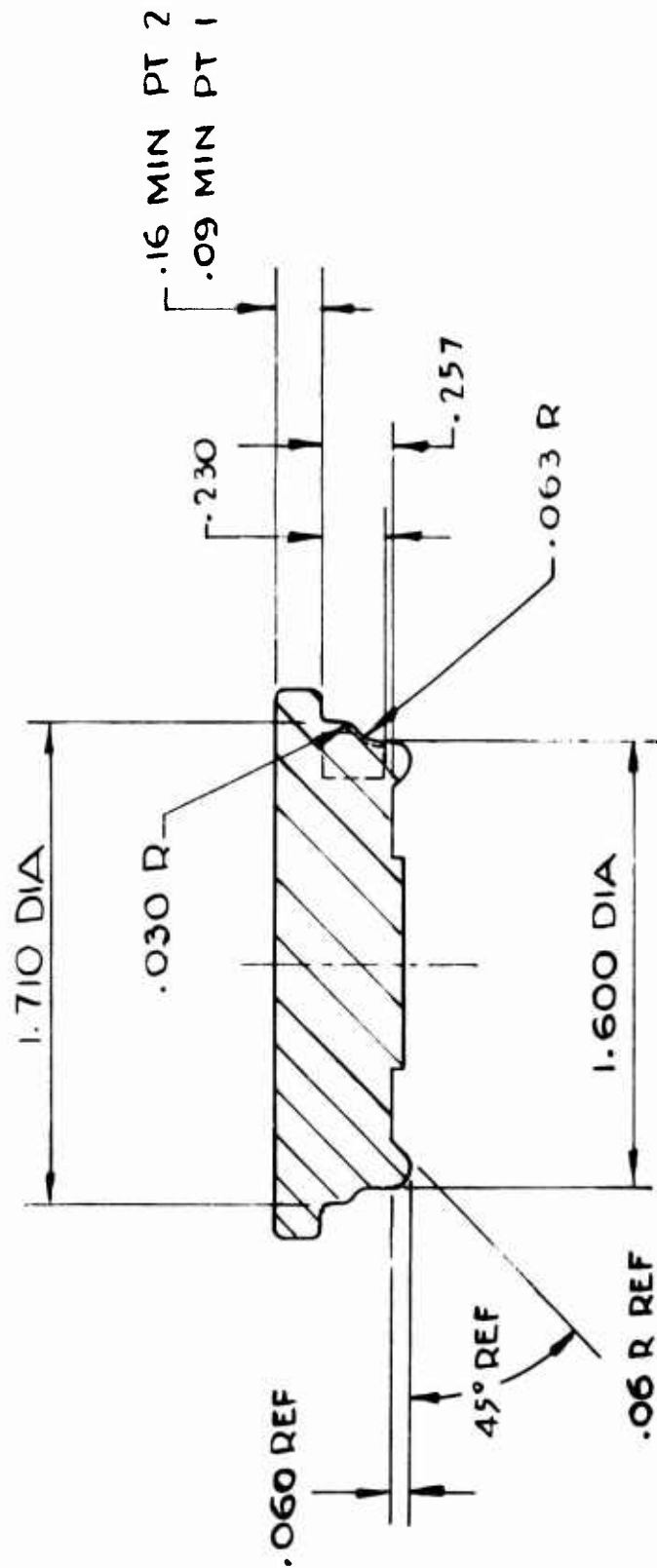
Figure 9. CEFF Energy Curves

.16 MIN PT 2
.09 MIN PT 1

.257

.063 R

.230

1.710 DIA

.030 R

1.600 DIA

.060 REF

45° REF

.06 R REF

PT 1 PLAIN SIDE
PT 2 PULLER SIDE

Figure 10. Inner Ring Forging Drawing

35

TABLE 2

35MM BEARING FORGINGS - MAJOR DIMENSIONS

Inner Race

	Max. O.D.	Min. O.D.	Height	
			(A)	(B)
Forging Dwg. S/N	1.710	1.600	.390	.450
1	1.710	1.607	.401	--
2	1.710	1.607	.396	--
3	1.711	1.606	.397	--
4	1.711	1.607	.396	--
5	1.711	1.609	.400	--
6	1.710	1.609	.401	--
7	1.711	1.610	.401	--
8	1.711	1.607	.395	--
9	1.711	1.608	.401	--
10	1.711	1.607	.396	--
11	1.711	1.607	.396	--
12	1.712	1.608	.398	--
13	1.711	1.608	.400	--
14	1.713	1.608	.395	--
15	1.712	1.610	.396	--
16	1.711	1.607	.400	--
17	1.711	1.607	.400	--
18	1.712	1.607	.399	--
19	1.710	1.608	--	.453
20	1.711	1.606	--	.458
21	1.712	1.607	--	.456
22	1.713	1.605	--	.456
23	1.712	1.606	--	.453
24	1.712	1.605	--	.457
25	1.711	1.606	--	.457
26	1.711	1.608	--	.454
27	1.713	1.607	--	.454
28	1.712	1.608	--	.460
29	1.711	1.605	--	.457
30	1.712	1.606	--	.458
31	1.712	1.606	--	.459
32	1.712	1.605	--	.455
33	1.712	1.606	--	.453
34	1.711	1.607	--	.454
35	1.713	1.605	--	.455
36	1.712	1.606	--	.453

36

Air Cool to room temperature

Stress relief 950°F - 120 min.

It was recognized that one of the critical operations in the above sequence was the time elapsed between the actual forging operation and the subsequent oil quench. In previous work[14] it had been observed that the transformation characteristics of the M-50 were altered as a result of the severe strain imposed during the ausforging operation. Consequently, for the current program, the die set was designed for rapid ejection of the forged blank, thus reducing the transfer time to the oil to a minimum. In actual practice, this transfer time averaged 5-7 seconds and never exceeded 10 seconds.

Photographs of the as-ausforged inner rings are shown in Figure 11.

The outer ring forgings were made by forward extrusion. The forging drawing for this part is shown in Figure 12. Because of the greater mass of material involved in this part, the ausforging temperature was raised to 1500°F - 1525°F in order to achieve improved metal flow. The sequence of operation was as follows:

Preheat 1400°F, 30 min.

Austenitize 2075°F, 30-40 min. (endothermic atmosphere)

Rapid Air Cool to 1500°F

Stabilize at 1500°F - 5 min.

Forge

Direct Oil Quench to 150°F

Air Cool to room temperature

Stress relief 950°F - 120 min.

Similar to the inner ring forgings, it was desirable to come as close as possible to the final I.D. and O.D. dimensions of the outer ring, in order to reduce the machining time and cost and to achieve optimum grain flow characteristics. This again was accomplished, as can be seen by the dimensional data presented in Table 3. Typical outer race forward extrusions are shown in Figure 13, and a production lot of inner and outer ring forgings is shown in Figure 14.

Along with the required dimensional controls, it was also imperative that the proper hardness and microstructure of the ausforged parts were assured. Hardness was a major consideration since it was necessary to achieve a Rc 62-64 hardness range in order to permit a direct assessment when compared to the baseline bearings, which were also in this hardness range. Table 4 shows the results of the hardness measurements of both inner and outer ring forgings after the 975°F stress relief treatment.
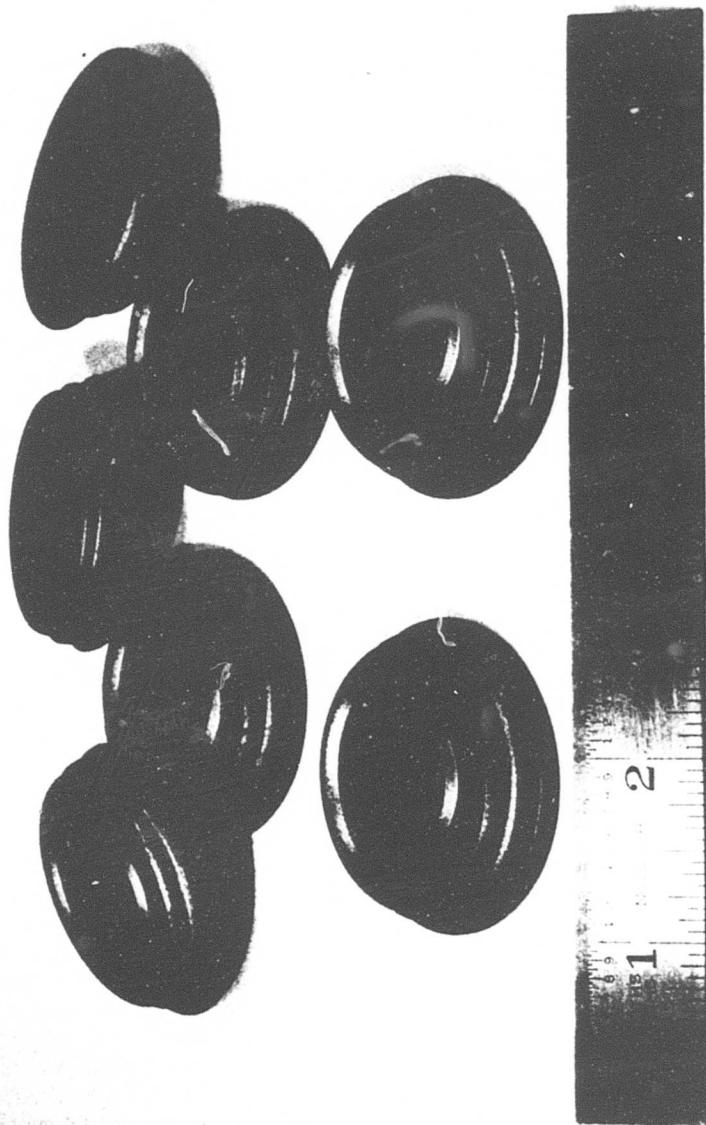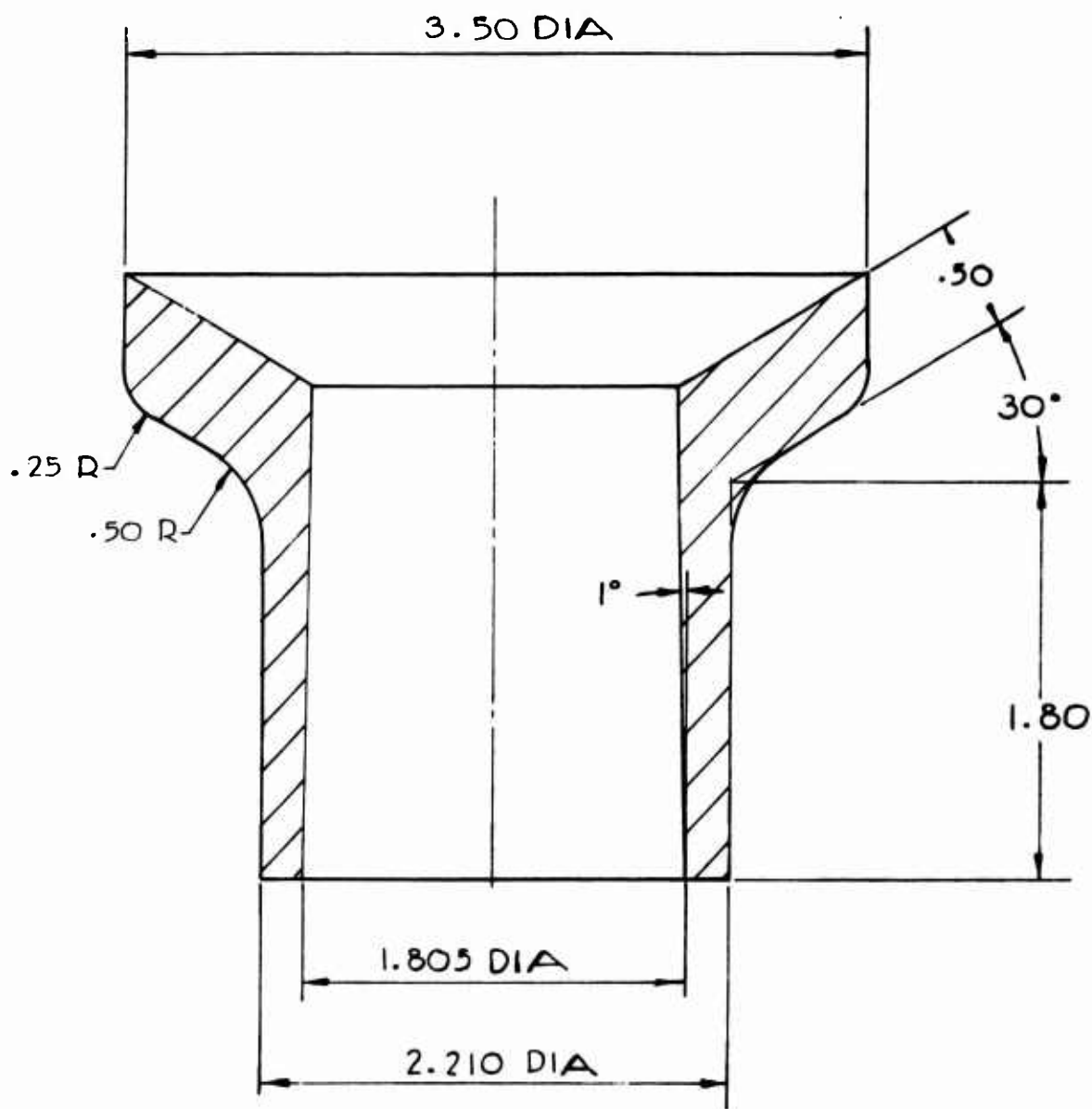
37

Figure 11. As-Forged 35MM Inner Ring Blanks

Figure 12. Forging Drawing - 35MM Outer Race
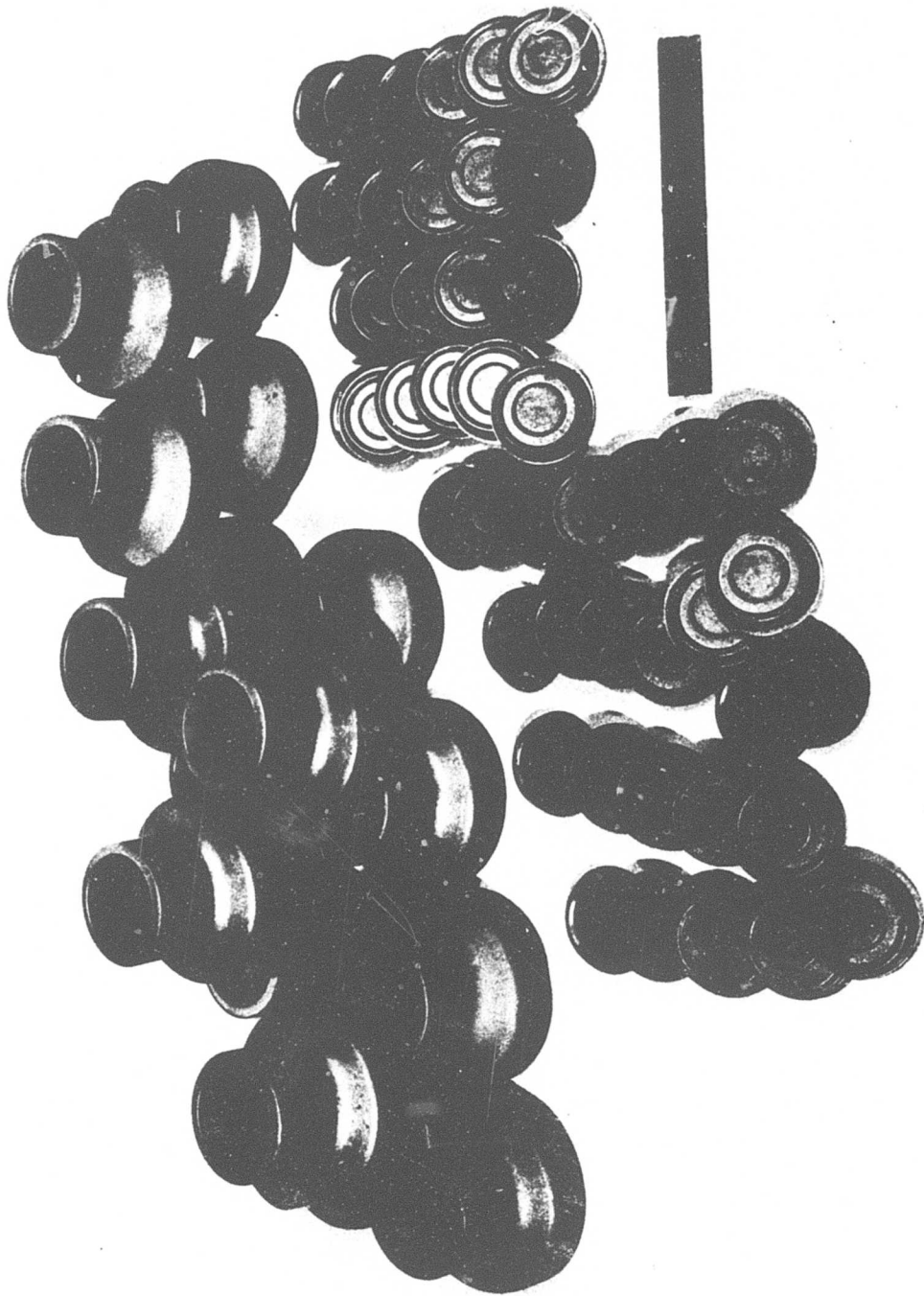
Figure 13. As-Forged 35MM Outer Ring Blanks

40

Figure 14. Production Forging Lot of 35MM Inner and Outer Race Forgings

TABLE 3

35MM BEARING FORGING - MAJOR DIMENSIONS

Outer Race

	O.D.	I.D.	Height
Forging Dwg.	2.210	1.805	1.8"
S/N			
1	2.228	1.801	1.3
2	2.232	1.800	1.25
3	2.232	1.796	1.3
4	2.230	1.797	1.3
5	2.234	1.798	1.3
6	2.229	1.798	1.25
7	2.230	1.800	1.25
8	2.228	1.798	1.25
9	2.232	1.798	1.4
10	2.234	1.799	1.4
11	2.228	1.798	1.3
12	2.229	1.799	1.3
13	2.234	1.799	1.35
14	2.235	1.800	1.3
15	2.236	1.801	1.4
16	2.235	1.799	1.4
17	2.234	1.801	1.4
18	2.235	1.801	1.45

TABLE 4

35MM BEARING FORGINGS HARDNESS SURVEYS

Inner Rings				Outer Rings		Ball Stock*	
S/N	Rc	S/N	Rc	S/N	Rc	Bar #	Rc
1	63	19	64	1	63	1	63.5
2	63	20	63.5	2	63	2	63
3	63.5	21	63	3	63	3	63.5
4	63.5	22	63	4	62.5	4	63
5	63	23	63.5	5	63	5	62.5
6	64	24	63.5	6	63	6	63
7	63	25	63	7	63.5	7	63
8	63.5	26	64	8	63	8	63.5
9	63.5	27	63	9	64	9	63
10	63	28	63	10	63.5	10	63
11	63	29	64	11	63	11	63
12	63	30	63	12	63	12	63.5
13	63.5	31	63.5	13	63	13	63.5
14	64	32	63	14	63.5		
15	63	33	64	15	63		
16	64	34	63	16	64		
17	64	35	63.5	17	63		
18	64	36	63.5	18	63.5	*2nd forging run	

43

Ball Ausforming

Because of the small-diameter balls required for the test bearing, it was decided to use the bar extrusion technique proved to be successful in previous work[12] to ausform the balls. The method, described pictorially in Figure 15, consists of aus-extruding bar stock and subsequently machining the balls from these bars. While the grain flow induced by this method is not ideal, the good performance of balls made by the method has been amply demonstrated.[13]

To achieve the desired 80 percent of deformation[11] in the ball material, the initial 0.625 inch diameter bar was reduced to 0.271 inch diameter, thus producing the 80 percent reduction in cross-sectional area. The as-extruded diameter contained adequate material to finish machine the required 0.1875 inch diameter ball.

For the ball extrusion a mechanical 650-ton press was used. Since the press action is considerably slower than the high-energy-rate forging facility used for the rings, several variations in the process had to be introduced. The major one of these dealt with the ausforging temperature. Previously, the preform was rapidly air cooled to the ausforging range (1200°-1500°F) prior to being placed into the forging die. In the present case, however, because of the small mass of the preform (.625 inch diameter by 1.00 inch high), the cooling rate from the 2075°F austenitizing temperature was very rapid. Coupled with this was the 10-15 seconds delay encountered between placing the preform into the extrusion die, activating the press, and the actual contact of the punch to start the extrusion process. Despite the fact that the die was preheated to 600°F, a considerable chilling effect was encountered. Consequently, initial efforts to extrude the bar were unsuccessful. Heat transfer studies and measurements showed that in order for the preform to be in the proper ausforming range at the moment of extrusion, the part would have to be placed into the die at a much higher temperature. After a series of experimental extrusions utilizing different preform temperatures, and taking into account the slight amount of adiabatic heating due to the extrusion process, it was found that the preform could be transferred directly from the austenitizing furnace to the extrusion press. The transfer time was controlled, and at the time the billet was placed into the die it was measured by infrared pyrometry to be within 1700°-1800°F. With the additional dwell time in the die the actual temperature at the moment of extrusion was estimated to be between 1200°-1300°F.

A second problem was occasioned by the physical setup of the extrusion process. Since immediate oil-quenching was required, it was decided to have the extruded part fall directly (propelled is perhaps the more correct term) into the quenching tank. The configuration of the press fortunately permitted the placement of an oil reservoir beneath the extrusion die. The problem then was completely extruding the bar through and free of the
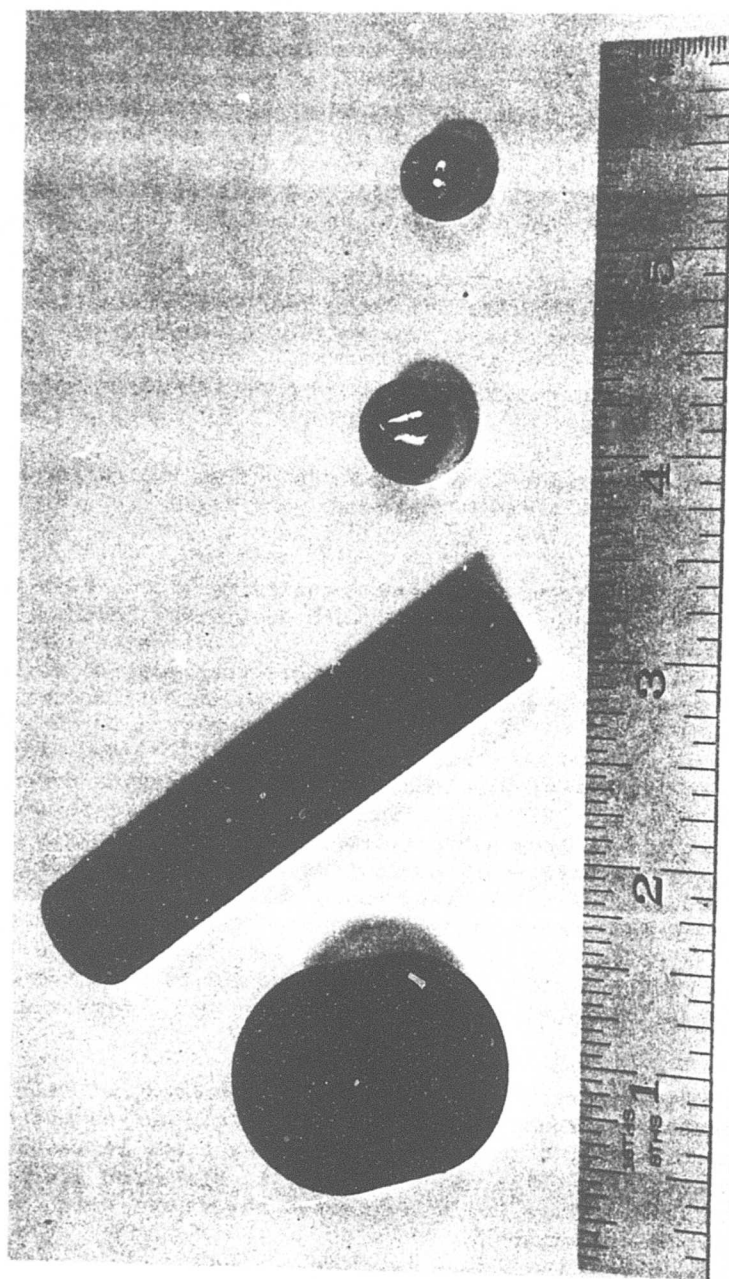
Figure 15. Ball Forging Sequence

45

die. Since the punch has a larger diameter than the throat of the die and since the total travel of the punch was limited, it was necessary to introduce a "pusher" bar into the system. Various materials were tried, with the most satisfactory being a graphite block having the same diameter as the preform. To accommodate this, the upper end of the extrusion die was lengthened. This system worked extremely well, and sufficient bar stock was extruded to produce all of the 300+ balls required for this program.

The above described process is quite repeatable. This was demonstrated when the entire set of ausformed balls had to be reforged because the initial set had been ground undersize by the ball vendor during the final lapping operation.

Metallurgical Evaluation

Comprehensive metallurgical evaluations were preformed on the ausformed rings and balls. The specific items of interest were grain flow, microstructure and hardness.

Initially all of the parts were visually and magnetic particle (MPI) inspected to remove those with obvious defects such as cracks, folds, forging laps, etc. Several extruded bars were removed by this method primarily due to forging laps. Rockwell hardness measurements were made on all of the parts. Only parts having the restricted hardness range of Rockwell C 62-64 were accepted.

Eighteen outer ring forgings were produced, all of which met the dimensional and hardness requirements. Fifty-five inner ring forgings were made, consisting of 27 short and 28 long parts (corresponding to the plain and puller groove inner ring halves). Six parts from each batch were used for metallographic and grain flow studies, and from the remaining number, 18 of each met the required dimensional and hardness tolerances. This is documented in Tables 2, 3 and 4. If the hardness range had been the normal Rc 60-64, all of the parts would have been acceptable, as the only cause for rejection was the fact that several forgings had a hardness range of Rc 61-62.

Approximately 174 inches of extruded ball stock was achieved, of which approximately 120 inches was sound. Rejection was mainly on the basis of having to remove approximately 1 to 1.5 inches from each bar representing the tail end of the extrusion which had a tendency to flare and crack, as well as rejecting several bars due to excessive curvature, which precluded further machining operations.

Micro-hardness surveys and grain flow examinations were made in the critical raceway sections of the inner and outer rings. Typical hardness results are shown in Figures 16, 17 and 18. The desired grain flow was achieved as shown in Figure 19. Metallographic examinations were conducted
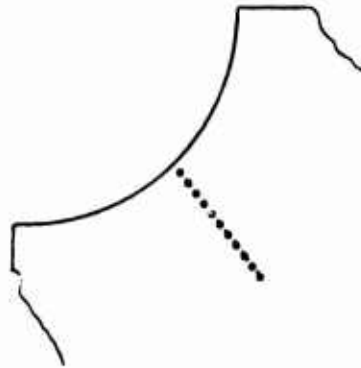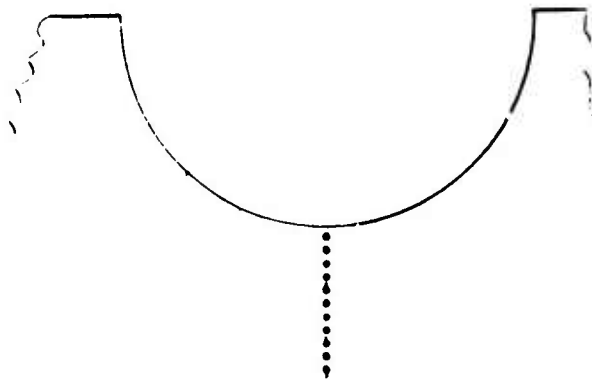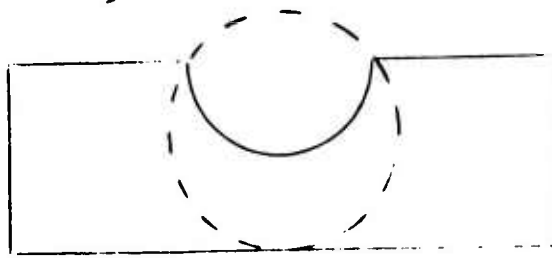
Depth Below Surface (in.)	Hardness Rc
.002	64.0
.005	64.0
.008	64.0
.0115	64.5
.0145	64.0
.018	64.0
.0205	64.0
.024	64.0
.028	64.0
.033	64.0
.040	64.0
.070	64.0

Figure 16. Hardness Survey 35MM Inner Race
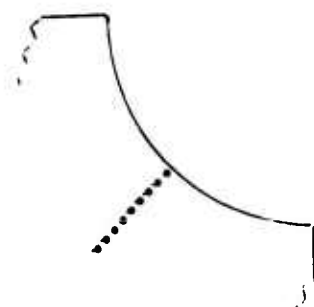
Depth Below Surface (in.)	Hardness Rc
.002	64.0
.0045	64.0
.0075	64.0
.011	64.0
.0135	64.5
.017	64.0
.020	64.5
.022	64.0
.025	64.0
.040	64.0

Figure 17. Hardness Survey 35MM Inner Race "Puller" Groove

Depth Below Surface (in.)	Hardness Rc
.002	64.5
.0045	64.5
.0065	64.5
.0095	64.5
.0125	64.5
.0155	64.5
.0185	64.5
.023	64.5
.026	64.5

Figure 18. Hardness Survey 35MM Outer Race
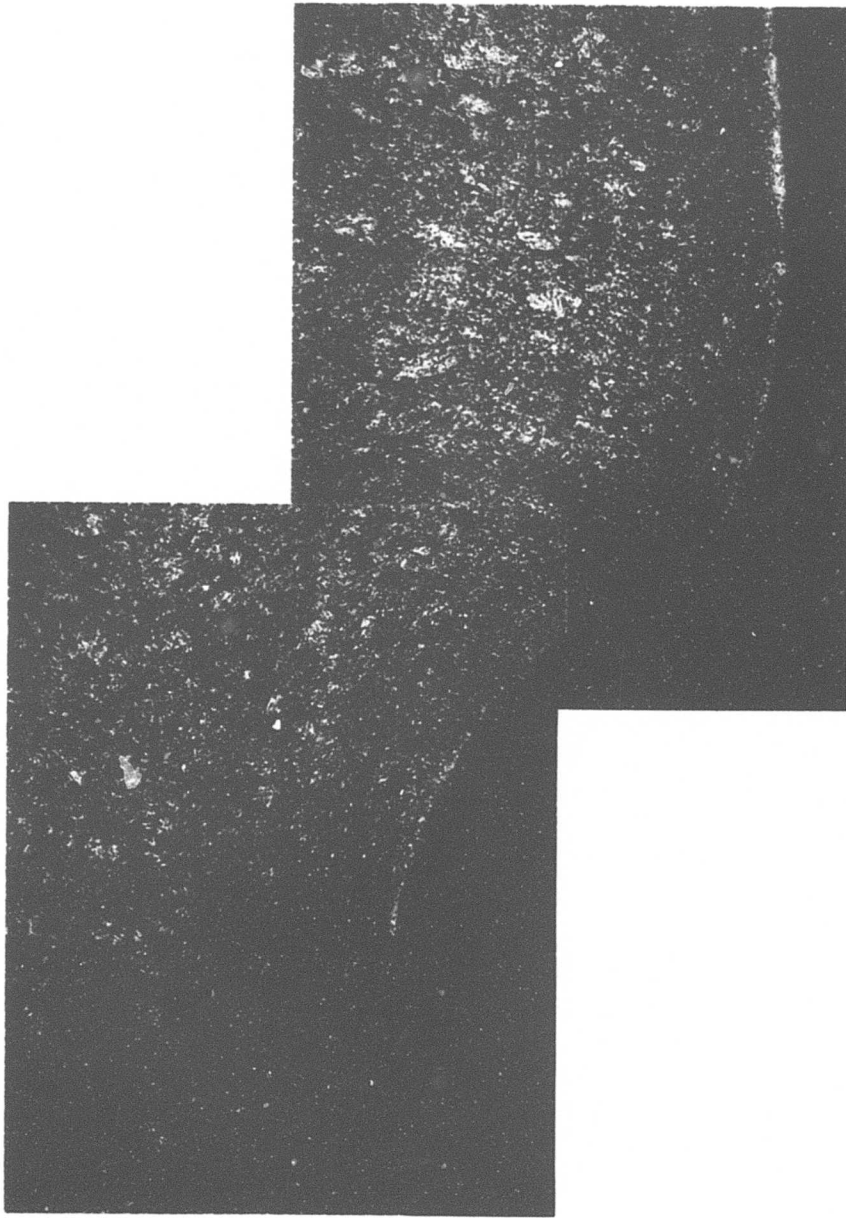
Etchant: 5% Nital   50X

Figure 19. Grain Flow Orientation in As-Forged 35MM Inner Ring Raceway
(Diamond-Shaped Indentations Are Vickers Hardness Surveys)

50

on the rings and balls, and typical results are presented in Figures 20 through 22.

X-ray diffraction measurements were taken on sample components to establish retained austenite content. These measurements showed the retained austenite to be below the realistic sensitivity of the test method, which indicated a retained austenite level of 0 to 2 percent.

Bearing Manufacture

Following the metallurgical and dimensional evaluation, selected forgings and ball stock were pre-processed prior to submittal to the bearing manufacturer for final processing.

The inner ring forgings were trepanned as shown in Figure 23. This operation was critical in that close concentricity had to be maintained between the bore and the as-forged raceway in order to assure a uniform (and minimum) metal removal from the ausformed raceway section during final machining. Consequently, the electrical discharge machining (EDM) circular electrode was indexed on the as-forged raceway pitch diameter. The parts were then nondestructively reinspected to check for any possible damage due to the machining operation. None was found. Figure 24 illustrates the manufacturing sequence, from the as-forged blank to the finish-machined inner ring.

It had originally been intended to make two outer rings from each forward extrusion. Since the length of the extrusions was marginal (see Table 3) and previous work had shown that optimum grain flow was limited to the center section of the extruded area,[14] it was decided to remove only one outer race segment from each extrusion. This was done by EDM and is illustrated in Figure 25. Since the as-forged extruded section was close to the final dimensions of the outer ring, no additional machining of these parts was required prior to submittal to the bearing vendor. Figure 26 illustrates the production lot of rough machined inner and outer rings prior to final machining by the bearing vendor.

The extruded bar stock was reduced to .225 inch ± .005 inch diameter ball blanks. This operation, performed by Acra-Sphere Ball & Mfg. Co., Gardena, California, consisted of a combination lathe turning and honing process.

No undue difficulties were reported by the bearing vendor in final machining the inner and outer races. An unfortunate incident occurred when the balls, being finish honed to a Grade 10 ball, were ground undersize (averaging about -.002 inch), thus making them unusable for the bearings. This necessitated a complete restart of the manufacturing cycle for this component, since insufficient bar stock remained from the original batch to complete the order. This was accomplished with outstanding cooperation from the forging source and the ball rough-machining vendor. The second
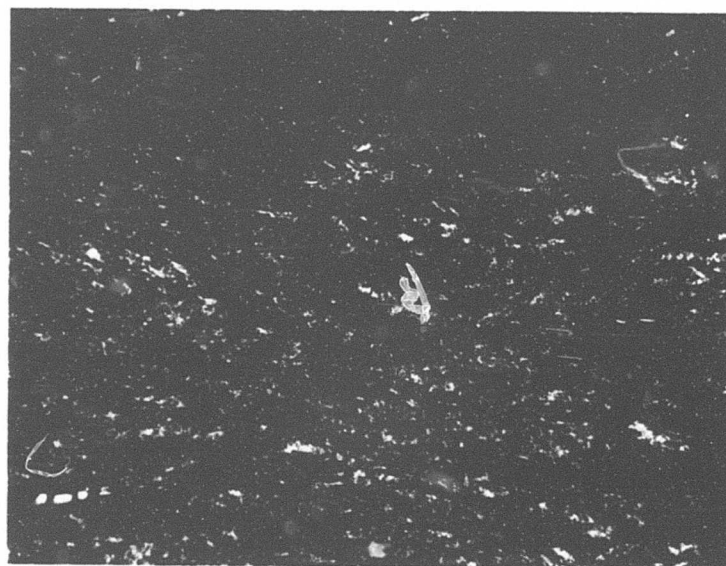
51
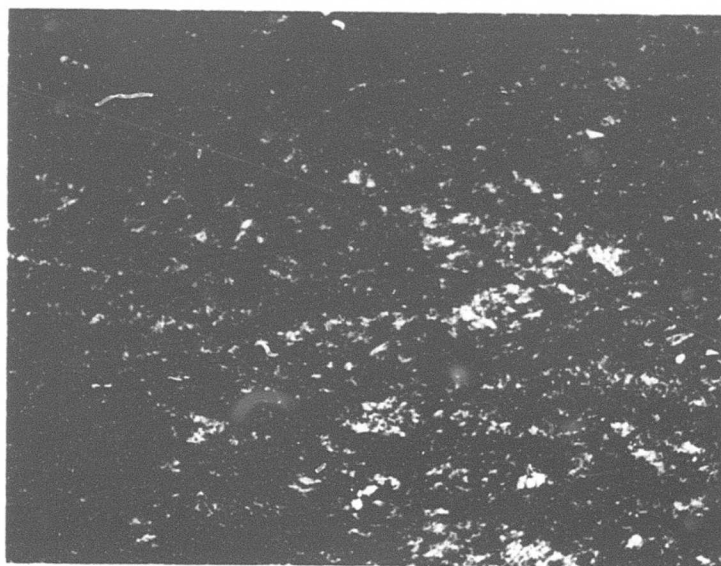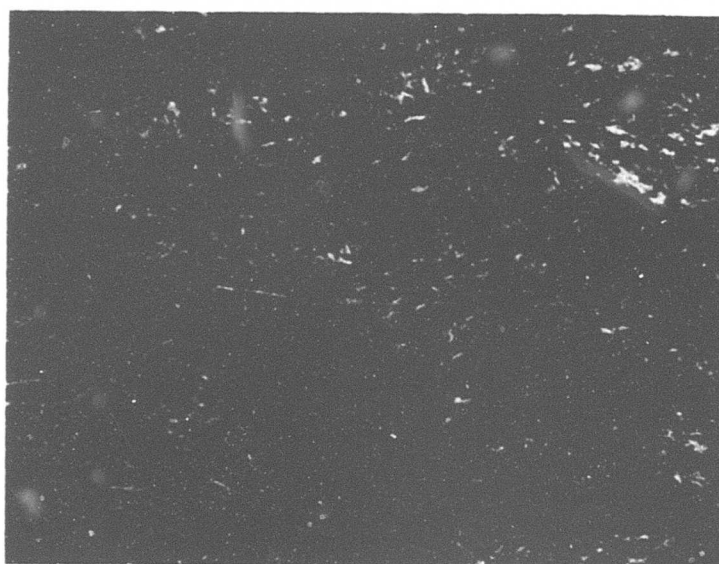
500X

1000X

Etchant: 5% Nital

Figure 20. Microstructure of Ausformed M-50 Inner Race
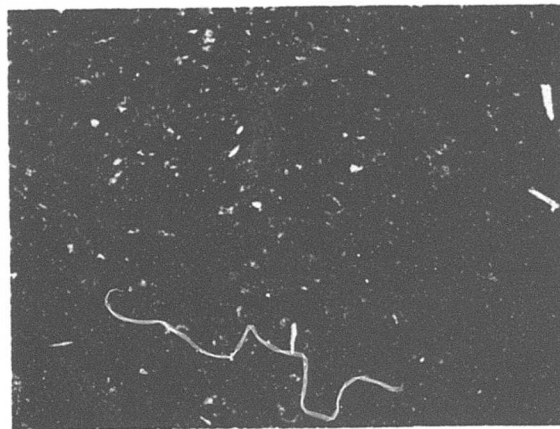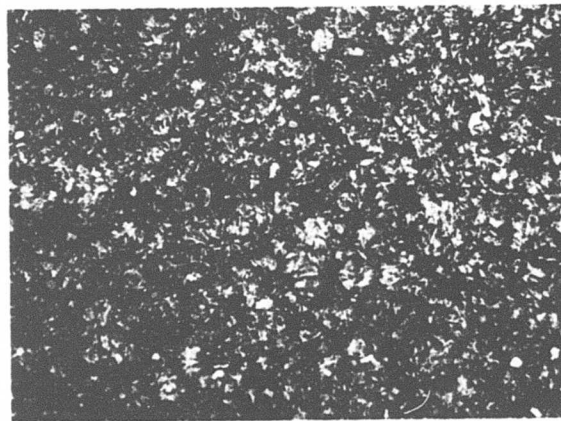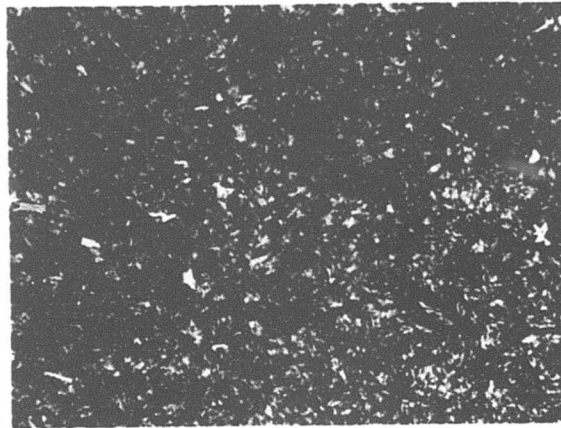
500X

1000X

Etchant: 5% Nital

Figure 21.   Microstructure of Ausformed M-50 Outer Race

53

Etchant: 5% Nital   500X

Figure 22.   Typical Microstructure of Ausformed Balls for
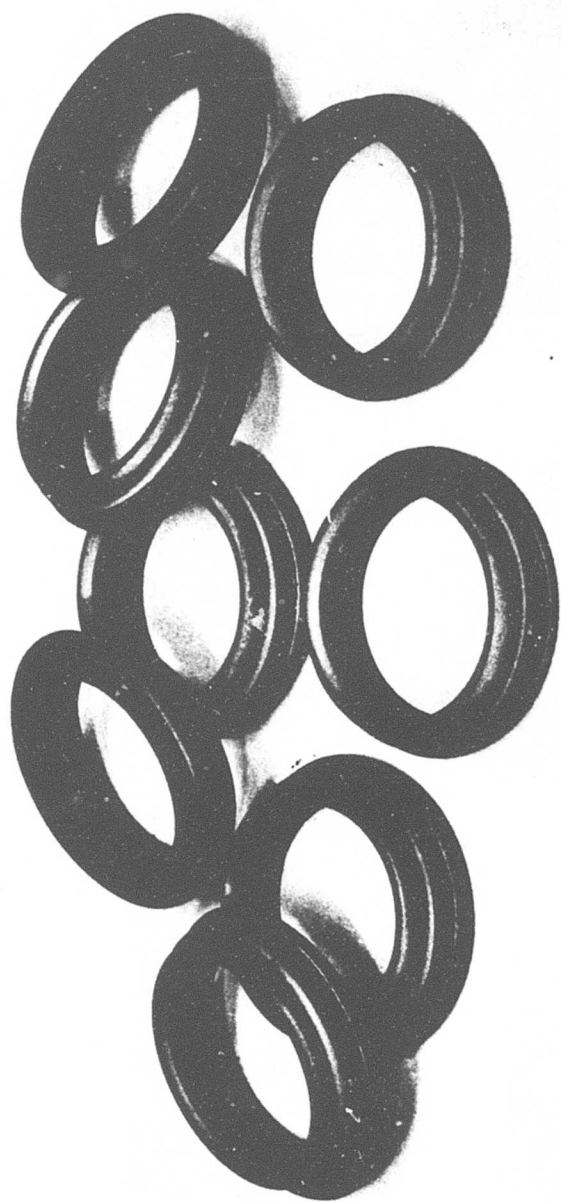   35MM Bearings

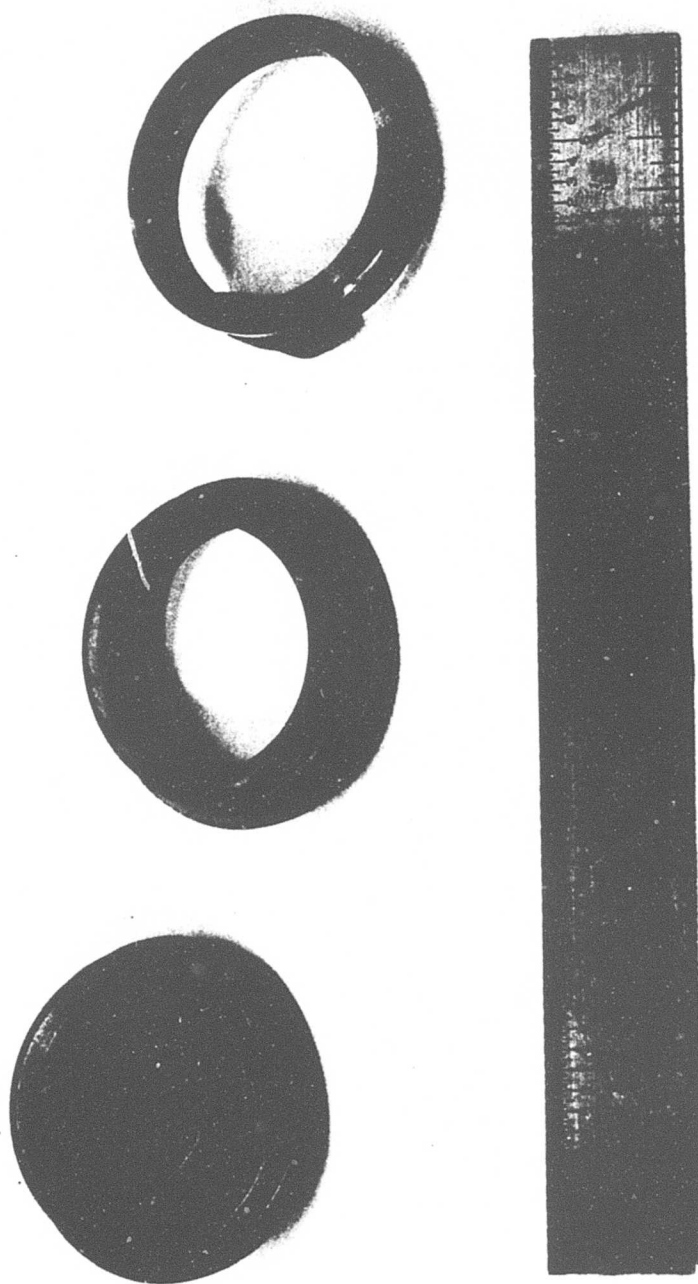Figure 23. Semifinish Machined Ausforged Inner-ring Blanks

55

Figure 24. Manufacturing Sequence for 35MM Inner Race
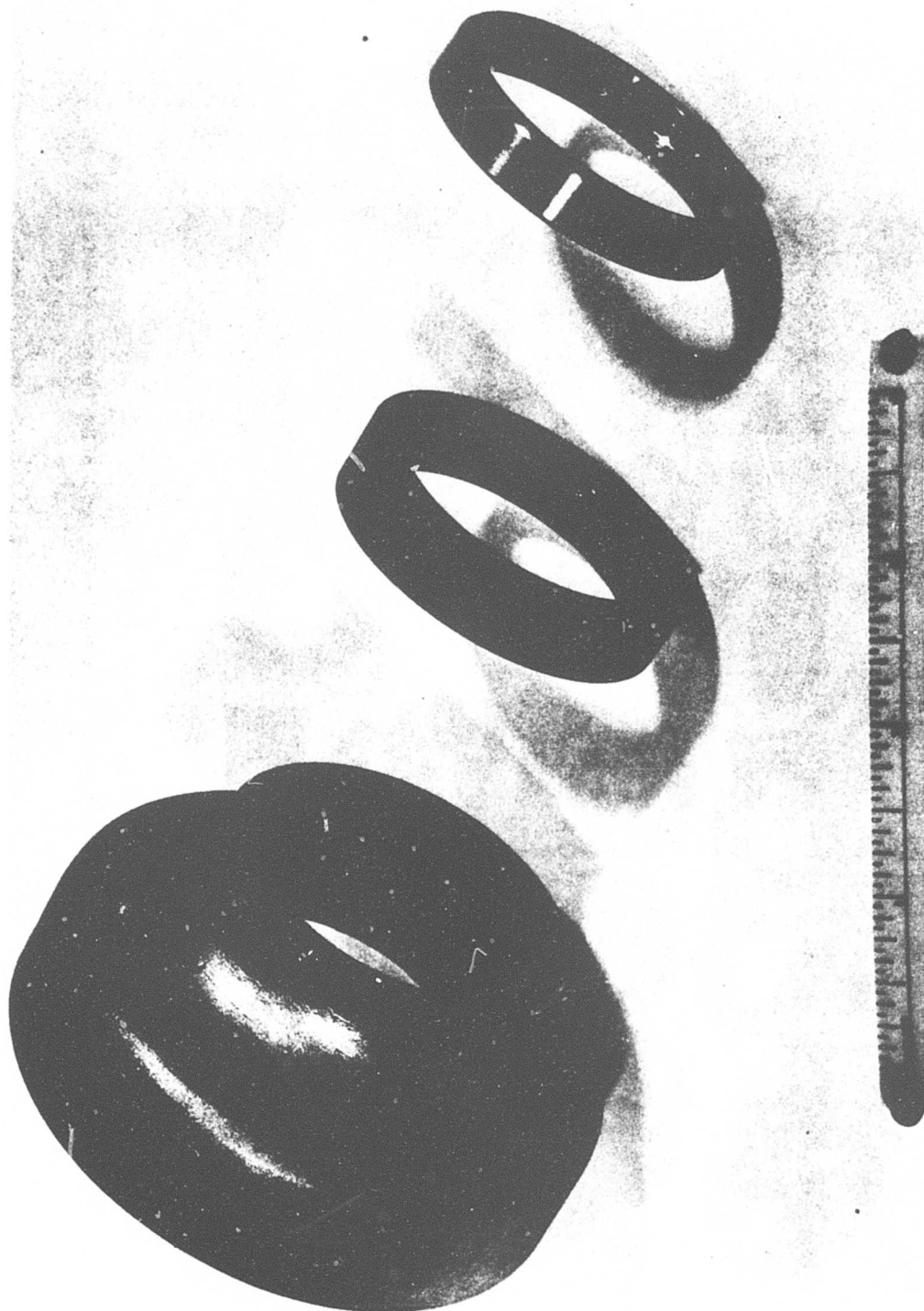From left to right: as forged, trepanned, finish machined

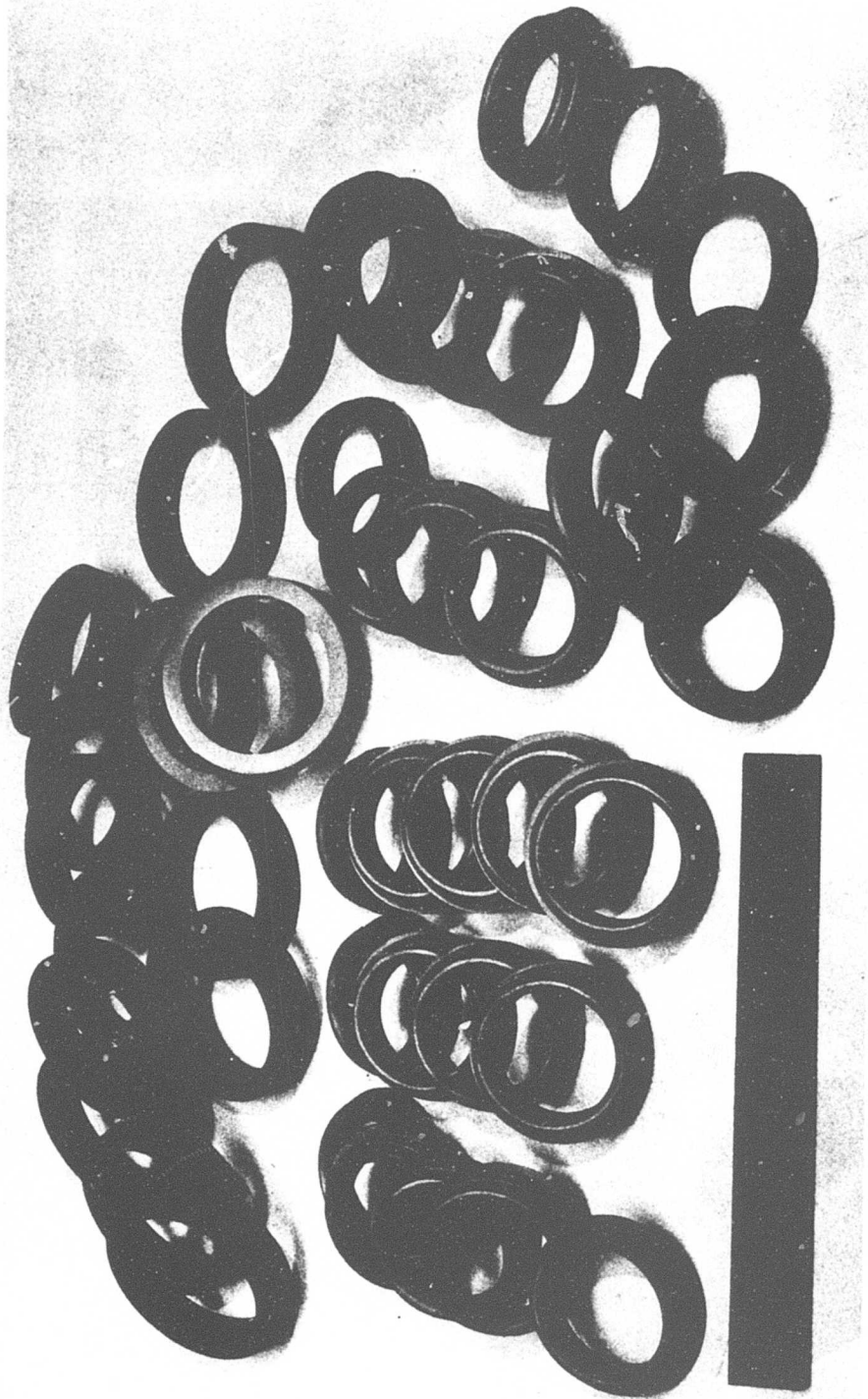Figure 25. Schematic of Manufacturing Sequence for 35MM Ausforged Outer Ring

Figure 26. Production Lot of Semifinish Machined Ausforged 35MM Inner and Outer Rings

set of balls had a hardness range from 62.5 to 63.5, excellent microstructure, and a retained austenite content of less than 2 percent.

Ten bearings were manufactured and delivered to General Electric for testing. All print dimensions were met with the exception of inner and outer width, which were as shown in Table 5. The deviation in this dimension was not considered to be critical to the planned test program. Figure 27 shows a disassembled view of one of the ausformed bearings.

TEST FACILITY

Test Facility Design

A cross section of the original test rig housing is shown in Figure 28. This was the assembly used for the initial rig checkout runs. The part numbers in the parts list (Table 6) are referenced in the following description.

The rig housing, item (1), consists of an accurately bored and lapped cylinder of nominal 5 inches diameter, into which fit the drive-end bearing housing, item (2), and a hydrostatically "floated" piston, item (4). The opposite-drive-end bearing is located within the piston by the adapter, item (3). The drive-end housing is provided with drilled oil passages supplying integral oil jets from an O.D. annulus fed by connections through the item (1) housing wall; item (2) housing is restrained from rotation by the dowel pin, item (20). O-ring seals are used to isolate supply oil to the drive-end housing O.D.

Oil supply to the opposite-drive-end bearing enters through the torque arm, item (18), which protrudes through a slot in the item (1) housing wall, allowing angular motion of the piston. Drilled oil passages in the adapter, item (3), are similar to those in item (2), and O.D. sealing is similarly by O-ring. Oil jet sizing initially was 3/64 inch diameter (.0469), two jets per bearing, as shown. Face slots and transfer holes are provided in items (2) and (3) to allow oil drainage and venting from bearing outboard sides to the center sump, from which all oil is scavenged through a single port.

The piston/cylinder clearance as manufactured was .0015/.0025 inch (on diameter). The housing (cylinder) bore was subsequently honed and the mating pair "lapped-in" to provide a satisfactory fit.

The shaft, item (6), supports the two 35mm (bore) test bearings on a common diameter, separated by a sleeve, item (8), the stack being clamped by the nut, item (11). The shaft driven-end protrudes through a labyrinth seal, item (10), and contains two 1/8 inch-diameter pins engaging slots in the driving spindle, item (9). The spindle is centered in a bore in the shaft with a light interference fit.
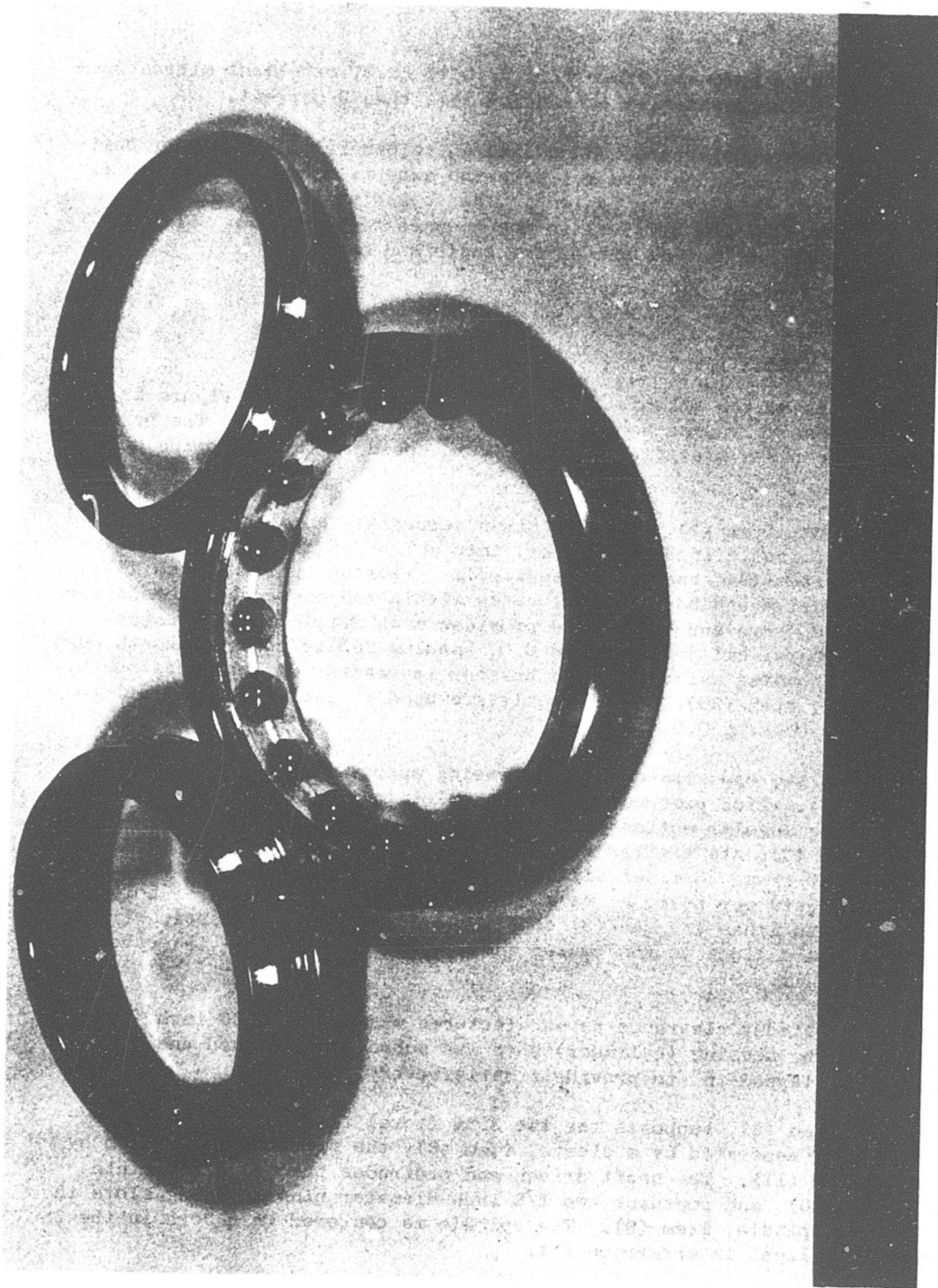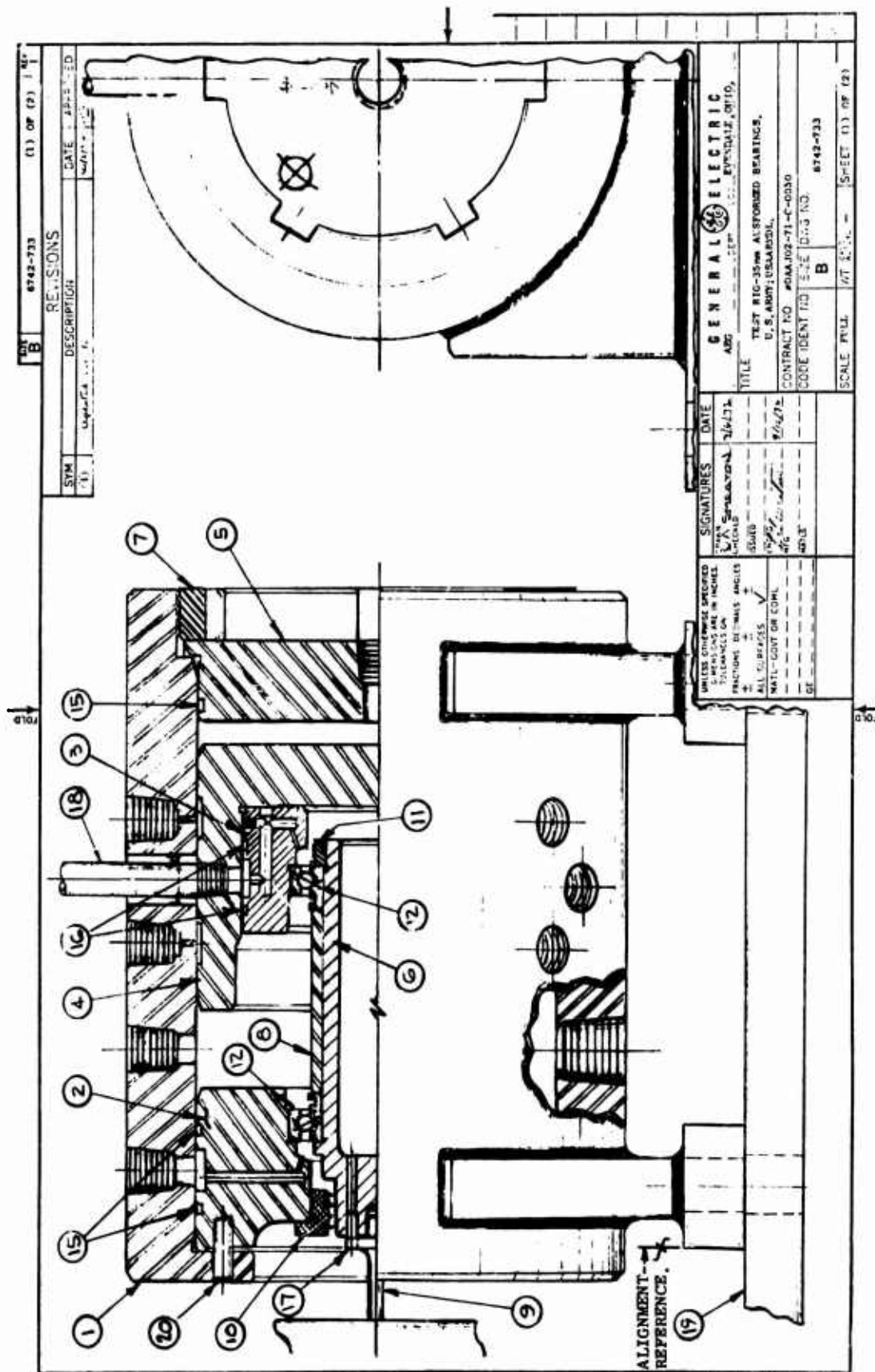
Figure 27. 35MM Ausforged Bearing

Figure 28. Cross Section of Original 35MM High-Speed Ball Bearing Tester

TABLE 5

PRINT DEVIATIONS ON 35MM AUSFORMED BEARINGS

Serial Number	Inner Width	Outer Width
Print Range	.5512 - .5462	.3937 - .3887
MDA E0001	.5497	.3912
MDA E0002	.5442	.3892
MDA E0003	.5232	.3897
MDA E0004	.5297	.3897
MDA E0005	.5307	.3895
MDA E0006	.5282	.3929
MDA E0007	.5252	.3897
MDA E0008	.5217	.3902
MDA E0009	.5307	.3897
MDA E0010	.5312	.3899

TABLE 6

MAJOR PARTS LIST - 35MM HIGH-SPEED BEARING TESTER

Part List

Pt.	Description	Dwg. No.
1	Housing, Test Rig	6742-739
2	Housing, Bearing	6742-740
3	Adapter, Bearing	6742-741
4	Load Piston	6742-742
5	Cover Plate	6742-743
6	Shaft	6742-790
7	Ring Nut	6742-745
8	Oil Jet Assembly	6742-792
9	Drive Spindle	6742-735
10	Labyrinth Seal	6742-747
11	Locknut	6742-791
12	Bearing, Ball, 35mm	6742-806
13	Bearing Sleeve	6742-807P02
14	Bearing Sleeve	6742-807P01
15	"O" Ring, Parker #2-156, 4.237ID X .103" W Parker Compound #77-545	
16	"O" Ring, Parker #2-42, 3.239ID X .070" W Parker Compound #77-545	
17	Dowel Pin (Rollpin) .125" Dia X .500" Lg.	
18	Torque Arm, 1/8" Sch. 40 Pipe, 8" Lg. NPT Both Ends	
19	Baseplate Assembly	6742-749
20	Dowel Pin .250" Dia X .750" Lg.	

Axial load is applied to the test assembly by either of two methods. The assembly shown is provided with an O-ring sealed cover plate, item (5), which allows pressurizing of the cavity between cover plate and piston with lube oil; leakage flow past the piston perimeter is scavenged from the annulus in the housing wall at piston mid-length. The second load method utilizes a spring loading assembly mounted in a plate interchangeable with item (5); a single die spring of 640 lb. maximum (solid) capability, 480 lb/in rate, is used and is calibrated prior to use.

The hydraulic load system is used when measurement of bearing torque output is required, since the piston is then free floating. Hydrostatic pads are milled into the outside diameter of the piston in two patterns of four, equally spaced circumferentially; pressurizing oil is applied through penetration in the stationary housing wall adjacent to each pad, while orifices and valves at each entry allow manual adjustment of oil flow until optimum piston "float" is achieved. Lube oil from the common system is used for pad pressurization so that oil leakage past the piston into the test bearing sump does not contaminate the test oil.

The mechanical (spring) load system is used for fatigue test runs of long duration and was the method used for all tests described in this report.

Material used for all rig components except baseplate, spring load system and drive spindle was AISI 4340. The shaft was heat treated to 33-38 Rc; other parts were heat treated to 28-32 Rc. Sump internal parts were black oxide coated for corrosion resistance. The drive spindle was AISI C1050.

The test oil system provides 3.0 gpm, maximum, to a 100-psi header, with bypass heat exchange returning spill to the reservoir. Full-flow 10-micron filtration is provided for bearing and pressurizing oil. A 2/1 scavenge ratio is maintained for "dry sump" operation.

The rig is driven through a 3/16-inch-diameter spindle which provides a flexible connection to the power source, a 2-inch Barbour-Stockwell Company air turbine, special model 1500, rated 10 HP at 65,000 RPM on 90 psia, 75°F air with atmospheric exhaust. The manufacturer's performance curve for this turbine is shown in Figure 29. The turbine is oil mist lubricated by a package unit mounted on the test frame.

Assembly of the rig is a bench operation, with the shaft, bearings, housing adapter and piston being preassembled and inserted into the cylindrical housing through the uncovered opposite drive end. Alignment between turbine and rig assembly is established upon each reassembly by use of a butt-plate dowelled to the common baseplate; a reference surface (see Figure 28) on the rig housing mates with a ground surface on the butt-plate. The butt-plate reference surface was initially located by taking indicator runout readings between the test shaft and the turbine shaft extension.
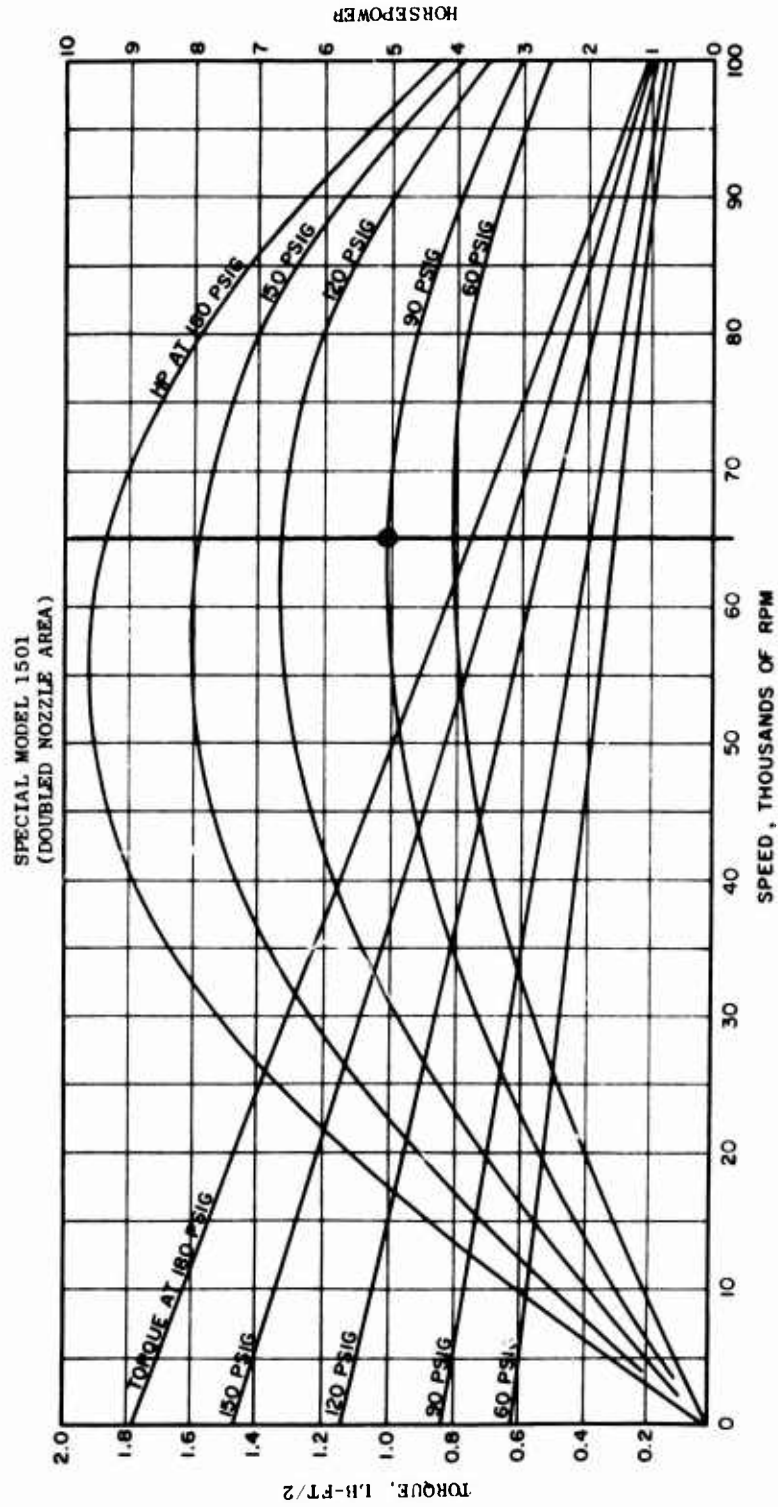
Figure 29. Barbour Stockwell 2 Inch Turbine Performance on Air at 75°F With Atmospheric Exhaust Total Nozzle Cross Sectional Area. 200 Sq. In.

65

Turbine speed control originates with a six-impulse/rev magnetic pickup mounted on the turbine. The pickup signal is amplified and rectified to a D.C. voltage linear with shaft speed; the D.C. signal is applied to the bridge circuit of an electropneumatic controller which controls turbine air supply by pneumatic valve. A manually operated bypass valve allows initial setting of turbine speed. The D.C. signal is also applied to a D.C. volt meter with high and low trip to allow adjustable overspeed and underspeed shutdown of the facility.

Emergency shutdown of the facility is effected by interruption of any unit in a series circuit through the following devices:

a) Pressure switch on test rig oil supply.

b) Pressure switch on turbine air supply.

c) Pressure switch on turbine oil-mist unit air supply.

d) Trip switch activated by vibration meter.

e) Oil-level-actuated float switch in turbine mist unit oil reservoir.

f) High-temperature trip switch on bearing O.R. temperature recorder.

g) Turbine overspeed/underspeed trips (on D.C. volt meter).

h) Chip detector in rig oil scavenge line.

Test bearing outer-race temperatures are determined by Chromel/Alumel thermocouples held against the outer-race exposed faces in the sumps by spring clips. Thermocouple leads are pulled through an access hole in the drive end bearing housing, item (2). Two thermocouples are used for each bearing.

In practice, the turbine required 75-80 psi air to maintain a test shaft speed of 65,000 RPM with the bearings under axial test load of 500 lb. Since the required airflow is close to the maximum available from the 90 psi supply header, deterioration of the test bearings usually resulted in shutdown of the facility via underspeed trip in the control circuit prior to serious damage to the facility. The underspeed trip proved to be more sensitive than vib pickup in this respect, while turbine air demand provided a good indication of test bearing deterioration via increase in power loss.

Test Facility Checkout

The contractually required test conditions, i.e., shaft speed of 65,000 RPM and bearing axial load of 500 lb, were achieved for 15 hours total running time during which period all emergency shutdown systems described above were activated and found to perform properly.

Because of the limited number of bearings available for the baseline tests, slave bearings having the same dimensional envelopes as the test bearings were utilized for these tests.

Test Rig Modifications

As reported in the checkout and baseline bearing test summary (Table 1), various modifications were undertaken to limit an apparent nonuniform temperature distribution in the test bearings. Figure 30 is a cross section of the modified rig assembly, with under-race oil supply into the shaft, and other changes as listed in order of implementation.

a) Shaft redesign: Early disassemblies of the rig for interim inspection proved to be difficult due to the necessity of pulling the separating sleeve (item 8 in Figure 30) and the shoulder-end bearing off of the full-length interference fit; this resulted in cumulative galling damage to the bearing fit surfaces. The 6742-744 shaft (Figure 31) was redesigned to eliminate the sleeve. The 6742-790 shaft (Figure 32) was used for tests following the rig checkout runs, up to test #25 (see Table 1).

b) Additional oil jets: These were added to supply oil to the sump sides of the test bearings. One pair of the two added is shown in the cross section. Additional oil passages drilled into the opposite-drive-end bearing adapter, item (3), provide the oil supply; oil delivery is through 1/8-inch-diameter tubing, plug welded and drilled at the ends to provide jet sizing. Similar tube jets were added to the drive-end side of the drive-end bearing to make jet exit positions identical for both bearings. Simultaneously, all jets were plug welded and resized to .030 inch diameter (from .0469 inch diameter) to allow increase of supply pressure to 40 psig with resultant higher jet velocity. Theoretical flow of MIL-L-7808 oil at 75°F and Δp of 40 psi is 0.84 lb/min per jet, using a flow coefficient of 0.65.

Coincident with the above, the test bearing O.D. supports were changed to provide "soft" mountings to alleviate transient thermal expansion effects which could result in changes to bearing internal radial clearances during startup, prior to temperature stabilization of the rig.

The thin-wall cylinders (item 14, sleeves) were added by press fit into the item (2) housing and item (3) adapter. Nominal sleeve wall thickness is .10 inch.

c) Under-race cooling: The assembly of Figure 30 incorporates the redesigned shaft 6742-853 of Figure 33, used to introduce under-race cooling for the bearings of test #27 and thereafter. Separate 1/8-inch tubing jets were provided to separately supply the bearings,
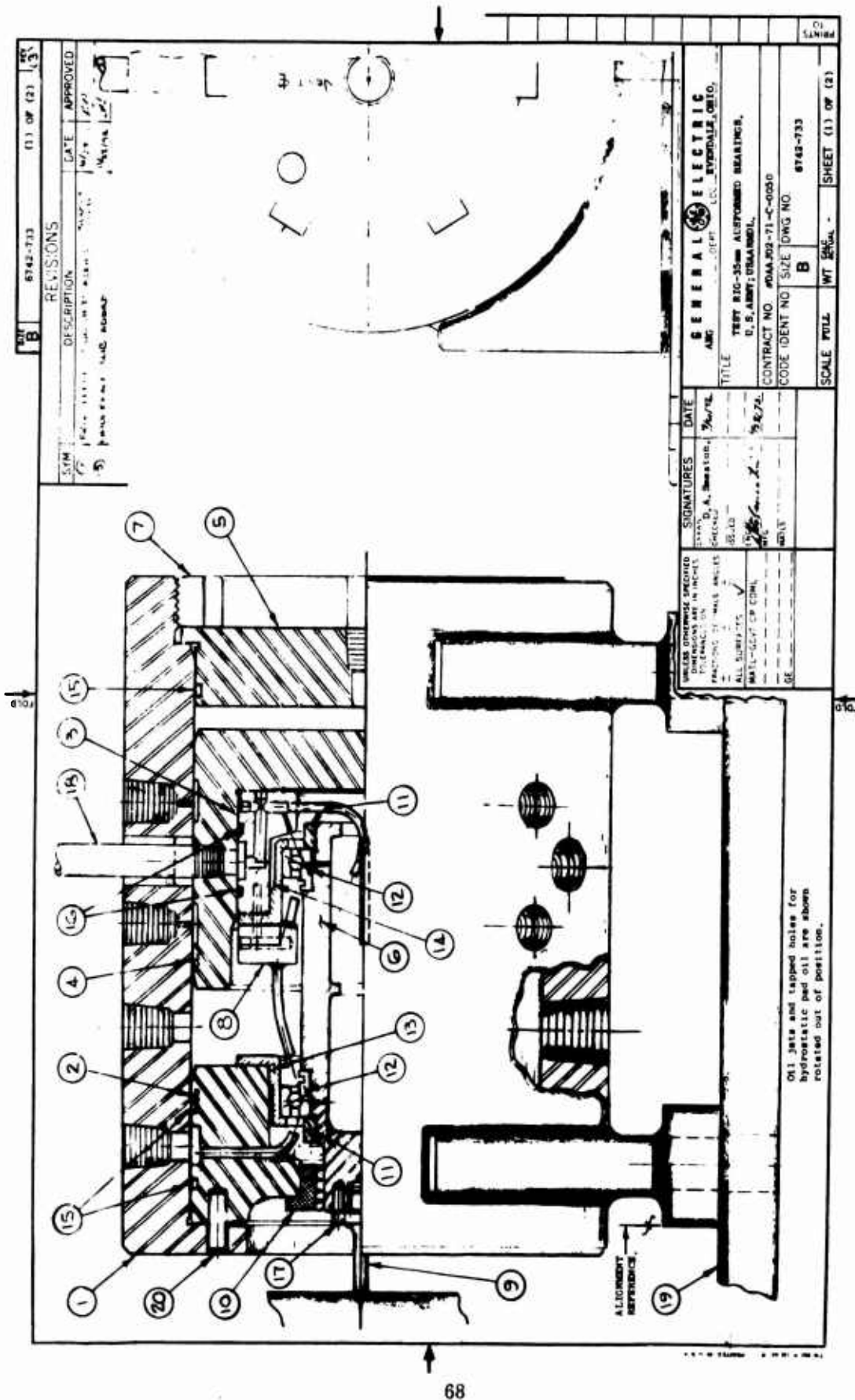
67

Figure 30. Modified High-Speed 35MM Bearing Tester

Figure 31. Drive Shaft — 35MM High-Speed Bearing Tester

69

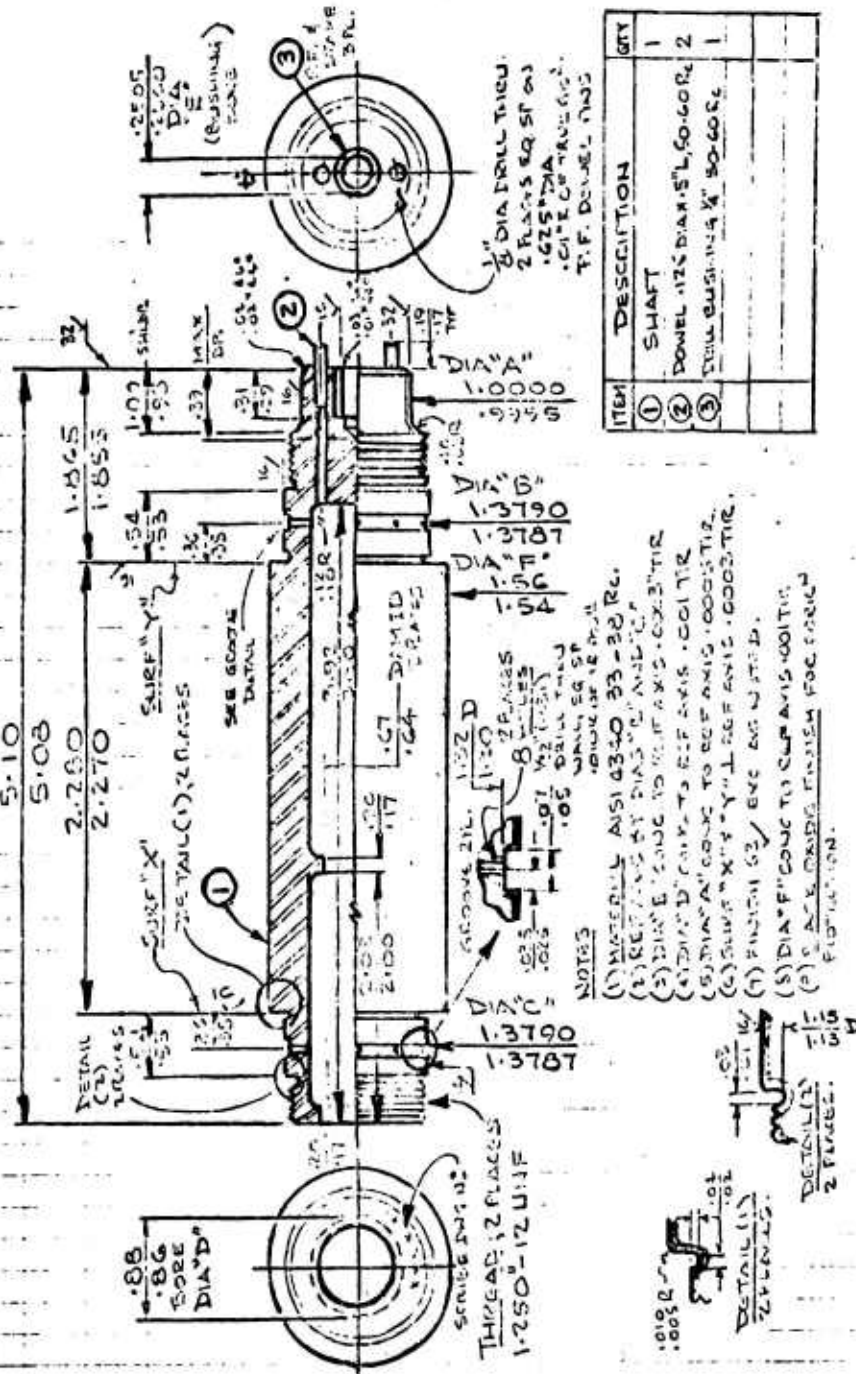Figure 32. First Modification to Drive Shaft - 35MM High-Speed Bearing Tester

Figure 33. Second Modification Drive Shaft - 35MM High-Speed Bearing Tester

71

oil separation in the bore being effected by a dam. The tubes were
brazed into drilled passages in the item (3) adapter, as shown.
Eight .032-inch-diameter feed holes to a supply annulus under each
bearing inner race split line were provided in the shaft. Metering
normally takes place in the oil transfer slots in the bearing inner
ring split faces; hence oil supply to the shaft bore is maintained
in excess to produce constant spillover of the lip at the shaft
opposite drive end. The dam allows metering of oil inlet, through
supply limitation, as an alternative.

Coincident with the above, a hardened bushing was added to the
spindle-fit in the shaft end, as shown, to alleviate wear; a similar
bushing was added to the turbine shaft at the spindle end to ensure
continuous close-clearance fit and support of the spindle mid-length;
replacement spindles were hardened at wear points by heat treatment.

TEST CONDITIONS AND TEST RESULTS

The standard practice when running bearing fatigue tests is to run at over-
load conditions to reduce running time. The loads were selected based on pre-
vious testing on the NASA program,[2] and testing accomplished on CF6 and
F101 main engine bearings.

Based on the life and stresses calculated by the Bearing Design Technology
Computer program RECAP3 and a comparison to AFBMA predicted life, the fol-
lowing test conditions were established:

Bearing Load	=	500 lb
Shaft Speed	=	65,000 RPM
Oil-In Temperature	=	160°-180°F
Effective Contact Angle	=	16.8°
Outer-Race Hertz Stress (S_{max}) =		301,000 PSI
Inner-Race Hertz Stress (S_{max}) =		297,000 PSI
Computer Calculated Life (B_{10}) =		6.7 Hr (26.3 x 10^6 revolutions)
AFBMA Calculated Life (B_{10})	=	5.4 Hr (21.1 x 10^6 revolutions)

The difference in AFBMA and computer life calculations is due to the approx-
imations used in the AFBMA method. The computer life is considered the
more accurate, but the AFBMA life is normally quoted to provide a common
base to parties who would not have access to the computer results.

In a previous section, the problem of operating the test bearings was out-
lined. Table 1 presents a chronological tabulation of shakedown testing
to obtain proper operation.

Table 7 presents the endurance test results for the control, or baseline, and the ausformed bearings. Four control bearings and ten ausformed bearings were tested. Two bearings in the ausformed group are not considered as legitimate fatigue failures (S/N 0007 and 0008). Bearing S/N 0008 appeared to fail due to overheating and caused sufficient damage to S/N 0007 to preclude additional running. The rig was running unattended when the failure occurred, and shutdown was due to overtorque. No evidence was found in the control system to indicate oil loss, but the possibility of oil interruption due to under-race cooling passage blockage exists. No fatigue was evident, and the failure is not included in the following statistical analysis.

The test results in Table 7 are presented graphically in Figure 34 and Figure 35 using the statistical techniques developed by Weibull.[17] In calculating the two curves, the suspended tests are included using the industry-wide accepted practice per Reference 18. The two curves are combined in Figure 36, which illustrates the improvement in fatigue life obtained by utilizing the ausforming process. The slight divergence in the slope of the two curves (~.7 for the standard bearing versus ~1 for the ausformed) is typical, having been observed in all of the previous ausformed bearing test programs. The steeper slope is indicative of less scatter and effectively indicates a more homogeneous material. The elimination or attenuation by ausforming of some of the more massive carbide particles and/or agglomeration normally found in M-50 is believed to be mainly responsible for this apparent higher level of homogeneity.

Admittedly, the number of tests performed is minimal in terms of the usual bearing test programs. Yet it is encouraging to note the directional trend of the data that was generated; more importantly, it can be reinforced by previous test results on similar size bearings. This will be discussed in greater detail in the ensuing discussion section of this report.

35MM BEARING FAILURE EVALUATION

One of the more frustrating problems in the testing of ultrahigh-speed small bore bearings, is the fact that despite the most sensitive failure detection control, termination of the test upon failure is rarely rapid enough to prevent a relatively massive failure propagation. This problem was compounded in the present case by the recognized marginality of the cage. Consequently, only a few of the failures, either standard or ausformed bearing, were as "clean" as would ideally be desirable. Nevertheless, failure initiation (and propagation) was adequately traceable to permit a valid engineering evaluation. In Figure 37 through Figure 45, typical examples of failed and unfailed bearings are presented. In all but one case (S/N MDA 0009) the initial fatigue failure was on the inner race, with subsequent and probably immediate ball and cage distress. In S/N MDA 0009, fatigue failure initiation was at the outer raceway, again followed closely by ball and cage failure. The photographs are essentially self-explanatory. It is interesting to note that in the tester

TABLE 7

BASELINE AND AUSFORMED BEARING TEST RESULTS

Baseline Test Summary

Bearing S/N	Speed (rpm)	Load (lb)	Total Time (hr)	Remarks
20	65,000	500	371.0	Suspended
21	65,000	500	30.5	Failed
22	65,000	500	180.6	Failed
23	65,000	500	521.1	Failed

Ausformed Bearing Test Summary

Bearing S/N	Speed (rpm)	Load (lb)	Total Time (hr)	Remarks
0001	65,000	500	373.1	Suspended
0002	65,000	500	373.1	Failed
0003	65,000	500	482.0	Suspended
0004	65,000	500	482.0	Failed
0005	65,000	500	500.0	Suspended
0006	65,000	500	500.0	Suspended
0007	65,000	500	34.1	Suspended*
0008	65,000	500	34.1	Failed*
0009	65,000	500	92.3	Failed
0010	65,000	500	92.3	Suspended

*Overtemperature failure - no fatigue.

74

TEST CONDITIONS:
SPEED: 65,000 rpm
LOAD: 500 lb axial
LUBRICANT: MIL-L-7808
BEARING TEMP: 160°F-180°F
FAILURE INDEX: 3/4
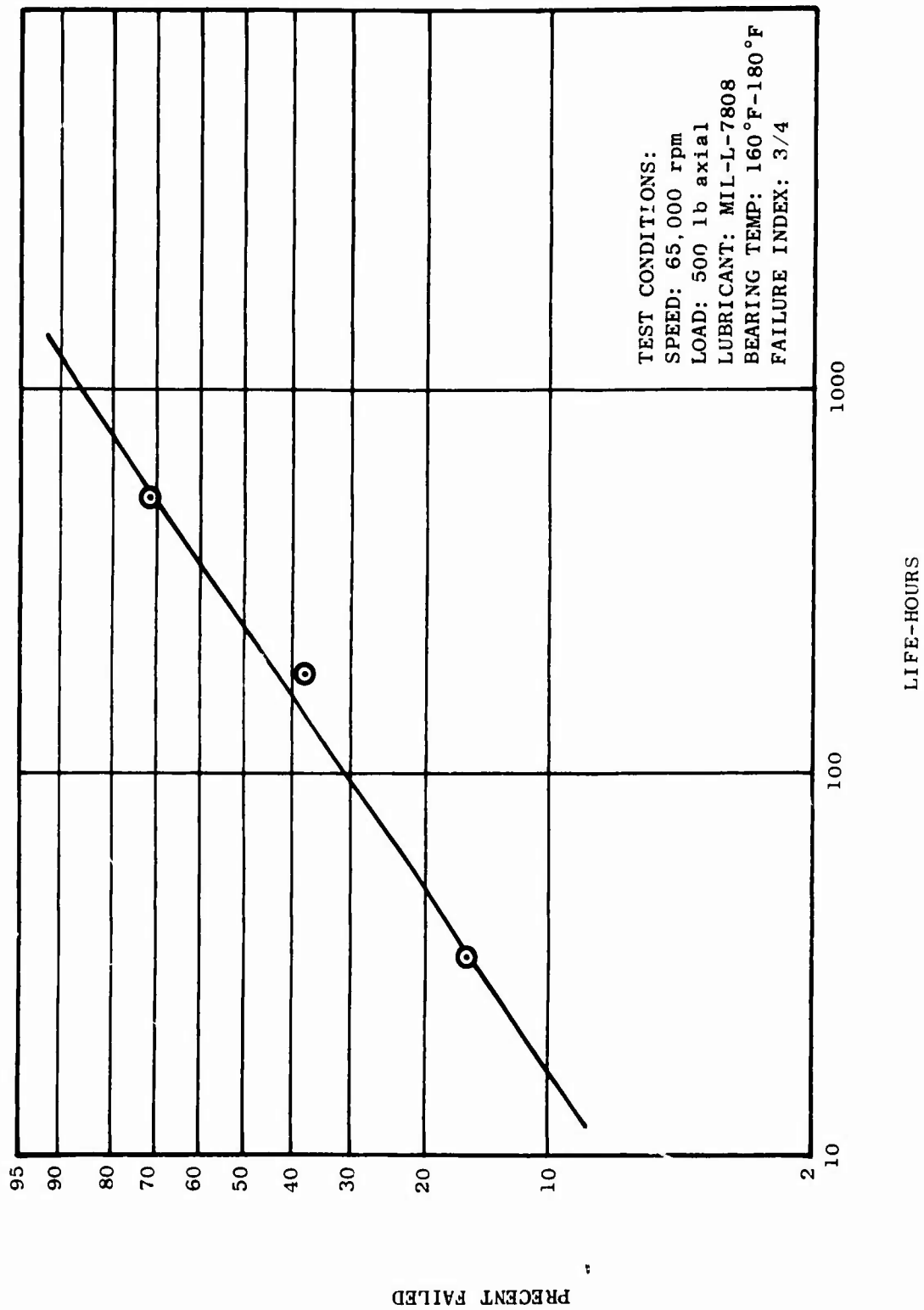
Figure 34. Life Test Results - 35MM Bore Ball Bearing
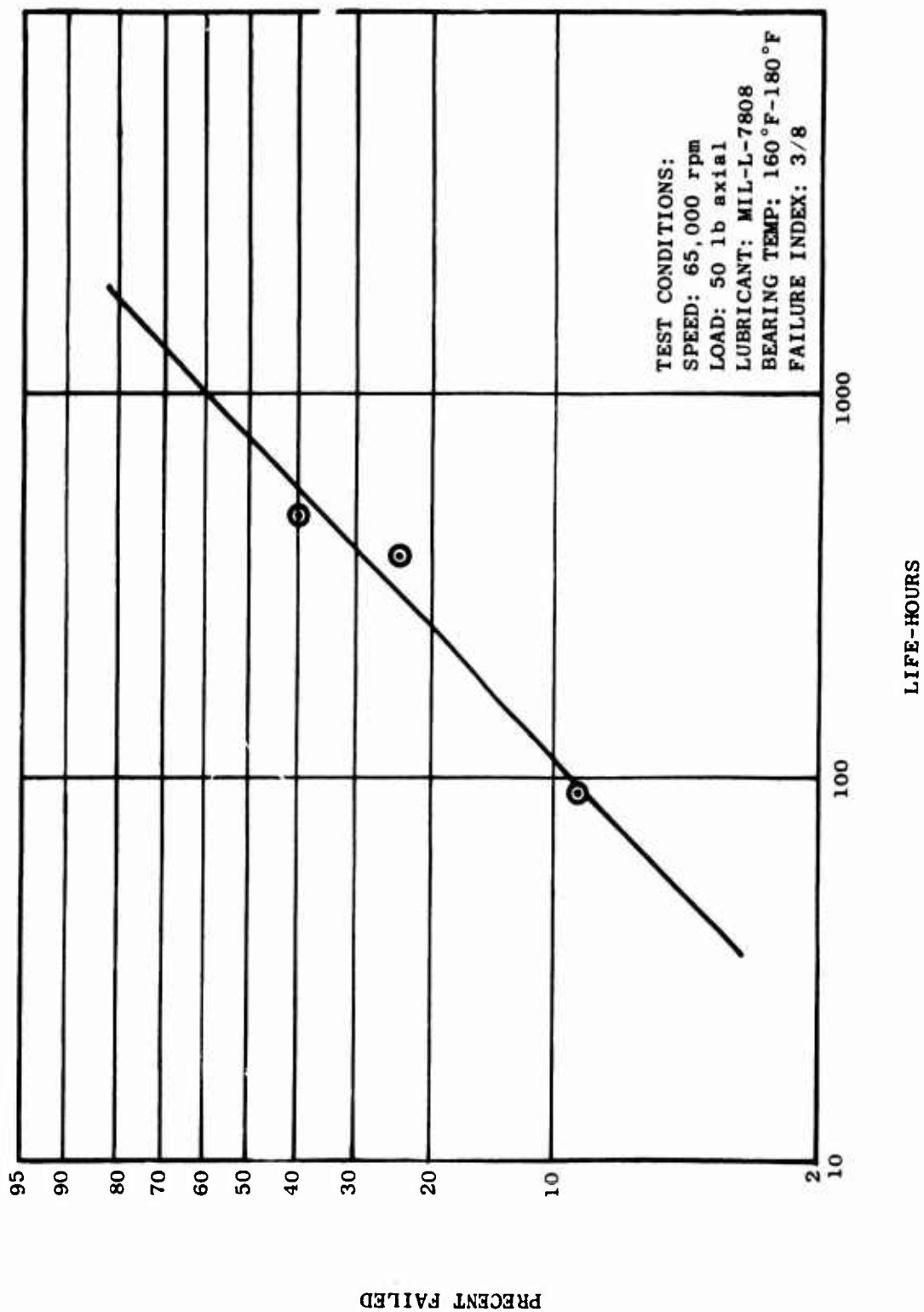
Figure 35. Life Test Results – Ausformed 35MM Bore Ball Bearing
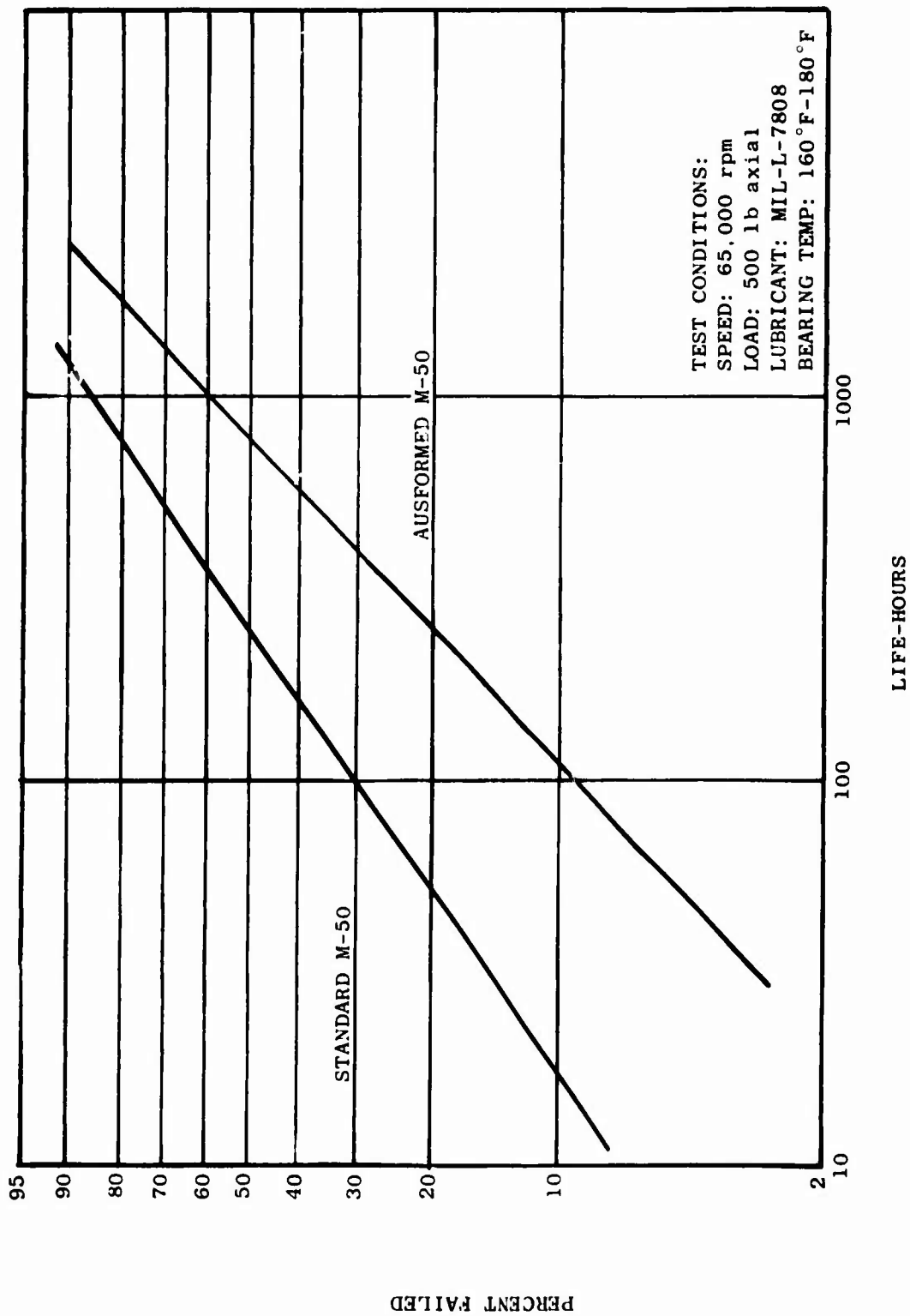
Figure 36. Life Comparison Stand – M-50 vs Ausformed 35MM Bearing
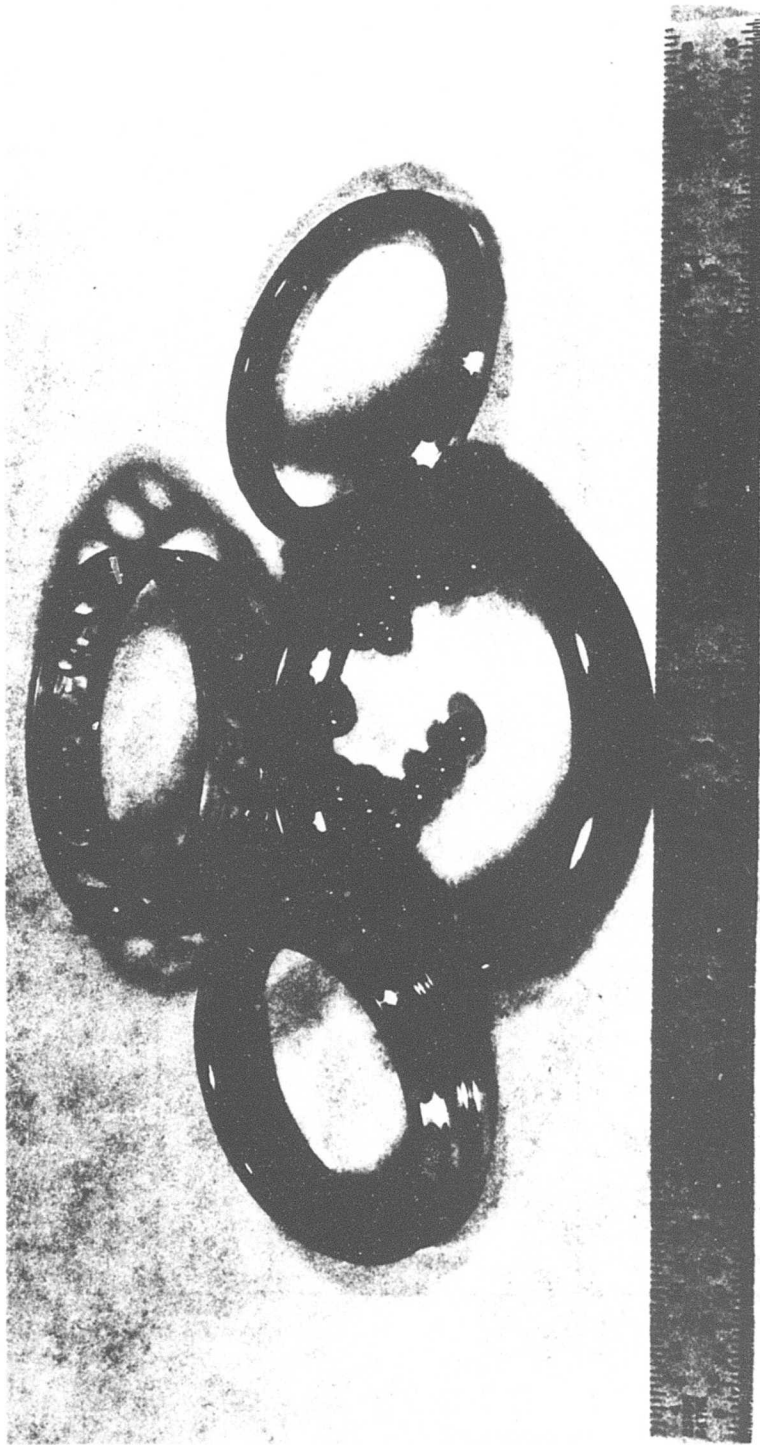
Figure 37.   35MM Ausformed Bearing (S/N 0006) After 500 Hours at 65,000 rpm and at an Axial Load of 500 lb
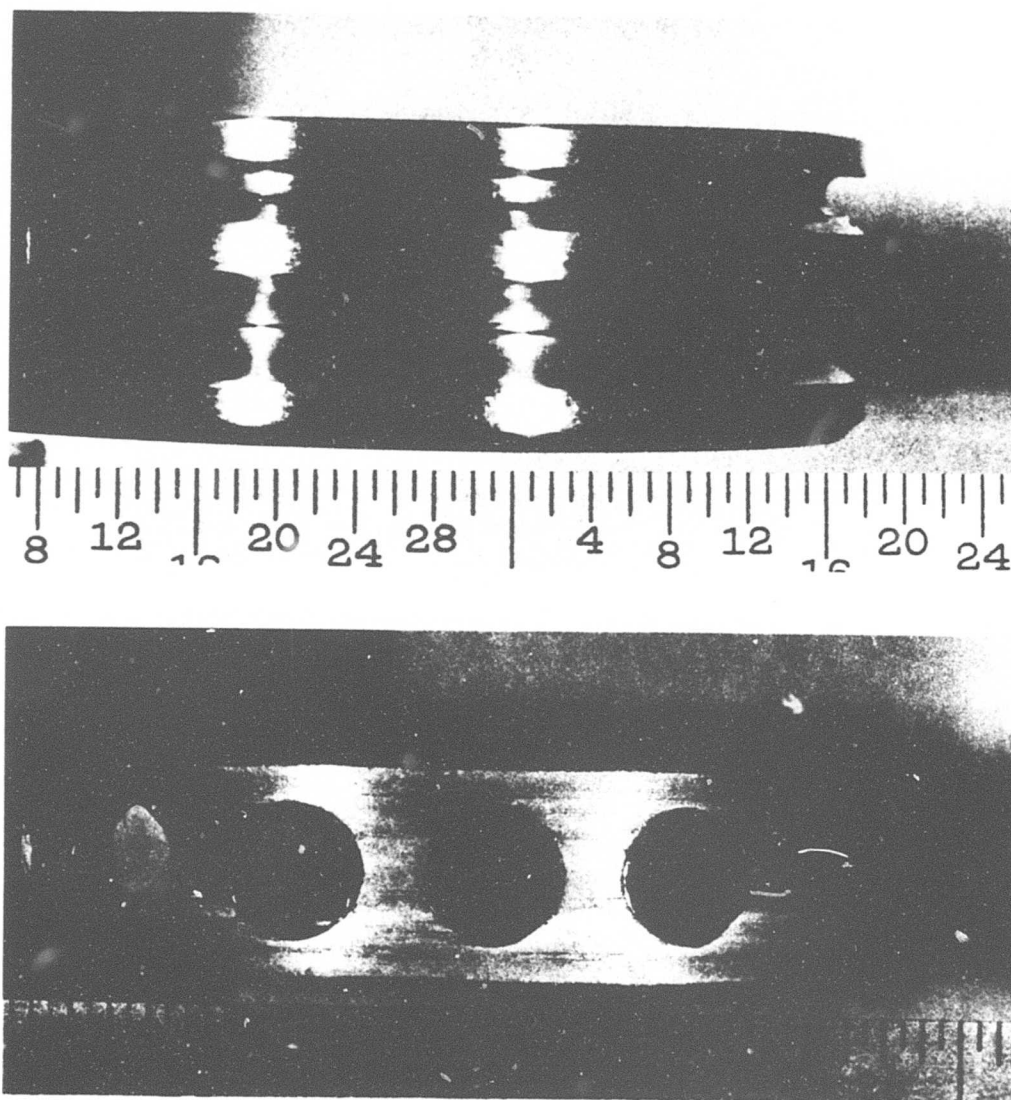
Figure 38. Condition of Inner Races & Cage of Bearing S/N 0006 After 500 Hours of Test. Except for Slight Extrusion of Silver Plate on Ball Pockets, All Components Are in Excellent Condition
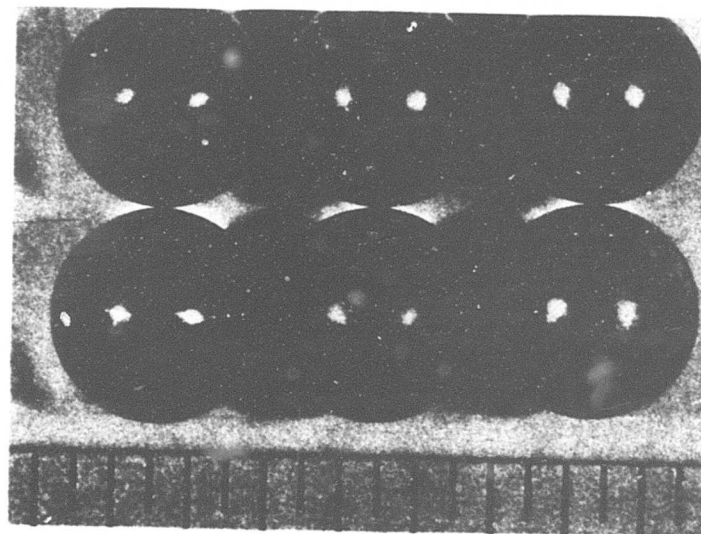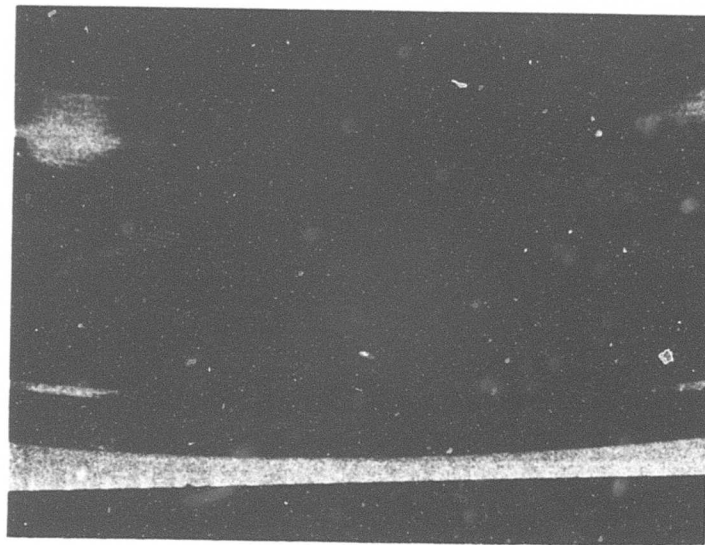
Figure 39. Condition of Outer Raceway and Balls of Bearing S/N 0006 After 500 Hour-Test
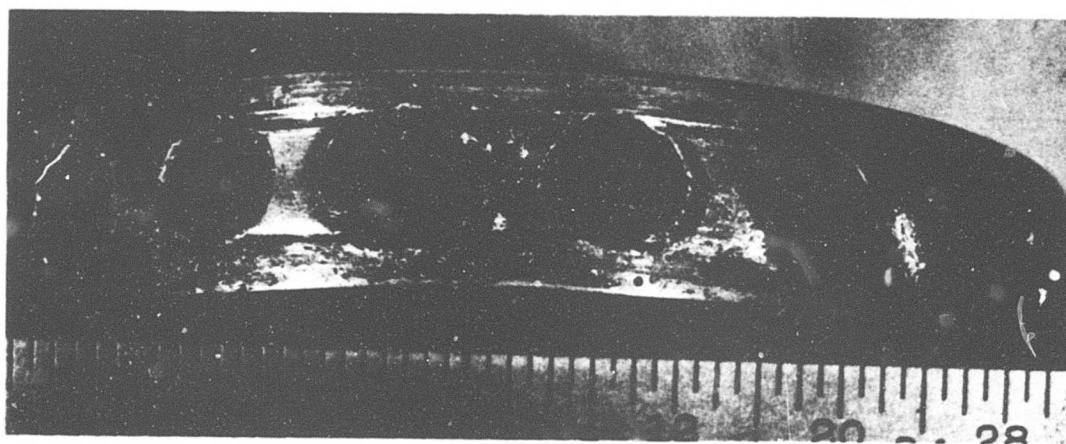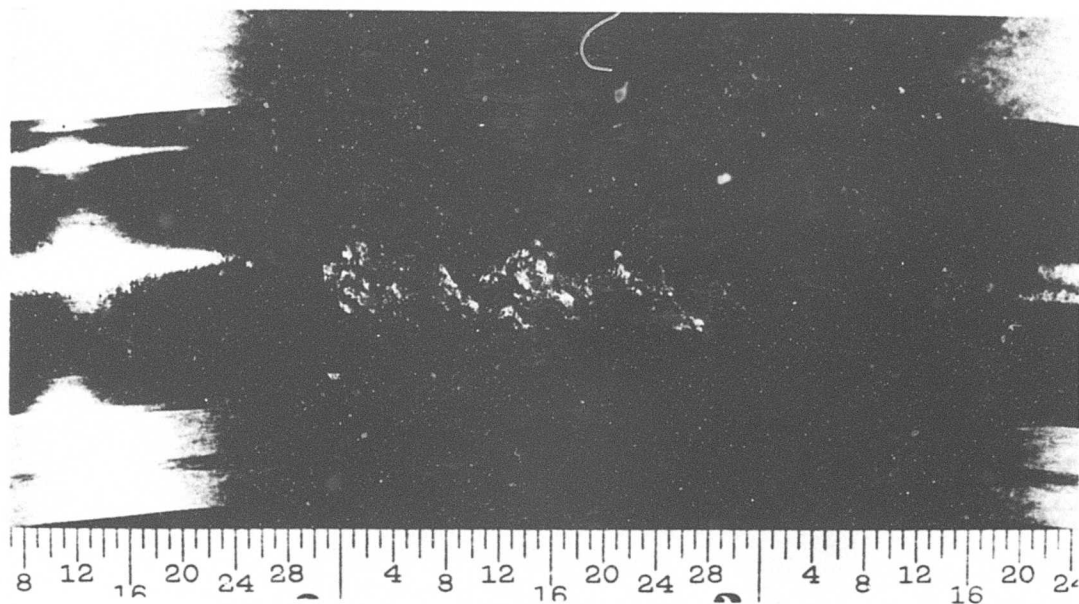
Figure 40. Ausformed Bearing (S/N 0004) After 482 Hours at 65,000 rpm
and at an Axial Load of 500 lb. Initial Outer-Race Fatigue
Failure (Top) Followed by Cage Distress (Bottom) and Ball
Damage (Figure 41.)

81
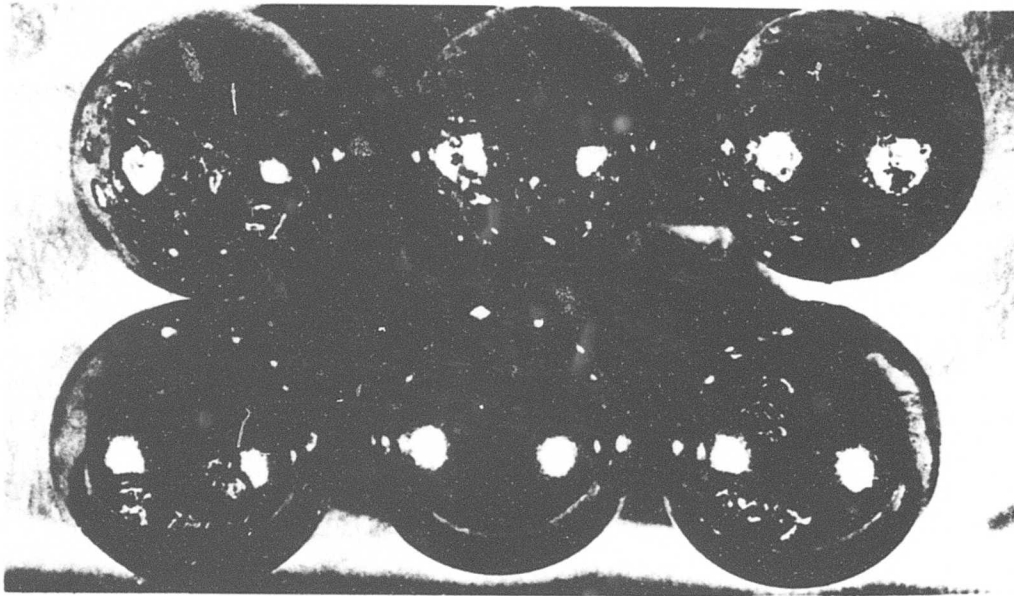
Figure 41. Balls From Bearing S/N 0004, Showing Damage as a Result
of Outer-Race Fatigue Failure
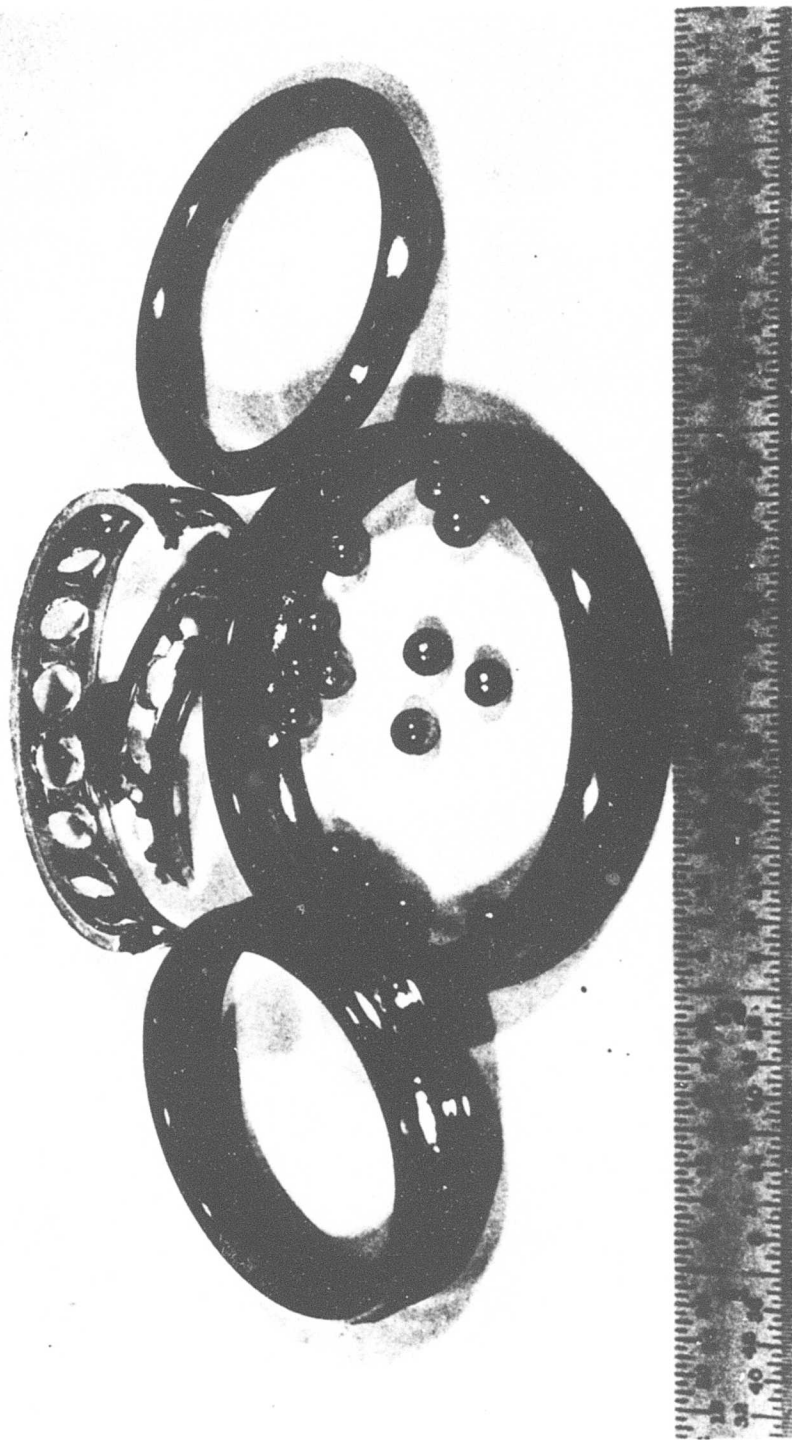
Figure 42. Ausformed Bearing S/N 0009 After 92 Hours at 65,000 rpm and at an Axial Load of 500 lb
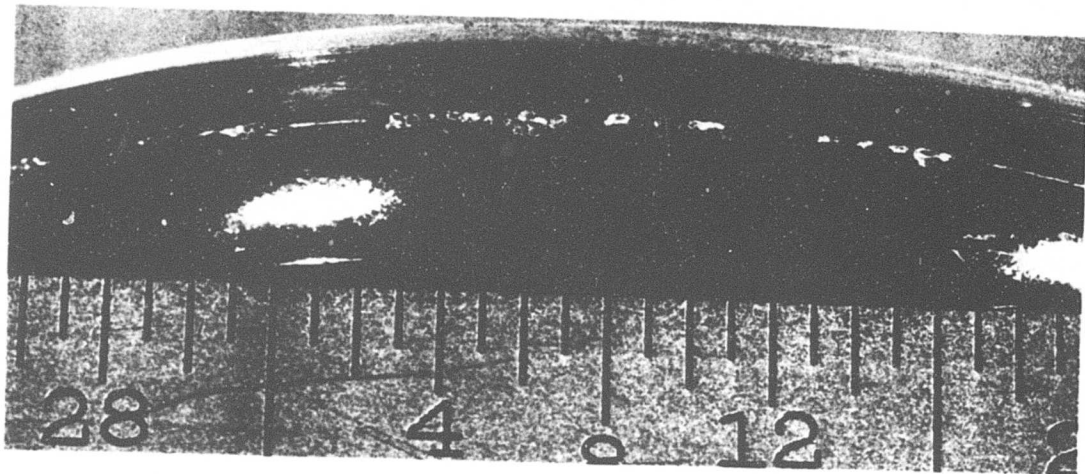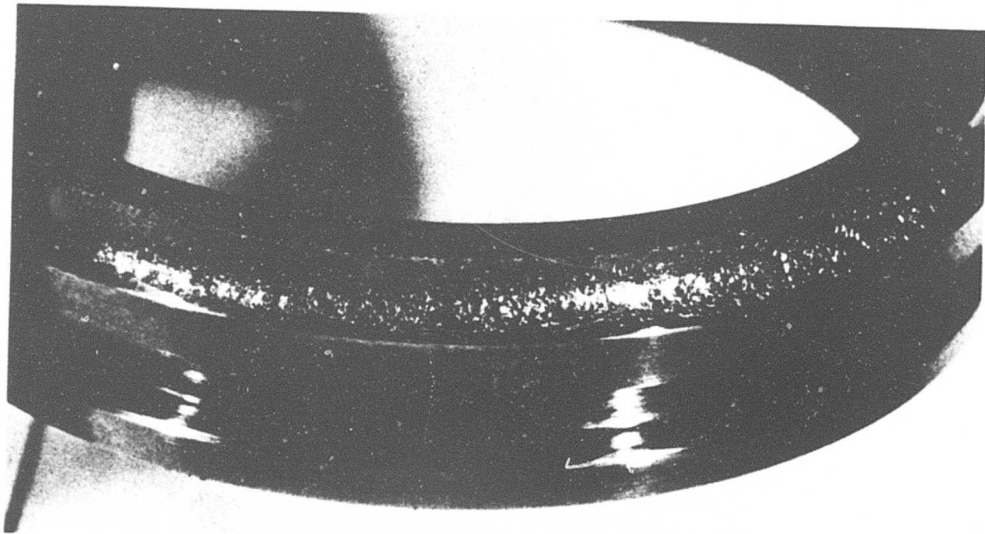
Figure 43. Primary Fatigue Failure on Puller Groove Half Inner-Race
Bearing S/N 0009. Slight Split-Line Damage on Plain
Inner-Race Segment (Bottom)

84
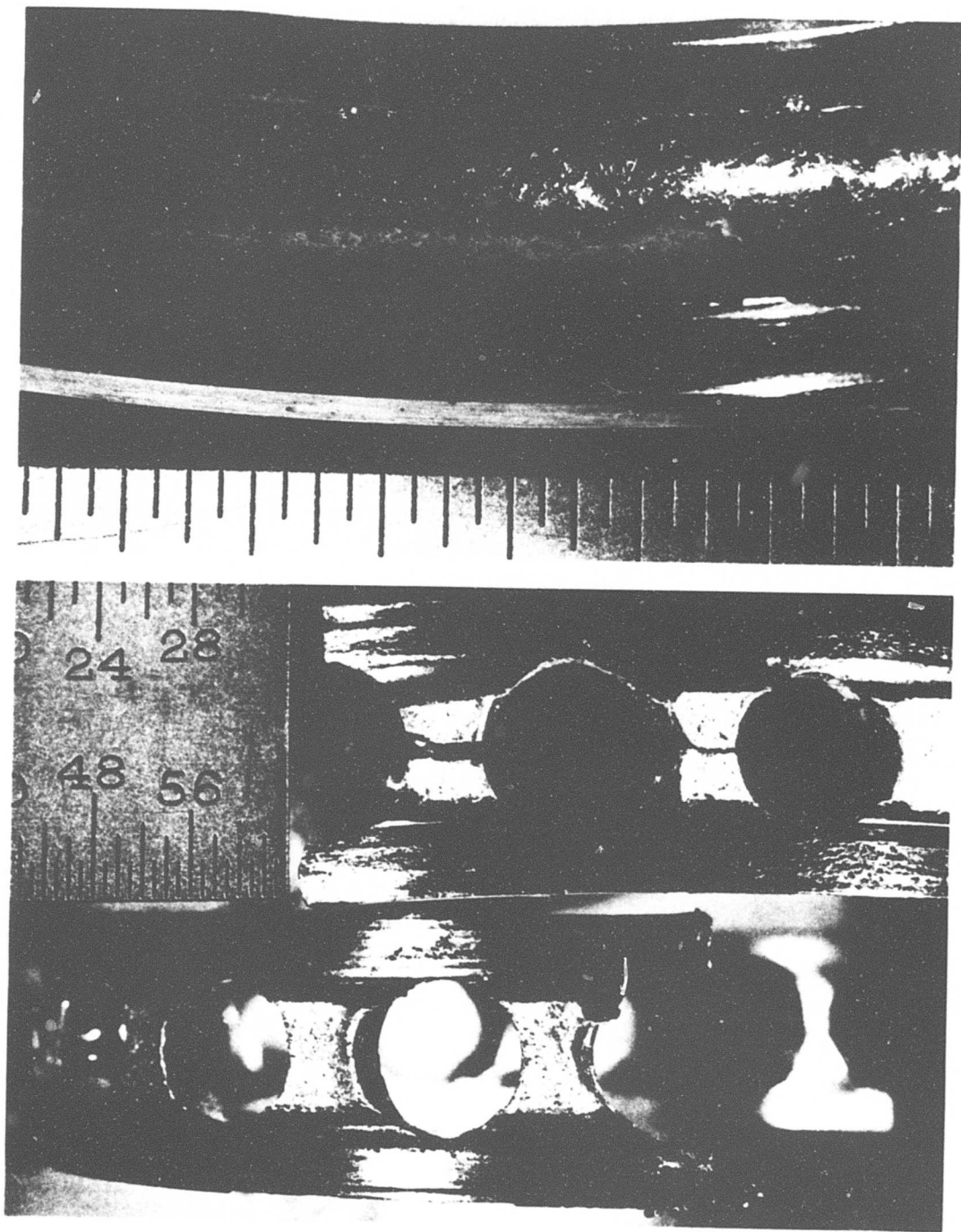
Figure 44. Secondary Outer Race and Cage Damage on Bearing S/N 0009

85
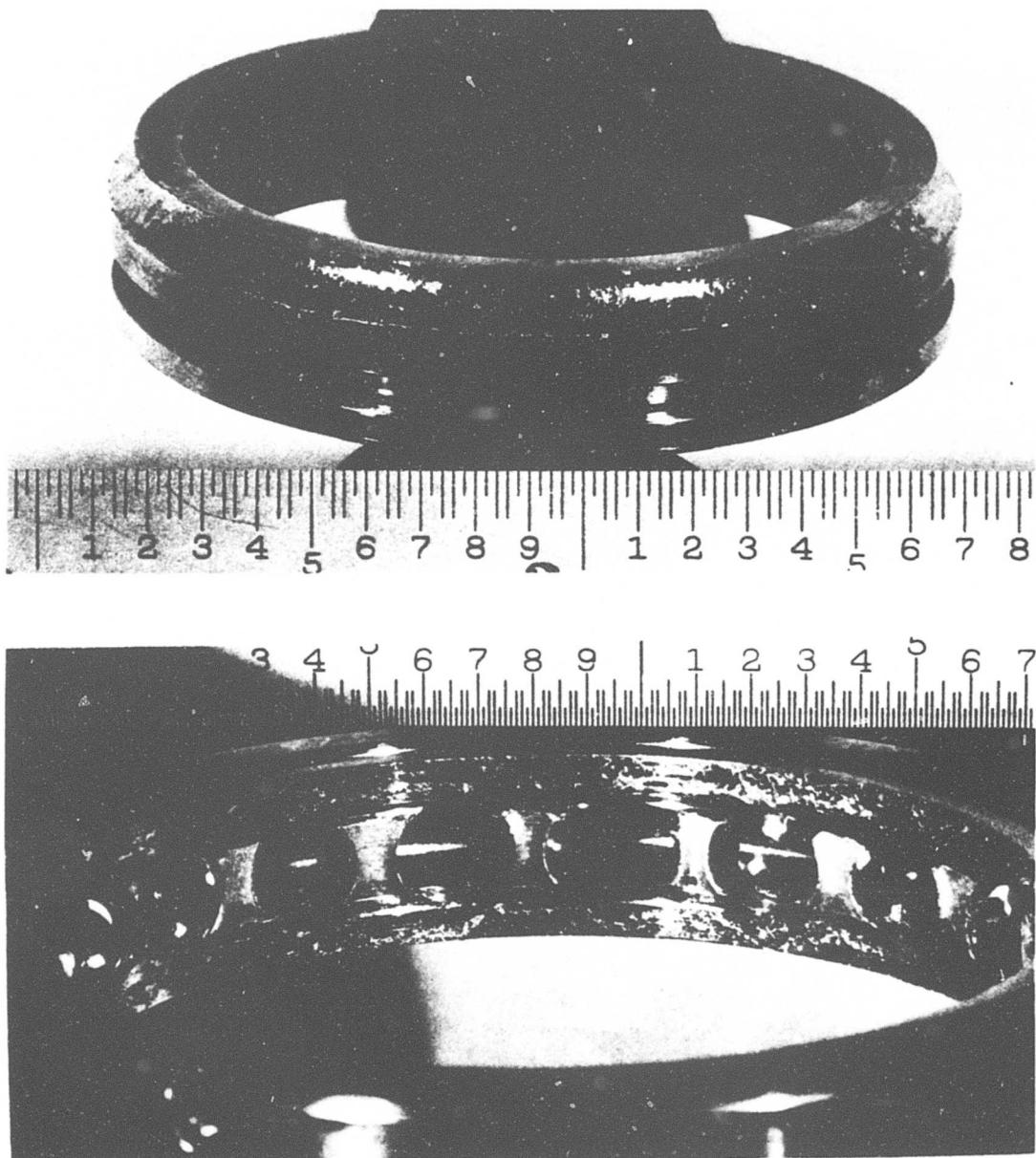
Figure 45. Typical Inner Ring Surface Fatigue Failure and Cage Distress
on M-50 Control Bearing, With Bearing in Original Configuration

86

checkout runs with a bearing utilizing a large diameter ball (Split-Ball P/N HDB-007), failure was on the outer race, obviously initiating at the site of the split line (see Figure 46), but did not result in cage and/or ball damage.

Metallurgical evaluation did not reveal any unusual condition in either the standard or the ausformed bearings which could be construed as abnormal. Failures were subsurface initiated and appeared to be classical spalling type rolling element fatigue.

DISCUSSION AND RECOMMENDATIONS

The prime objective of the work reported herein was the evaluation of rolling-element bearings utilizing thermomechanically processed components in the size range common to U.S. Army propulsion systems. A second objective was to establish a feasible production process for this type of bearing. Both of these objectives were successfully accomplished.

As is often the case, relatively straightforward tasks such as the two cited in the preceding paragraphs can generate complementary activities which are at least as difficult and complex as the primary objectives. This program was no exception. The report has covered these areas in detail. The two appendixes are a direct result of these excursions; and while they were not a contract requirement, it is felt that their inclusion will provide a more complete story and serve as a practical guide in future, similar efforts.

The beneficial influence of the ausforming procedure has been demonstrated on a bearing which, at best, was of marginal design. There is no doubt that the results would have been equally satisfactory, and perhaps even more so, with a properly designed high-speed bearing. It is interesting to note that the degree of improvement ($\sim 7X$) achieved over a standard processed bearing is in excellent agreement with previously published data on similar size bearings.[12] This latter fact is demonstrated in Figure 47. This agreement is especially beneficial from the standpoint that the present test series were performed with a minimal number of tests and consequently standing by itself would have a relatively low statistical confidence level. The results of the previous program, however, are based on an adequately large test population, such that a totally valid statistical judgement can be made. The agreement between the two programs thus validates to a great extent the results of the test program reported herein.

It will be recognized that thermomechanical processing does incorporate several more or less difficult steps into the manufacturing cycle of rolling-element bearings. Based on past experience, the degree of difficulty is an almost linear function of bearing size. In the size range of interest to the U.S. Army, i.e., ~ 25mm -75mm, the metal-working processes required for ausforming are on the lower order of the difficulty scale;
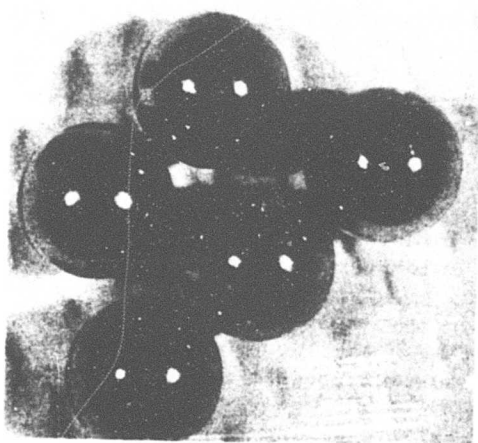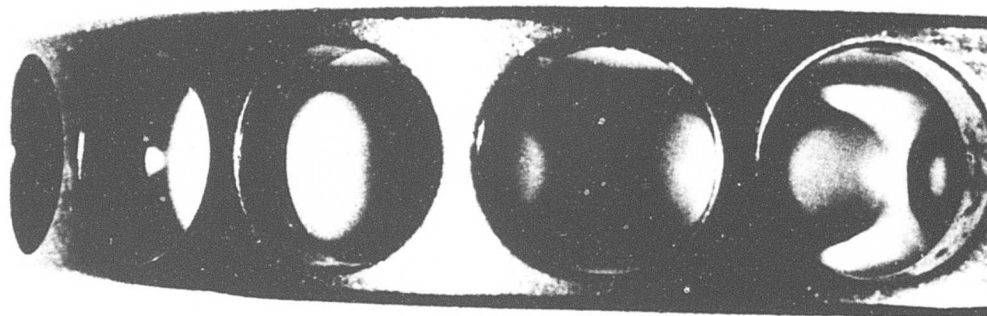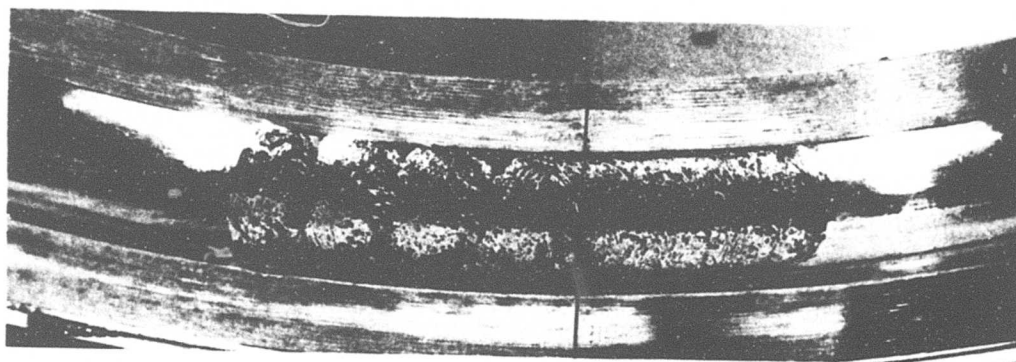
Figure 46.   Outer Race, Cage, and Balls From Split-Ball Bearing Checkout Run.
Note Fatigue Spall on Outer Race Originating at Split-Line.
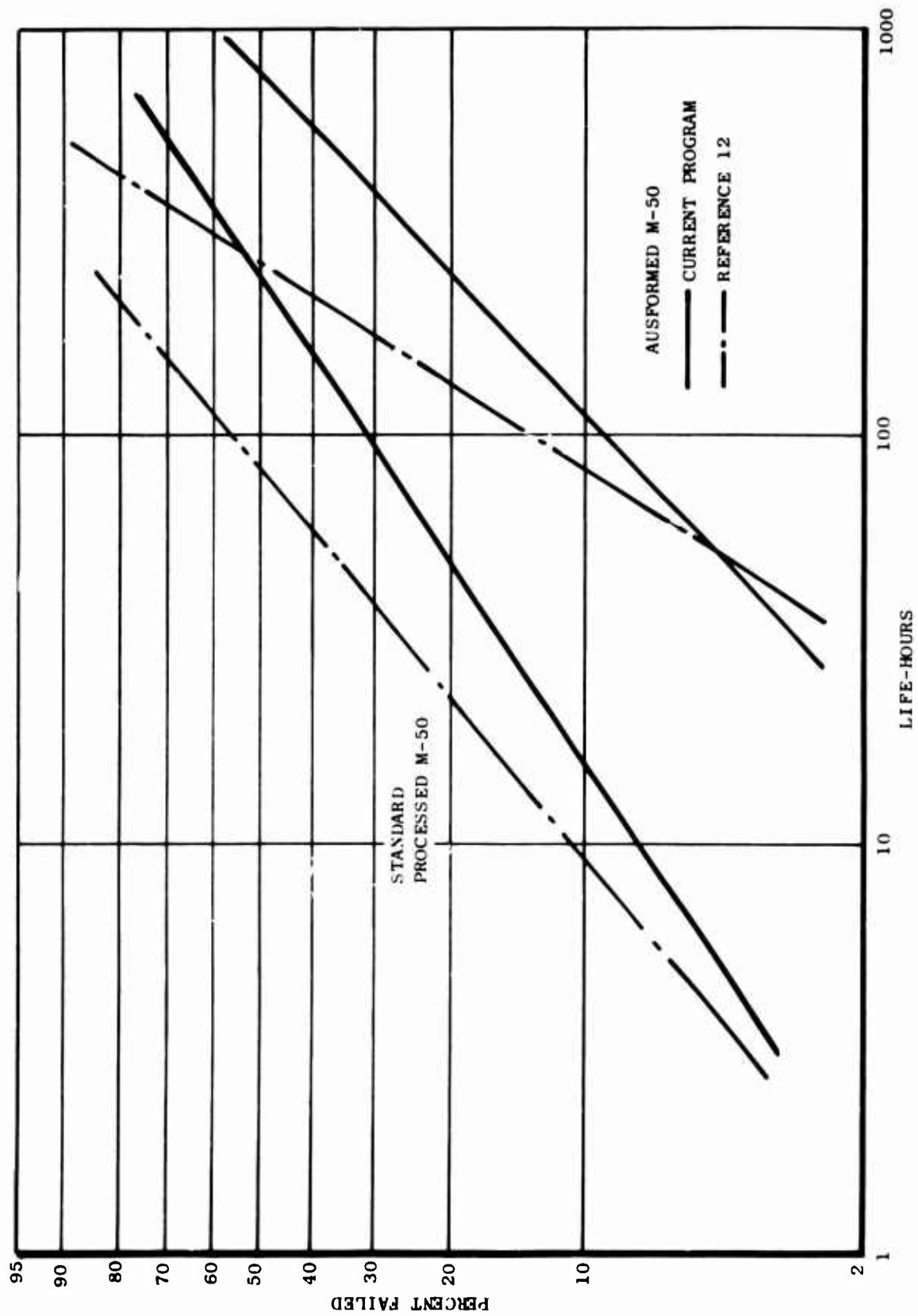Other Components Are in Excellent Condition

Figure 17. Comparison of 35MM Bore Ball Bearing Test Results

thus ausforming represents a viable approach to fatigue life extension of critical engine bearings.

Obviously, because of the extra manufacturing steps required, bearing costs will be increased. The exact cost increase is difficult to assess, since it depends greatly on bearing size and configuration and more specifically on quantity. Thus, the engine designer will have to make a judgement weighing the life-improvement potential against the economic consideration. In the cases of hypercritical fatigue limited bearings, the argument will, admittedly, be rather one-sided.

The high-energy-rate forging process utilized for making the rings is well suited for the ausforming of smaller diameter (up to ~ 100mm) bore bearings. It is a repeatable and reproducible process and should lend itself well to high-volume production levels. The manufacture of the ball, while cumbersome, is repeatable, although improvements in the forging of this part seem warranted.

In summary, ausforming of small to medium size bore rolling element components is a viable process and does result in sizable improvements in bearing fatigue life. It is recommended that work be continued in this area, concentrating on refining the process to improve ball manufacturing techniques and increasing the yield from the outer ring forgings. Additional component testing is suggested utilizing an actual engine bearing size and configuration, with the ultimate aim of introducing thermomechanically processed bearings into operational U.S. Army propulsion systems.

REFERENCES

1. Scibbe, H.W., and Zaretsky, E.V., "ADVANCED DESIGN CONCEPTS FOR HIGH SPEED BEARINGS", ASME Paper 71-DE-50, 1971.

2. Signer, H., Bamberger, E.N., and Zaretsky, E.V., "PARAMETRIC STUDY OF THE LUBRICATION OF THRUST LOADED 120-mm BORE BALL BEARINGS TO 3 MILLION DN", ASME Paper 73-Lub-24, 1973.

3. Bamberger, E.N., "EFFECT OF MATERIALS - METALLURGY VIEWPOINT", Inter-disciplinary Approach to the Lubrication of Concentrated Contracts. NASA SP-237, 1970.

4. Potts, J.R., "MANUFACTURING METHODS FOR PRODUCTION OF HOLLOW BALL BEARINGS FOR USE IN GAS TURBINE ENGINES", P&W Aircraft Division, First Interim Report IR-121-0(1), AF Contract F33615-70-C-1524.

5. Lips, E.M., Van Zuilen, H., "IMPROVED HARDENING TECHNIQUE", Metal Progress, August 1954, pp. 103-104.

6. Schmatz, D.J., Zackay, V.F., "MECHANICAL PROPERTIES OF DEFORMED META-STABLE AUSTENITIC ULTRA-HIGH STRENGTH STEELS", Trans. A.S.M., 1959, pp. 476-488.

7. Marschall, C.W., "DRAFT LITERATURE SURVEY ON HOT COLD WORKING OF STEEL", Battelle Memorial Inst. Project AF 33(657)9139, September 1962.

8. Koppenaal, T.J., "THE CURRENT STATUS OF THERMO-MECHANICAL TREATMENT OF STEEL IN THE SOVIET UNION", ASM Trans. Vol. 62, No. 1, 1969.

9. Bamberger, E.N., Zimmerman, W.F., "HIGH STRENGTH MATERIALS FOR SOLID ROCKET MOTORS", Final Report, Bureau of Naval Weapons, Report No. Nord 18119.

10. Bamberger, E.N., "THE EFFECT OF AUSFORMING ON ROLLING CONTACT FATIGUE", Final Engineering Report. BuWeps Contract NOw 63-0144-d, December, 1963.

11. Bamberger, E.N., "THE EFFECT OF AUSFORMING ON THE ROLLING CONTACT FATIGUE LIFE OF A TYPICAL BEARING STEEL", Trans. ASME, J. Lub. Tech. Vol. 89F, No. 1, 1967.

12. Bamberger, E.N., "THE PRODUCTION, TESTING AND EVALUATION OF AUSFORMED BALL BEARINGS", Final Engineering Report, BuWeps Contract NOw-65-0070-f, June 1966.

13. Parker, R.J., Zaretsky, E.V., "ROLLING ELEMENT FATIGUE LIFE OF AUSFORMED M-50 STEEL BALLS", NASA TN D-4954, 1968.

14. Bamberger, E.N., "MANUFACTURE OF JET ENGINE THRUST BEARINGS BY AUSFORMING" AF Contract F33615-67-C-1723, Final Engineering Report AFML-TR-72-43, April, 1972.

15. Bamberger, E.N., "BEARING FATIGUE INVESTIGATION II", NASA CR 134621, June 1974.

16. Breznyak, E.J., "RECENT DEVELOPMENTS IN HIGH VELOCITY METAL-WORKING", Society of Manufacturing Engineering Paper MF70-228, 1970.

17. Weibull, W., "A STATISTICAL DISTRIBUTION OF WIDE APPLICABILITY", Journal of Applied Mechanics No. 18, 1951.

18. Johnson, L.G., "THE STATISTICAL TREATMENT OF FATIGUE EXPERIMENTS", General Motors Research Laboratory GMR-202, April, 1959.

19. Delaney, B.R., and West, H., "MULTIMISSION AIRCRAFT PROPULSION SIMULATOR INITIAL AERO/MECHANICAL TEST RESULTS AND EVALUATION", AFAPL-TR-73-77, December, 1973.

20. Dowson, D., and Higginson, C.R., "ELASTOHYDRODYNAMIC LUBRICATION", Pergamon Press, New York, 1966.

21. Archard, J.F., and Cowking, E.W., "ELASTOHYDRODYNAMIC LUBRICATION AT POINT CONTACTS", Proceedings of the Institution of Mechanical Engineers, Vol. 180, Pt. 3B, 1965-1966, pp 47-56.

22. Skurka, J.C., "ELASTOHYDRODYNAMIC LUBRICATION OF ROLLER BEARINGS, EFFECTS OF ENDURANCE LIFE ON FILM THICKNESS AND SURFACE FINISH", ASME Paper 69-LUB-18, 1969.

23. Danner, C.H., "FATIGUE LIFE OF TAPERED ROLLER BEARINGS UNDER MINIMAL LUBRICANT FILMS", ASLE Paper 69-LC-11, 1969.

24. Tallian, T.E., "ON COMPETING FAILURE MODES IN ROLLING CONTACT", ASLE Transactions, Vol. 10, No. 4, October 1967, pp 418-459.

APPENDIX A

DETAILED DESIGN OPTIMIZATION STUDIES

As an integral part of the 35mm ausformed bearing program, a parametric study was performed to isolate the critical geometry and operational variables and to attempt to optimize the bearing design around designated operating conditions.

The analytical tool utilized for the parametric study was the GE Bearing Design Technology computer program RECAP3. This program simulates the performance of high-speed, thrust-loaded angular-contact ball bearings. Inertial effects such as ball centrifugal force and primary and secondary gyroscopic moments due to ball orbital, rolling and sliding motions are included in the analysis. Also included are elastohydrodynamic lubrication traction forces acting on the balls, viscous drag forces owing to the ball orbital motion, and cage rail-to-bearing ring land friction forces. Lubricant viscosity data as a function of pressure and temperature are resident in the program and are used to determine lubricant film thickness and traction characteristics in the Hertzian contact zones. A sample program output is shown in Figure A-1.

Contact Angle

In discussing the contact angle relationships with bearing operating performance, it is necessary to define the proper contact angle in question, namely, the effective mounted contact angle or the contact angle that the bearing will exhibit after the decreases in internal radial clearance (IRC) due to the effects of interference fit and centrifugal and thermal growth have been accounted for. It is critically important to define the proper contact angle from a life prediction viewpoint and to properly assess the contact angle sensitivity to changes in IRC. A common error is to neglect the shaft, bearing and housing expansions due to centrifugal and thermal effects, as most computer programs utilize a rigid ring approach to determine bearing operating performance. For the 35mm bearing design tested in this program, the average free contact angle was 30°. Factoring in the IRC reduction due to the interference fit between the shaft and bearing inner race produces an assembled average contact angle of 23.8°. Further accounting for the IRC reduction due to centrifugal and thermal effects decreases the contact angle to an effective mounted value of 16.8°. It is this effective mounted contact angle along with the other geometrical and operational variables that determines the operating contact angles and associated bearing performance.

93

Figure A-1. Recap 3 Computer Program Sample Output

Figure A-1. Continued

As shown in Figure A-2 for the 35mm bore diameter bearing tested in the U.S. Army program, and at a specified thrust load of 250 lb, calculated bearing fatigue life generally increases with effective mounted contact angle, particularly in the normal range of interest of from 20° to 30°. As shown in Figure A-3 for the same bearing, an optimum value of contact angle can be achieved, but it usually occurs at excessively large values where the associated IRC and end play levels are prohibitively large for proper machine assembly and clearance control. The average effective mounted contact angle of 16.8° for the original bearing design is not considered to be satisfactory for this application because of fatigue life reduction and for sensitivity to changes in IRC to be subsequently discussed. An effective mounted contact angle range from approximately 22° to 26° is considered to represent a satisfactory compromise between fatigue life, tolerance to IRC reductions and required machine clearance control requirements. Following the subsequent discussion of the advantages of increasing the ball diameter and total curvature, Figures A-4 and A-5 show the contact angle versus life relationships for a 35mm bore diameter bearing with 15-5/16 inch diameter balls and outer and inner curvature ratios of 0.51 and 0.56, respectively. The 26.3 average effective mounted contact angle for this bearing is seen to effect a considerable improvement in predicted fatigue life at 250 lb applied thrust load when compared to Figure A-2 for the 18-3/16 inch ball diameter configuration.

Curvature

One of the most significant variables in small bearing technology is the ratio of raceway radius of curvature to ball diameter. A common value for main shaft size bearing inner- and outer-race curvature ratios is 0.52. Fatigue life increases with decreasing curvature ratio, but a minimum curvature ratio is not necessarily desirable for a small-diameter bearing operating at high speeds. For a given contact angle, a minimum curvature ratio also produces a minimum internal radial clearance and the greatest contact angle sensitivity to loss of clearance. An example of this effect is shown in Figure A-6 for a 12mm bore diameter ball bearing operating at 88,000 rpm (1.06×10^6 DN). In this bearing design, the initial curvature ratios of 0.52 predicted adequate fatigue life, but subsequent testing indicated that classical subsurface fatigue was not the limiting factor. Loss of clearance due to thermal effects produced a significant decrease in contact angle which led to increased bearing heat generation, further decreases in clearance and contact angle, etc., until eventual seizure. Noting the 0.52 curvature curve in Figure A-6, it can be seen that the slope of this curve is steeper than the slopes of the other curvature curves, producing the greatest sensitivity of contact angle change to small changes in internal clearance. Based on this test experience, the bearing was subsequently redesigned with curvature ratios of 0.53 to effect a satisfactory compromise between predicted fatigue life and contact angle sensitivity to small changes in internal clearance. This bearing design has been demonstrated in a propulsion simulator application for the USAF

Figure A-2. U. S. Army 35MM Bearing Fatigue Life vs Contact Angle
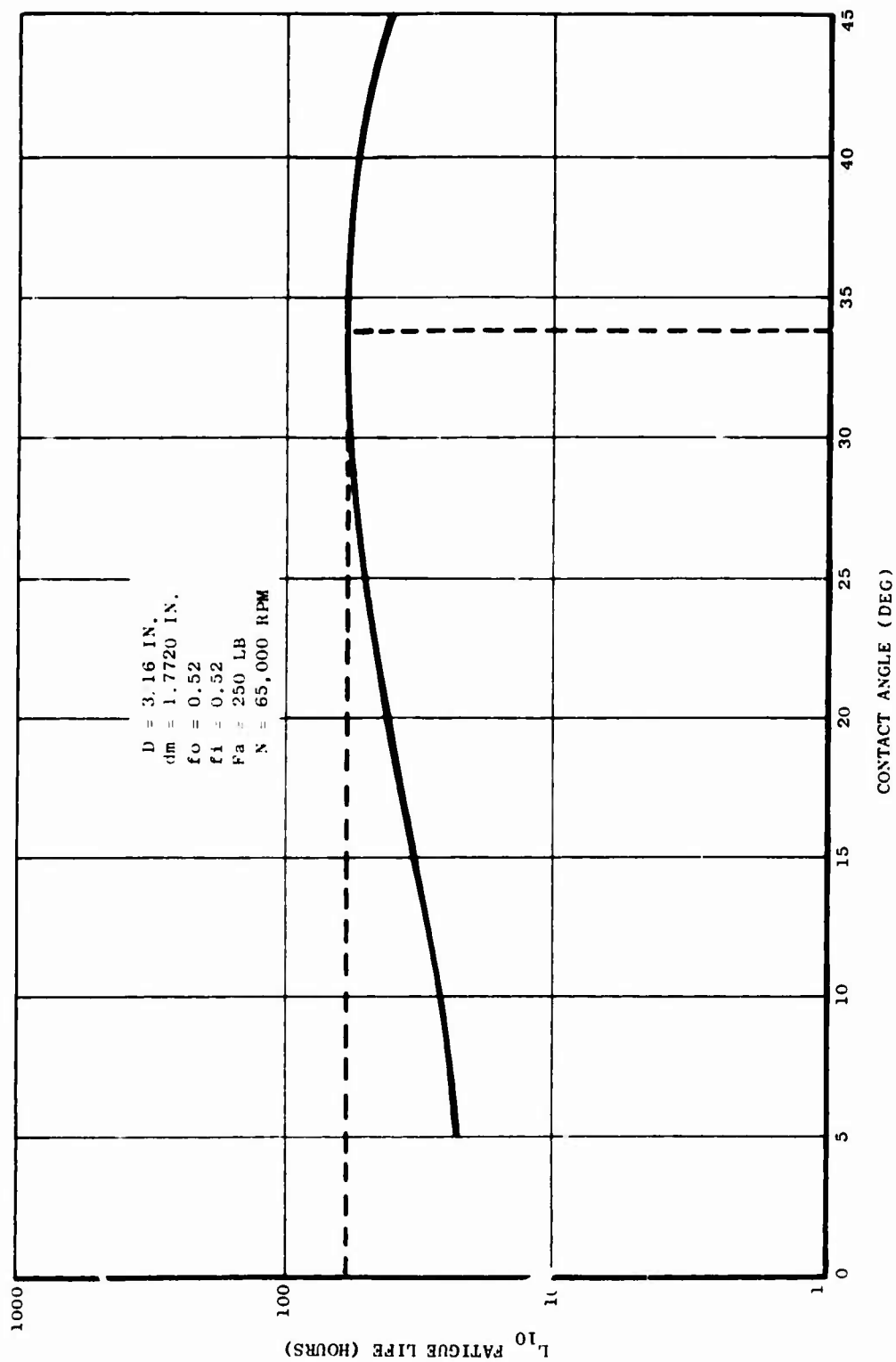
Figure A-3. U. S. Army 35MM Bearing Optimum Contact Angle

The chart shows L₁₀ Fatigue Life (Hours) versus Contact Angle (DEG) with the following parameters:

$$D = 3.16 \text{ IN.}$$
$$dm = 1.7720 \text{ IN.}$$
$$fo = 0.52$$
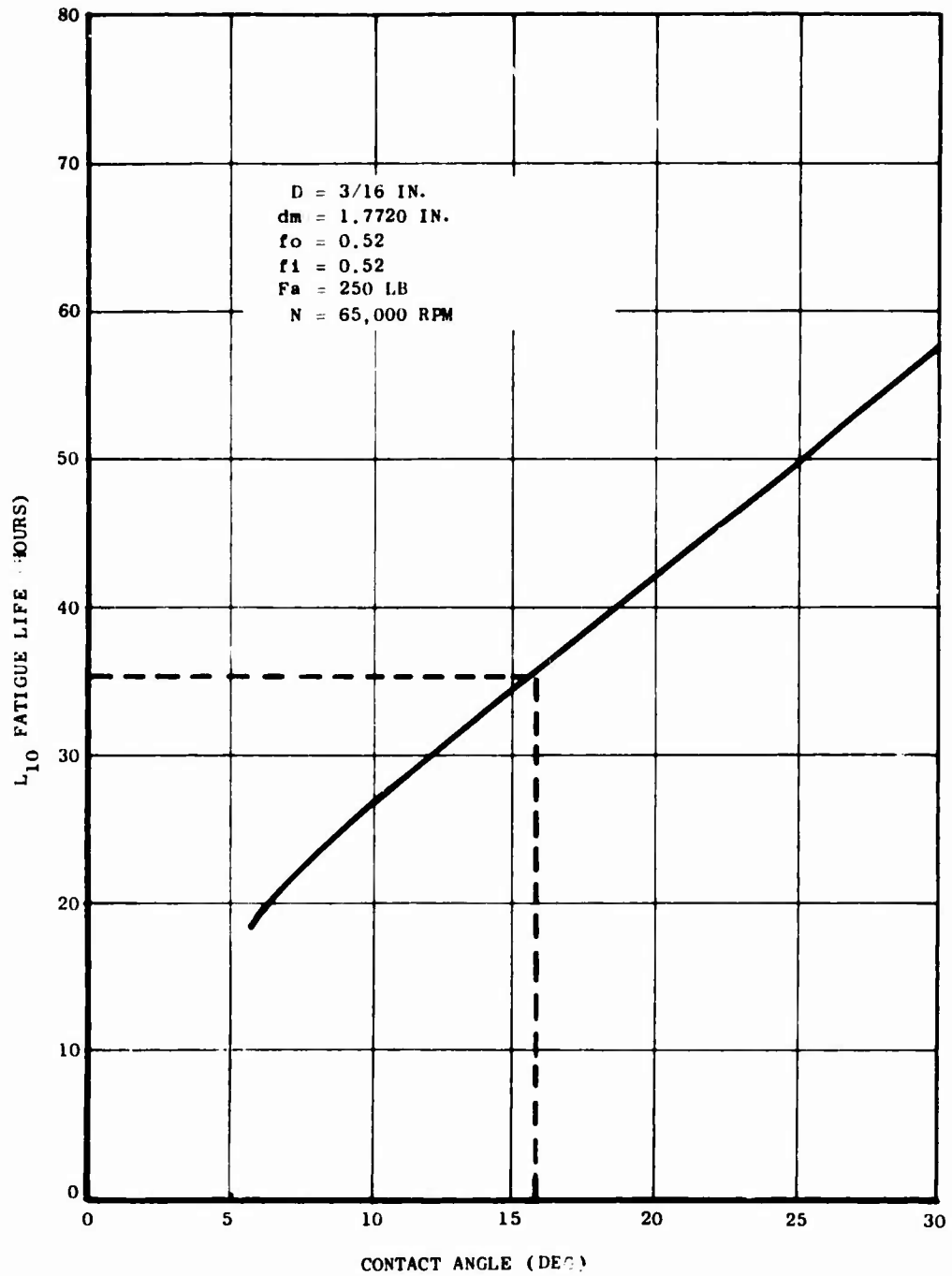$$fi = 0.52$$
$$Fa = 250 \text{ LB}$$
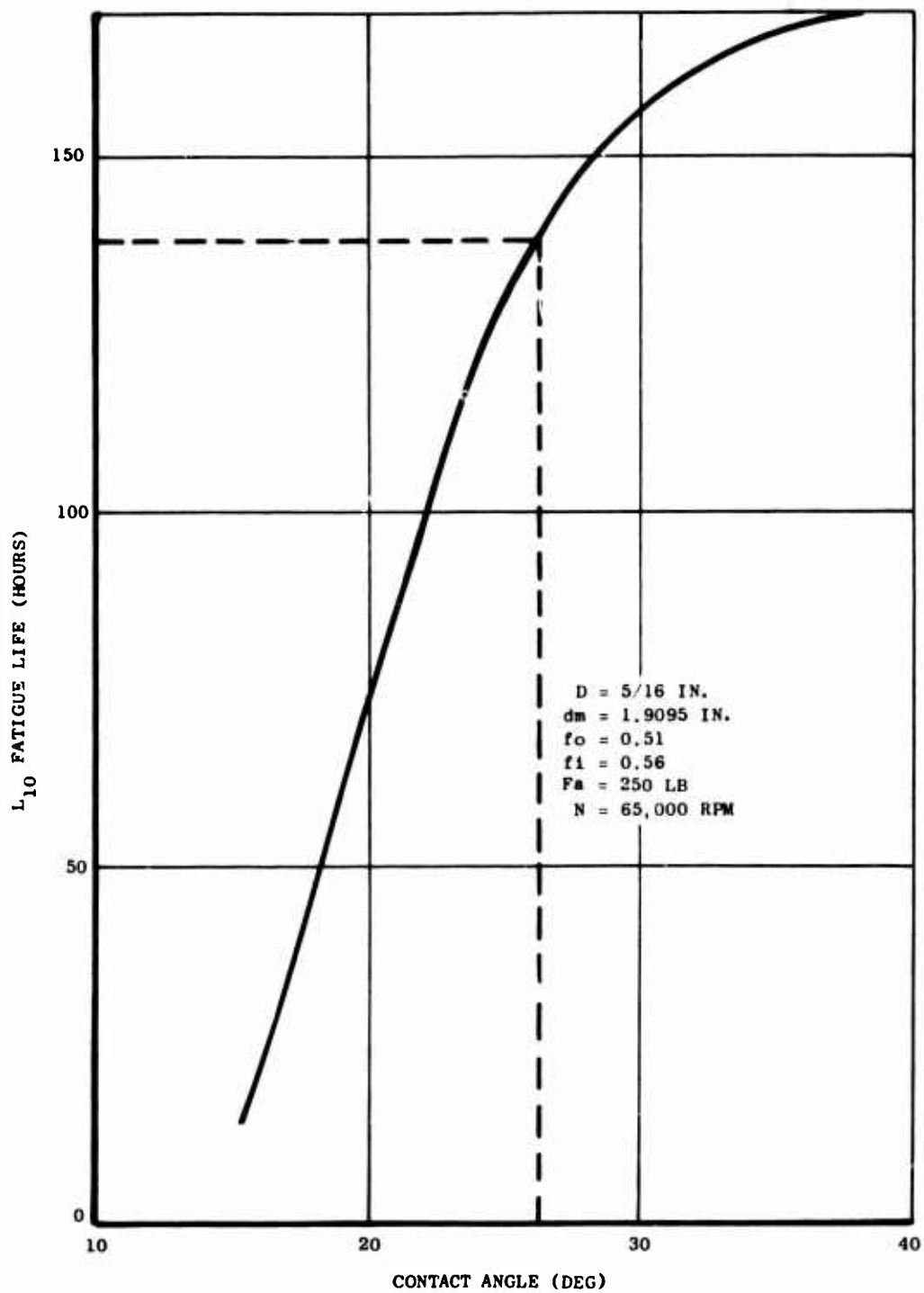$$N = 65,000 \text{ RPM}$$

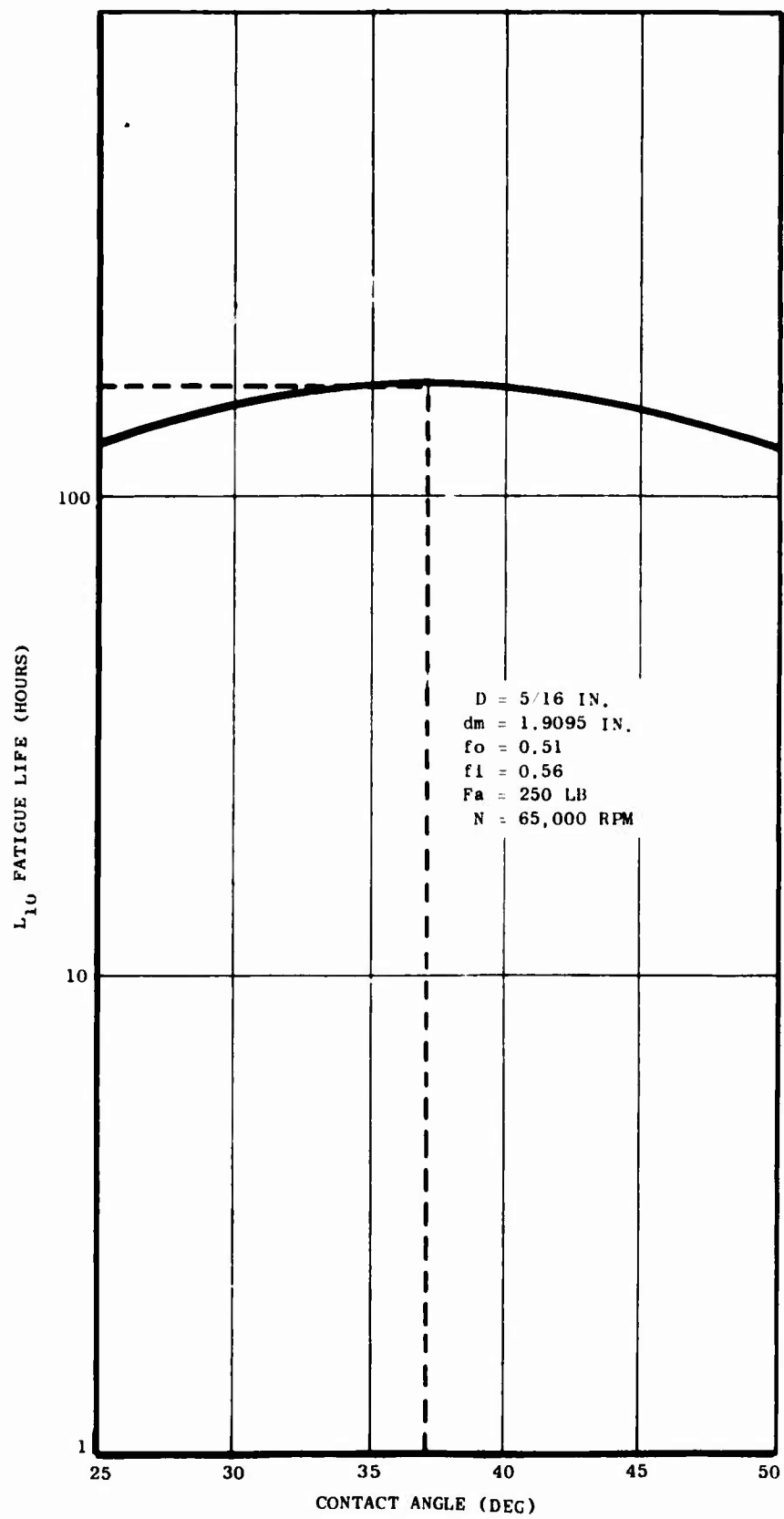**Figure A-4.** U. S. Army 35MM Bearing Fatigue Life vs Contact Angle

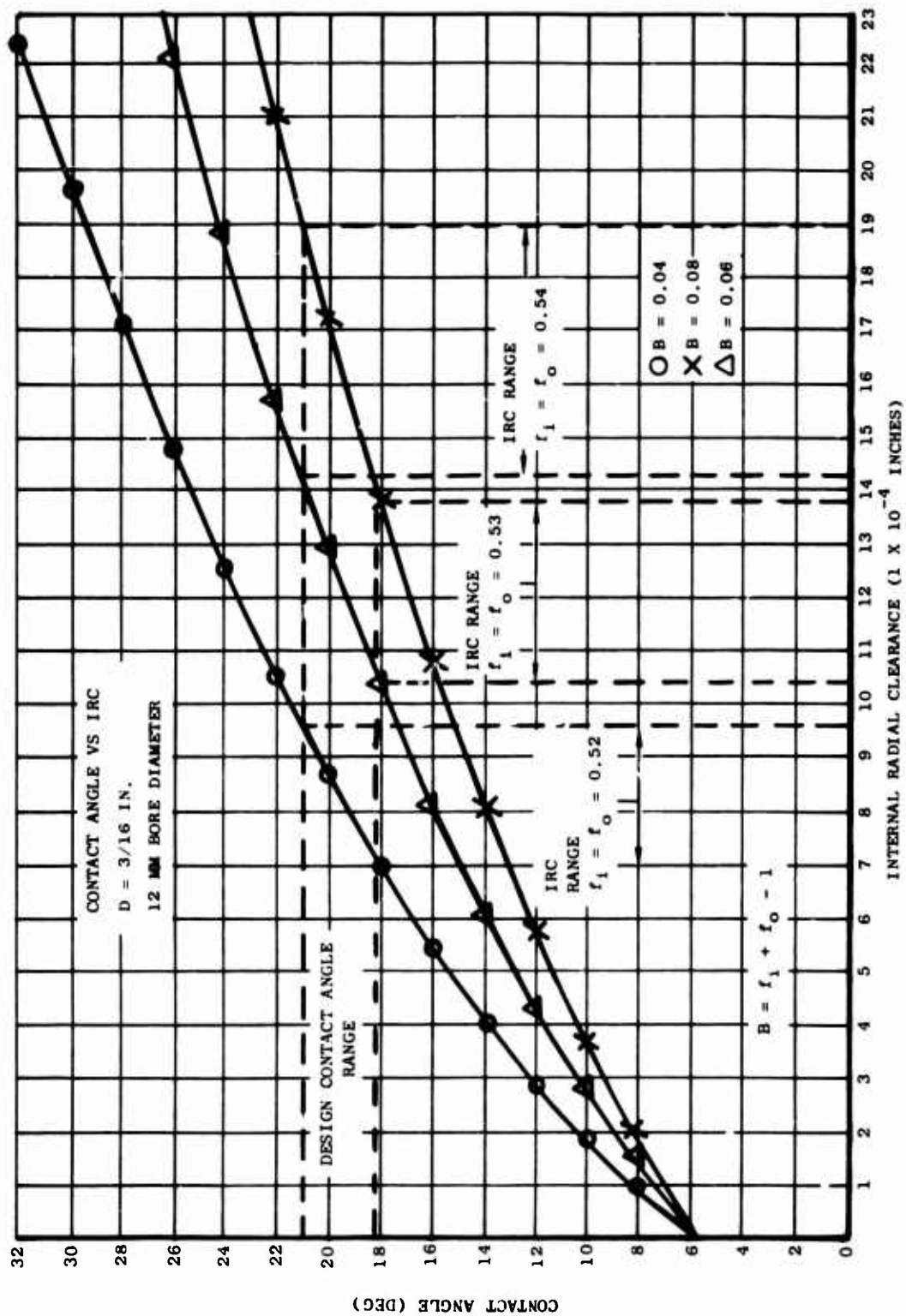Figure A-5. U. S. Army 35MM Bearing Optimum Contact Angle

100

Figure A-6. Propulsion Simulator Thrust Bearing

101

Aero Propulsion Laboratory.[19] It operates with minimal oil supply flow
rate (30 cc/hr), with bearing cooling being provided by flow path bleed
air. The bearing design, shown in Figure A-7, exhibits excellent toler-
ance to changes in internal clearance produced by changing operating con-
ditions.

The internal radial clearance (IRC) versus contact angle relationship for
various values of total curvature (B = $f_o + f_i - 1$ where f_o and f_i are the
outer and inner raceway curvature ratios, respectively) is shown in Figure
A-8 for a 35mm bore diameter bearing with a 3/16 inch ball diameter. The
current bearing design has a total curvature value of 0.04 ($f_o = 0.52$;
$f_i = 0.52$), a free contact angle range of from 28° to 32°, and an un-
assembled IRC range from 0.0017 to 0.0022 inch. Calculating the loss of
clearance due to the interference fit (0.0007"T to 0.0012"T) between the
bearing inner race and shaft (in the test rig the outer race is assembled
with a line-to-line to loose fit into an adapter and does not affect the
bearing IRC), the mounted IRC range is from 0.0008 inch to 0.0017 inch,
producing a corresponding mounted contact angle range of from 19.5° to
28.2°. Adding the shaft and bearing centrifugal and thermal effects of
65,000 RPM and 250°F operating temperature reduces the IRC further to an
average of 0.00065 inch and the contact angle to an average of 16.8°
(effective mounted contact angle). Noting Figure A-8, it can be seen that
at 16.8°, the slope of the contact angle versus IRC curve for B = 0.04 is
quite steep, and any small change in IRC will produce a significant change
in contact angle. As can be seen from the figure, a reduction of the IRC
by 0.0002 inch produces a contact angle decrease to 14.0°. This is a
highly unstable condition with only minor differences in radial thermal
gradient being capable of driving the bearing to seizure. In contrast,
for a total curvature value of 0.07, the effective mounted contact angle
is 23.5° and the corresponding IRC is 0.0022 inch. A reduction in IRC by
0.0002 inch reduces the contact angle to only 22.5°. Therefore, the con-
tact angle sensitivity to change in IRC can be significantly reduced by
increasing the total curvature, and one would expect a greater tolerance
to operating condition variation with the increased curvature design.

Maintaining the other bearing geometry variables at the same value, the
penalty paid for the increased curvature is loss of predicted fatigue
life. As seen from Figure A-9, increasing the inner-race curvature ratio
from 0.52 to 0.56 while maintaining the outer-race curvature ratio at
0.52 reduces the predicted fatigue life from 52 hours to 20 hours, respec-
tively, at 250 lb applied thrust load. With the ball centrifugal loading
at 65,000 rpm, the outer raceway-ball contacts are limiting in calculated
fatigue life so that to maximize fatigue life at an increased value of
total curvature, it is necessary to maintain or decrease the outer raceway-
ball curvature ratio while increasing the inner raceway-ball curvature
ratio. Furthermore, it should also be noted that the calculated fatigue
lives quoted assume no life multiple for the use of premium-quality M-50
material and are calculated at a reference contact angle of 25°. The
values specified are primarily for comparison purposes. Part of the
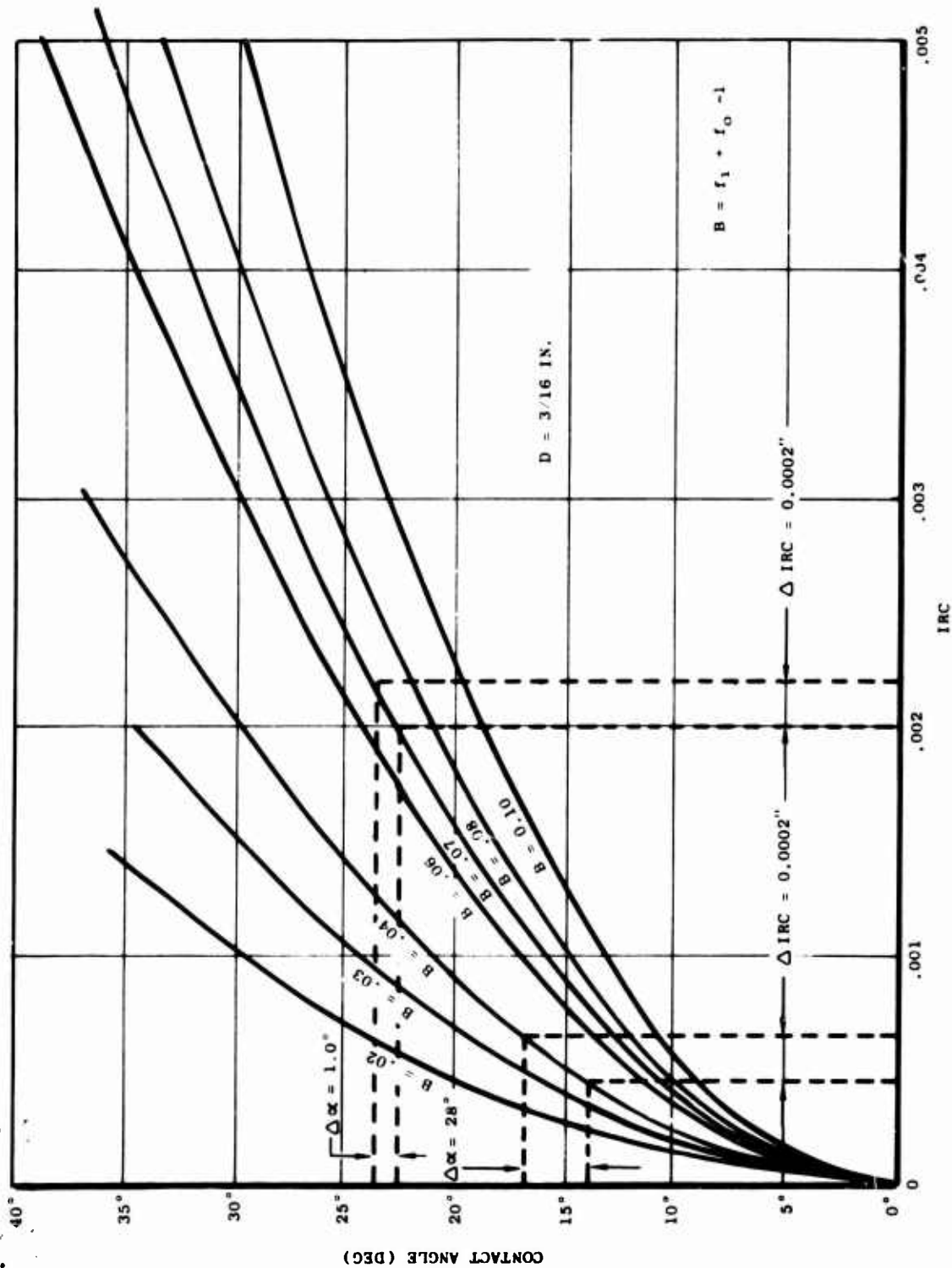
Figure A-7. Propulsion Simulator Ball Bearing

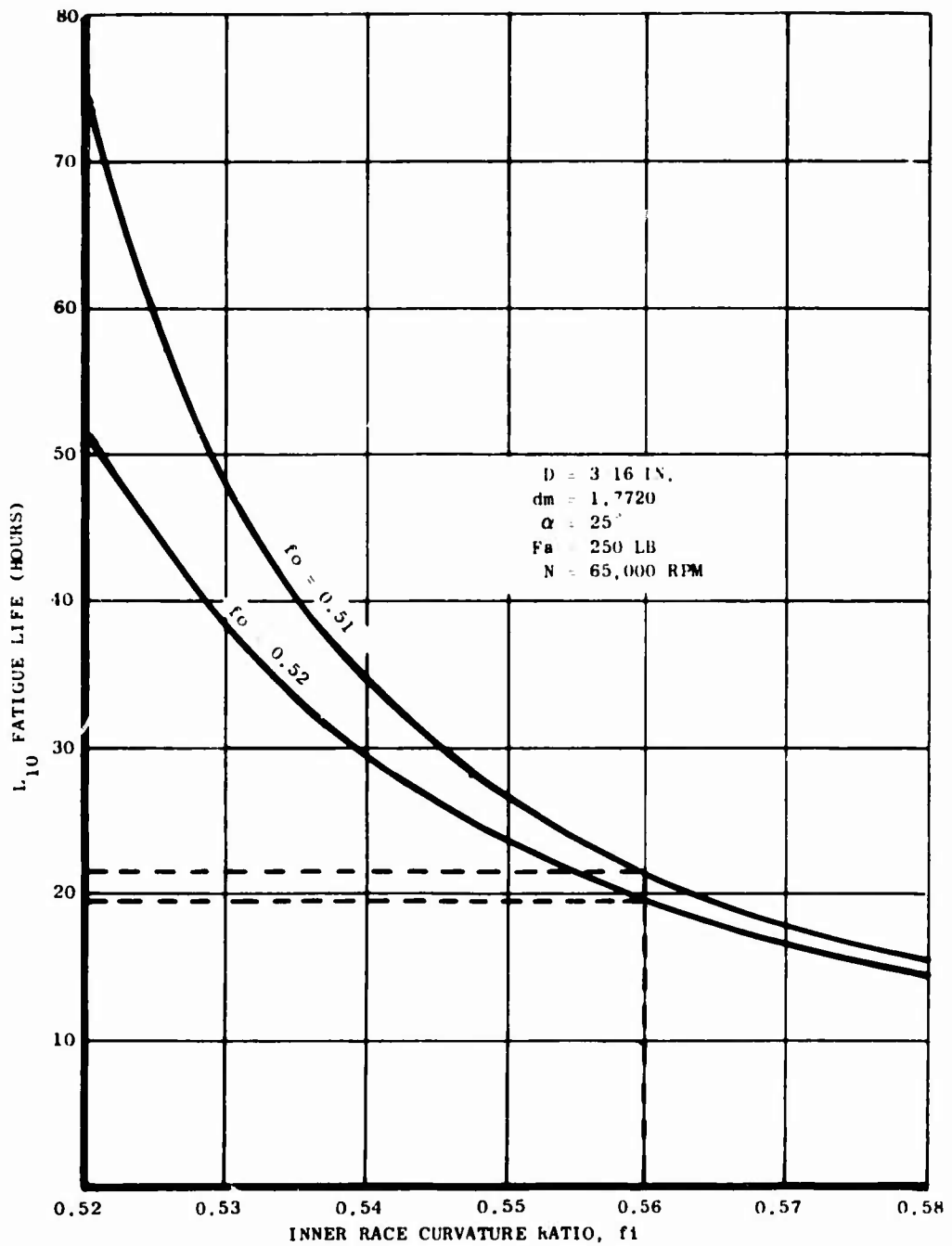Figure A-8. U. S. Army 35MM Bearing Contact Angle vs IRC

Figure A-9. U. S. Army 35MM Bearing Fatigue Life vs
Inner Race Curvature Ratio

fatigue life loss can be reclaimed by reducing the outer raceway-ball curvature to 0.51 as seen in Figure A-9.

Ball Diameter

Another significant bearing geometry variable is the ball diameter. One school of thought is that the bearing ball diameter should be made as small as practicable in order to minimize the ball centrifugal loading on the outer race and thus increase the bearing fatigue life. As seen from Figure A-10, this will be true only at low values of applied thrust load. At greater thrust loads the larger operating contact angles achieved with the increased loading produce an inverse effect in that a greater predicted fatigue life can be achieved with an increase in ball diameter. As noted in Figure A-10, an increase in ball diameter from 3 16 inch to 5/16 inch more than doubles the calculated fatigue life at 250 pounds applied thrust load. Figure A-11 shows the effect of ball diameter versus load for outer and inner raceway ball curvature ratios of 0.51 and 0.56 respectively. Comparison of this figure with Figure A-9 indicates that for larger values of thrust load, the fatigue life lost through increased total curvature can be regained by an increase in ball diameter. Furthermore, Figure A-12 shows that the contact angle sensitivity due to small changes in IRC is also decreased with increased ball diameter. With a 5 16 inch diameter ball (15-5/16 inch diameter balls versus 18-3 16 inch diameter balls), the average contact angle at $B = 0.04$ and including the effects of interference fit and centrifugal and thermal growth is 23.2°, and the IRC at this contact angle is 0.002025 inches. Reduction of the IRC by 0.0002 inches results in a contact angle of 21.9°, which is a significant improvement from the 14.0° noted at $B = 0.04$ for the 3 16 inch ball diameter. In addition, increasing the total curvature from 0.04 to 0.07 increases the effective mounted contact angle for the 5 16 inch diameter ball to 26.3°. A reduction of the IRC by 0.0002 inch results in a contact angle of 25.5° and represents a further reduction in sensitivity of contact angle with changes in internal radial clearance

Load

The effects of applied thrust load on the optimization of a given bearing design have already been alluded to in the previous paragraphs, where it was mentioned that for thrust loads greater than approximately 100 lb, fatigue life advantage can be gained by increasing the ball diameter. Although it is easy to quantify the effects of load on bearing design, determining the magnitude of the applied thrust loads in a given application can be difficult. Changing operating conditions causes fluctuations in thrust load and necessitates either a duty cycle life analysis or an analysis that uses a cubic mean thrust load. The accuracy of such load determinations is questionable and, for the loads of the magnitude considered for the 35mm application, can vary by as much as ± 50 lb, except for in precisely defined test rig applications. Bearing design optimization must therefore usually be attempted for a load range rather than a
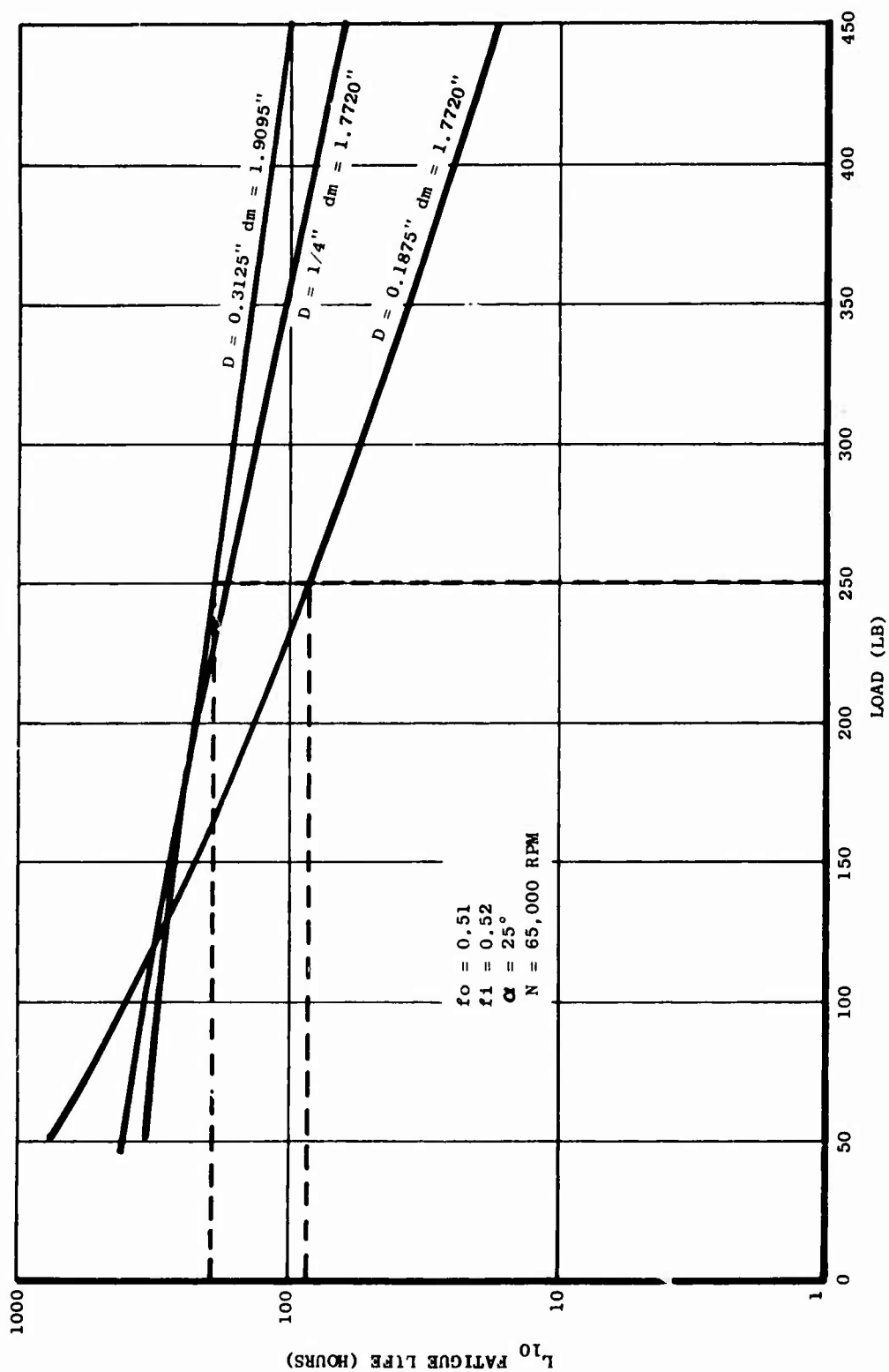
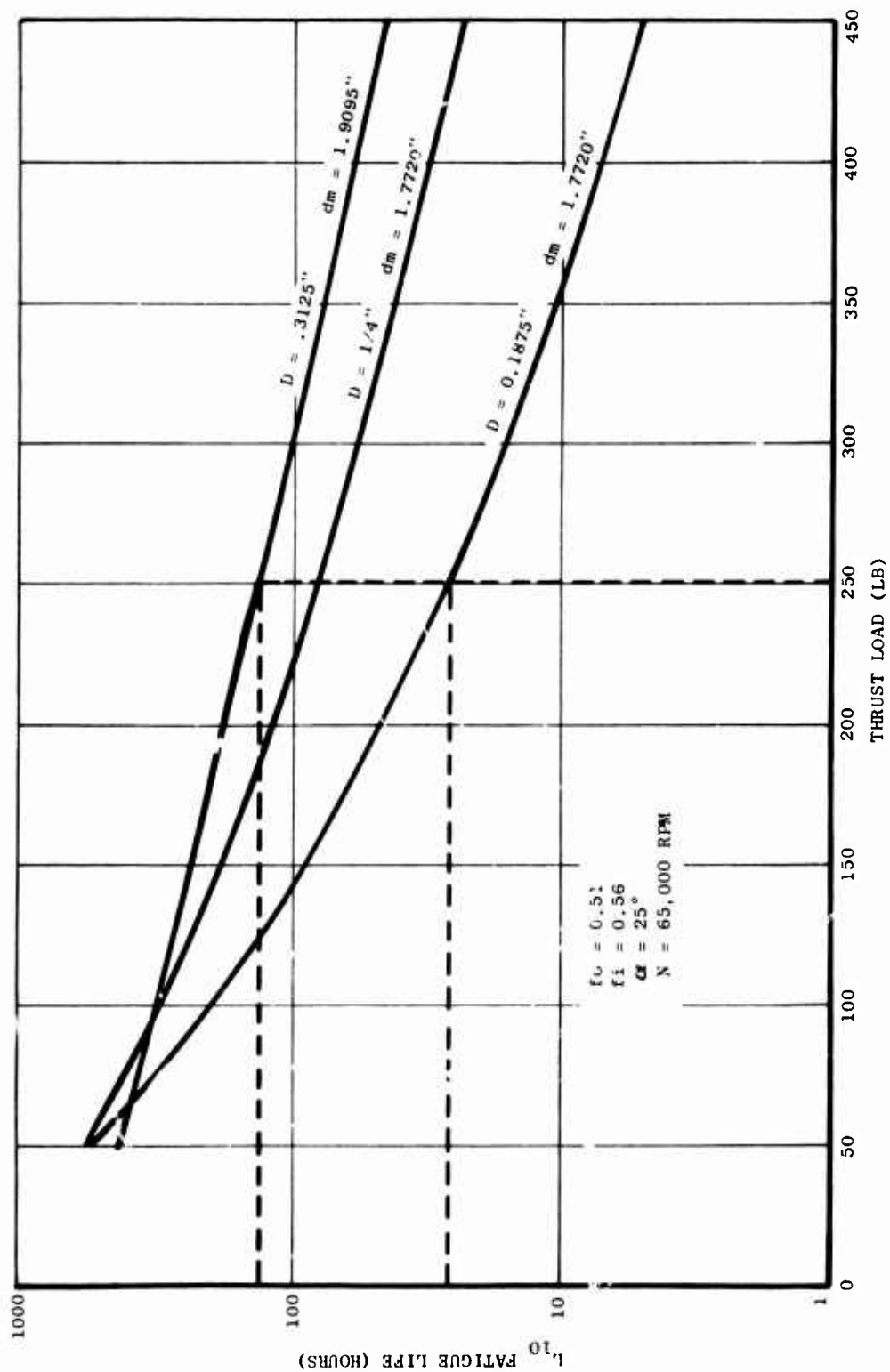Figure A-10. U. S. Army 35MM Bearing Fatigue Life vs Thrust Load

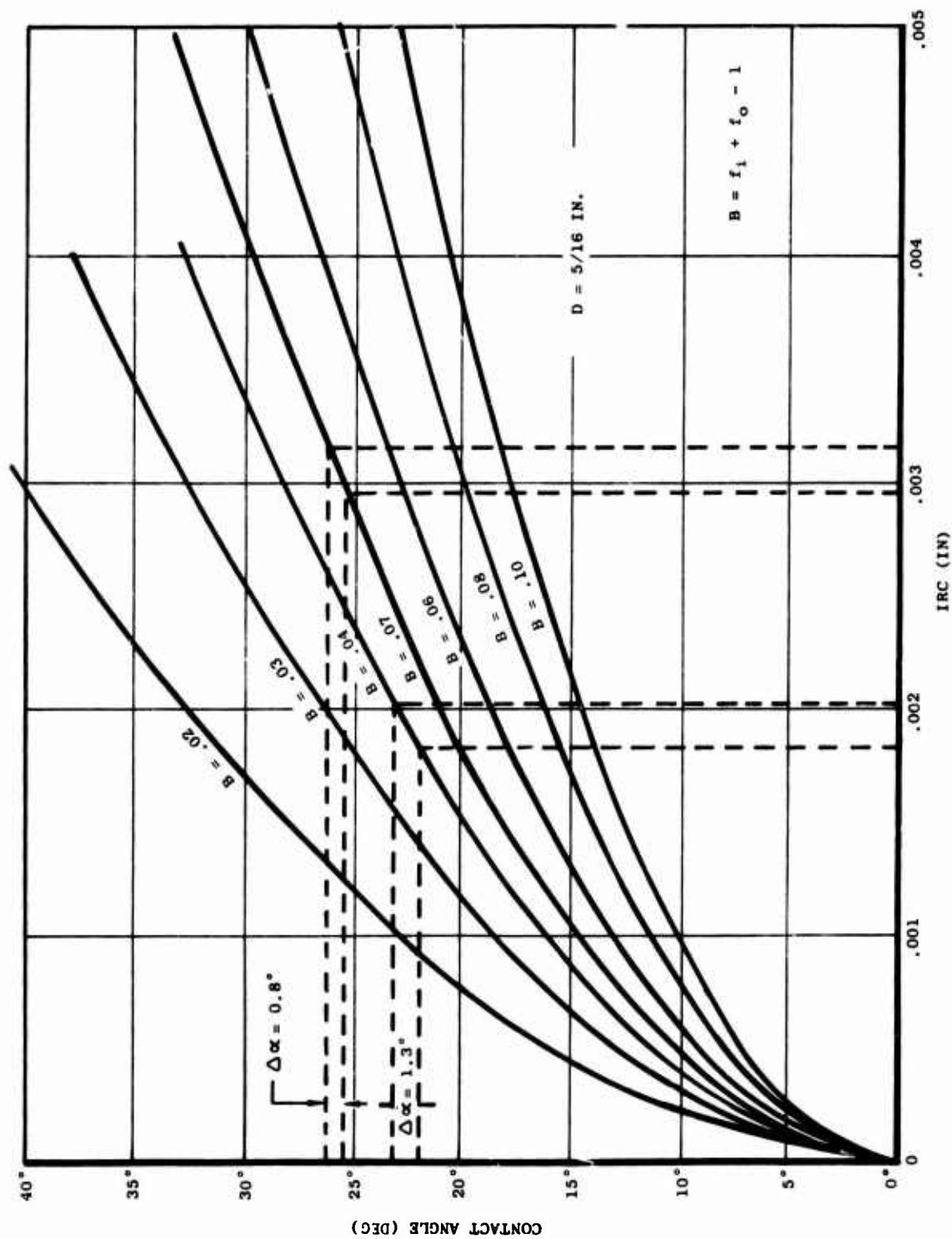Figure A-11. U. S. Army 35MM Bearing Fatigue Life vs Thrust Load

Figure A-12 U. S. Army 35MM Bearing Contact Angle vs IRC

specific load value, which places an additional degree of difficulty into the process.

The results of the parametric investigation of the 35mm ball bearing design indicate the following recommendations:

- Increase the total curvature from 0.04 to 0.07 by decreasing the outer race curvature ratio from 0.52 to 0.51 and by increasing the inner race curvature ratio from 0.52 to 0.56.

- Increase the ball diameter from 3/16 inch to 5/16 inch.

- Maintain the free contact angle in its present range of from 28° to 32°.

Decreasing the total curvature increases the effective mounted contact angle and decreases the contact angle sensitivity to changes in internal clearance. The loss in fatigue life due to the increased total curvature can be compensated for by increasing the ball diameter to 5/16 inch as long as the applied thrust load exceeds approximately 100 lb. The increase in ball diameter also further reduces the contact angle sensitivity to change in IRC. The existing free contact angle range should be satisfactory. Taken in conjunction with the increased total curvature and ball diameter, the average effective mounted contact angle is increased from 16.8° to 26.3°. Should machine clearance control requirements dictate, small changes in the contact angle range could be accommodated to lower the operating IRC and end play without significantly affecting the bearing operating performance.

APPENDIX B

ELASTOHYDRODYNAMIC LUBRICATION EFFECTS

Fundamental to the performance of the 35mm bore diameter ball bearing is an investigation of the elastohydrodynamic (EHD) lubrication effects on the bearing operating performance. The full EHD problem is to calculate the pressure and temperature distribution in the Hertzian contact, allowing at the same time for the effects of this pressure and temperature on the fluid and on the geometry of the solids. The solution must also provide the shape of the lubricant film, in particular the minimum clearance between the solids. This requires the simultaneous solution of the hydrodynamic, elasticity and energy equations with pressure and temperature dependent fluid properties and temperature dependent material properties. This is a lengthy and tedious process which requires numerical analysis utilizing a digital computer.

The primary concern of the design, however, is the minimum film thickness. With some simplifying assumptions, a reasonable estimate can be achieved for design purposes. Dowson and Higginson[20] succeeded in obtaining numerical solutions to the hydrodynamic and elasticity equations for wide ranges of three dimensionless parameters, W, U and G which are the load, speed and material parameters respectively. They assumed that the lubricant is incompressible, that the elastic displacements are those of a semi-infinite solid in a condition of plane strain, and that side leakage and thermal effects can be neglected. The neglecting of thermal effects was based on the analytical and experimental evidence which indicated that the film thickness is not appreciably influenced by the oil film temperatures generated in rolling/sliding contacts. They concluded that the isothermal film thickness formula gives good approximations to the measured film thickness if the lubricant viscosity corresponding to the temperature at the inlet to the contact is considered.

Following the work of Dowson and Higginson, which is primarily applicable to line contacts (roller bearings), Archard and Cowking[21] extended the empirical approach to ball bearings. They found that the best representation of minimum film thickness in a point contact over a wide range of operating parameters is given by

$$H = \frac{h_{min}}{R_x} = \frac{2.04\emptyset^{0.74} (GU)^{0.74}}{(W')^{0.074}}$$

where h_{min} = minimum film thickness
$\emptyset$ = ellipticity parameter

$$\emptyset = \frac{1}{(1 + \frac{2}{3} \frac{Rx}{Ry})}$$

Rx = equivalent radius of curvature in direction of rolling

Ry = equivalent radius of curvature normal to the direction of rolling

Inner-Race Contact

$$Rx_i = \frac{D}{2dm} (dm - D \cos\alpha) = \frac{D}{2} (1 - \gamma)$$

$$Ry_i = \frac{f_i D}{2f_i - 1}$$

D   = ball diameter
dm   = pitch diameter
α = mounted contact angle
γ = $D\cos\alpha/d_m$
f_i = inner raceway-ball curvature ratio

Outer-Race Contact

$$Rx_o = \frac{D}{2dm} (dm + D\cos\alpha) = \frac{D}{2} (1 + \gamma)$$

$$Ry_o = \frac{f_o D}{2 f_o - 1}$$

f_o = outer raceway-ball curvature ratio

Materials Parameter

$$G = \alpha E'$$

α = pressure viscosity coefficient

$$\mu = \mu_o e^{\alpha P}$$

μ = absolute viscosity

P = gauge pressure

$$E' = \frac{1}{\frac{1}{2} (\frac{1 - \delta 1^2}{E_1} + \frac{1 - \delta 2^2}{E_2})}$$

112

E' = equivalent modulus

δ = Poisson ratio

E = modulus of elasticity

Subscripts 1 and 2 refer to the contacting solids.

Speed Parameter

$$U = \frac{\mu_o \, u}{E' \, Rx}$$

μ_o = atmospheric pressure viscosity

u = equivalent velocity

$$u = \frac{1}{2} (u_1 + u_2)$$

$$u_i = \frac{dm}{4} \quad (1 - \gamma)(\omega_i - \omega_m) + \frac{\gamma}{\cos \alpha} \, \omega r$$

$$u_o = \frac{dm}{4} \quad (1 + \gamma) \, \omega_m + \frac{\gamma}{\cos \alpha} \, \omega r$$

i refers to inner-race contact
o refers to outer-race contact
ω_i = rotational speed of inner race, rad/sec
ω_r = roller speed about its own axis relative to the
inner race, rad/sec
ω_m = cage rotational speed, rad/sec
α = mounted contact angle, °

Load Parameters

$$W' = \frac{W}{E \, Rx^2}$$

W = load in point contact

This film thickness relationship is the one employed in the Bearing Design Technology computer program RECAP3 discussed in Appendix A and used for the performance analyses conducted on the 35mm bearing.

The work of several authors[22],[23],[24] has established the dependence of the fatigue life of rolling element bearings on the elastohydrodynamic film thickness in a Hertzian contact.

Generally, a lubricant life factor can be defined as a function of λ, which is the ratio of the minimum film thickness to the composite surface roughness:

$$\lambda = \frac{h_{min}}{\sigma}$$

$$\sigma = (\sigma_1^2 + \sigma_2^2)^{1/2}$$

where σ_1 and σ_2 are the surface roughnesses for the contacting solids.

Figure B-1 shows the life factor curve as a function of λ ratio. This curve has been generated as the result of a condensation of the data presented in References 22, 23 and 24 and a synthesis of engine bearing test data.

Three lubrication regions are defined in Figure B-1. At $\lambda \geq 1.8$, the full film region is defined in which the contact loads are entirely supported by the elastohydrodynamic lubricant film. In the mixed film region, $0.9 \leq \lambda < 1.8$, a life derating occurs due to asperity contacts that enhance the probability of surface-initiated fatigue. As λ approaches 0.9, the asperity contacts occur with increasing frequency as more of the contact normal load is supported by the asperity contacts. Finally, at $\lambda < 0.9$, the bearing is operating at full life deration in the boundary lubrication region where predominant metal-to-metal contact occurs and the lubricating function is provided essentially by the boundary additives in the lubricant.

The primary variables affecting λ and, thus, the lubricant life factor are temperature, speed, and surface finish. These effects are shown in Figures B-2, B-3, and B-4 for a representative main shaft ball bearing using MIL-L-23699 lubricant. Figure B-2 indicates the dependence of the lube life factor (L_f) on temperature for a fixed speed and surface finish, while Figure B-3 shows the effect of increasing speed at constant temperature and surface finish, and Figure B-4 depicts the surface finish effect at constant temperature and speed. The curve represented in Figure B-1 has been represented numerically and is used in the RECAP3 computer program to estimate the effect of lubricant film thickness on fatigue life.

The 35mm bearings tested in the U.S. Army ausformed bearing test program were intended to operate in the full film region with no life degradation due to EHD lubricant effects being contemplated. Oil supply temperature was maintained at approximately 170°F, and in combination with the operating speed and surface finishes, λ (h/σ) ratios well into the full film region were consistently calculated by the RECAP3 computer program. Many of the failures early in the test program, however, were determined to be due to surface initiated fatigue such as would be generated from the lack of a proper lubricating film.

This seeming inconsistency can best be explained by considering the operating clearances, contact angles, cage design, and cooling configuration. The low contact angle and the inherent low clearances result in bearing operation
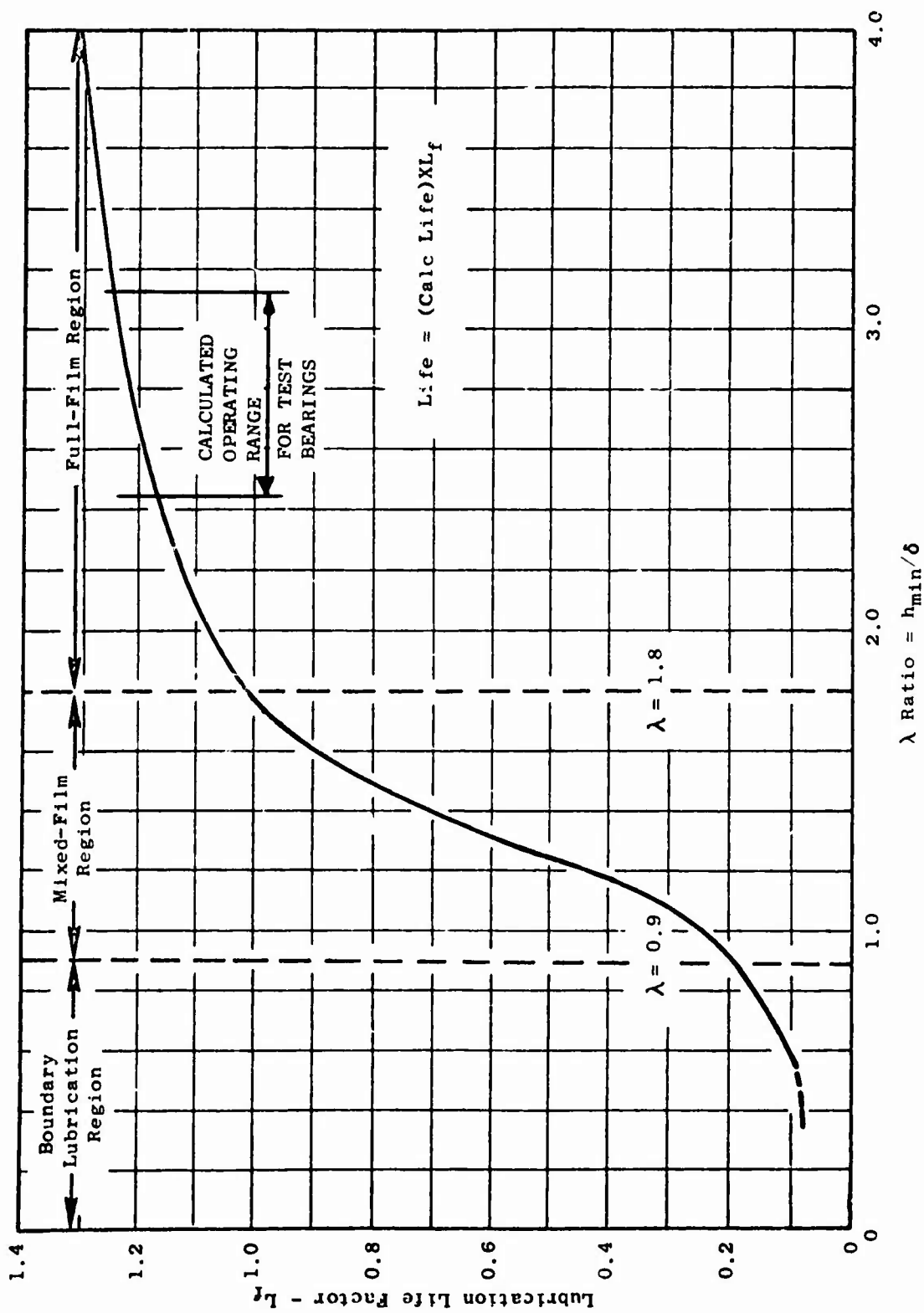
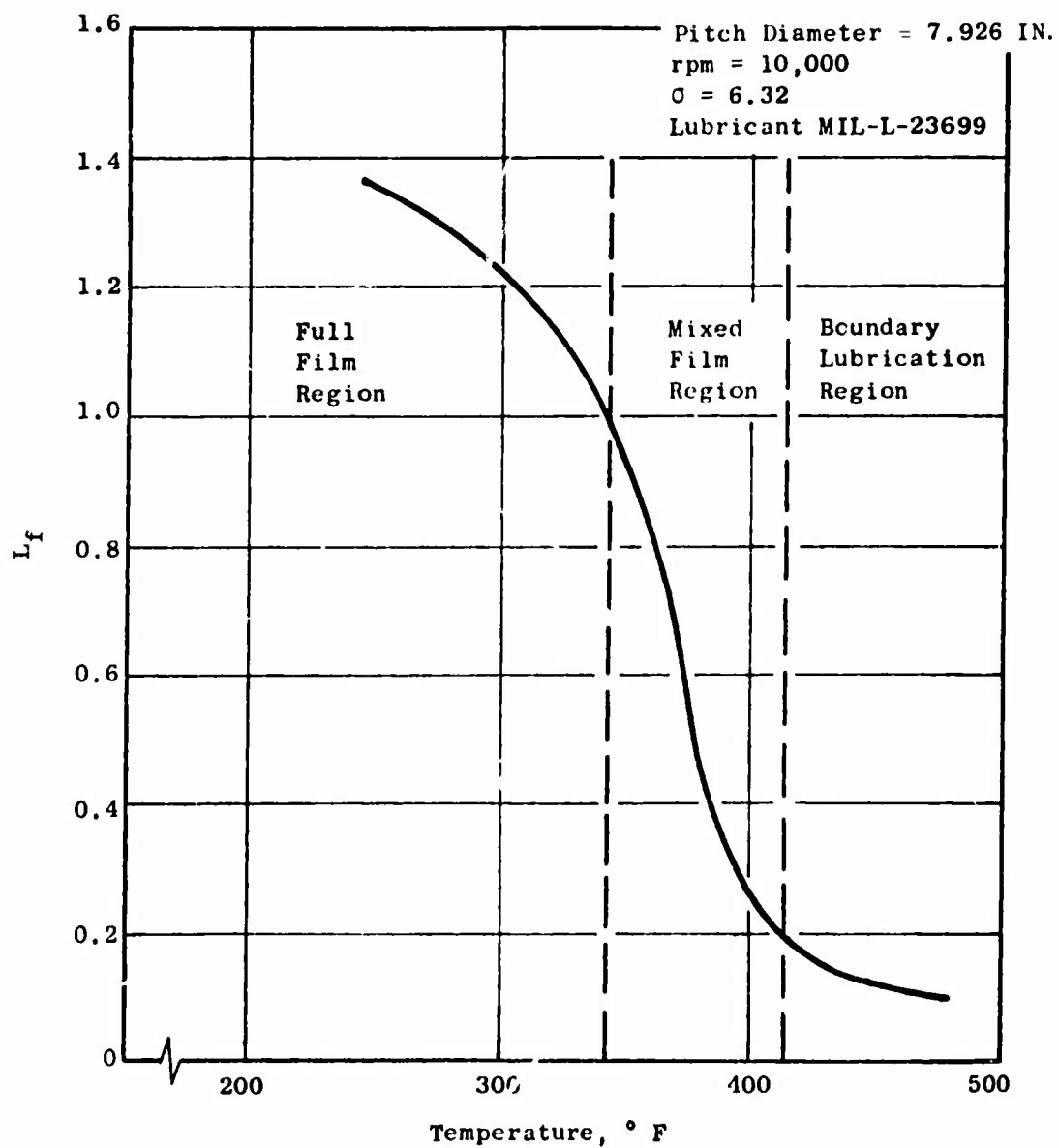Figure B-1. Lubrication Life Factor Versus λ Ratio

Figure B-2.   Lubrication Life Factor Versus Contact Temperature
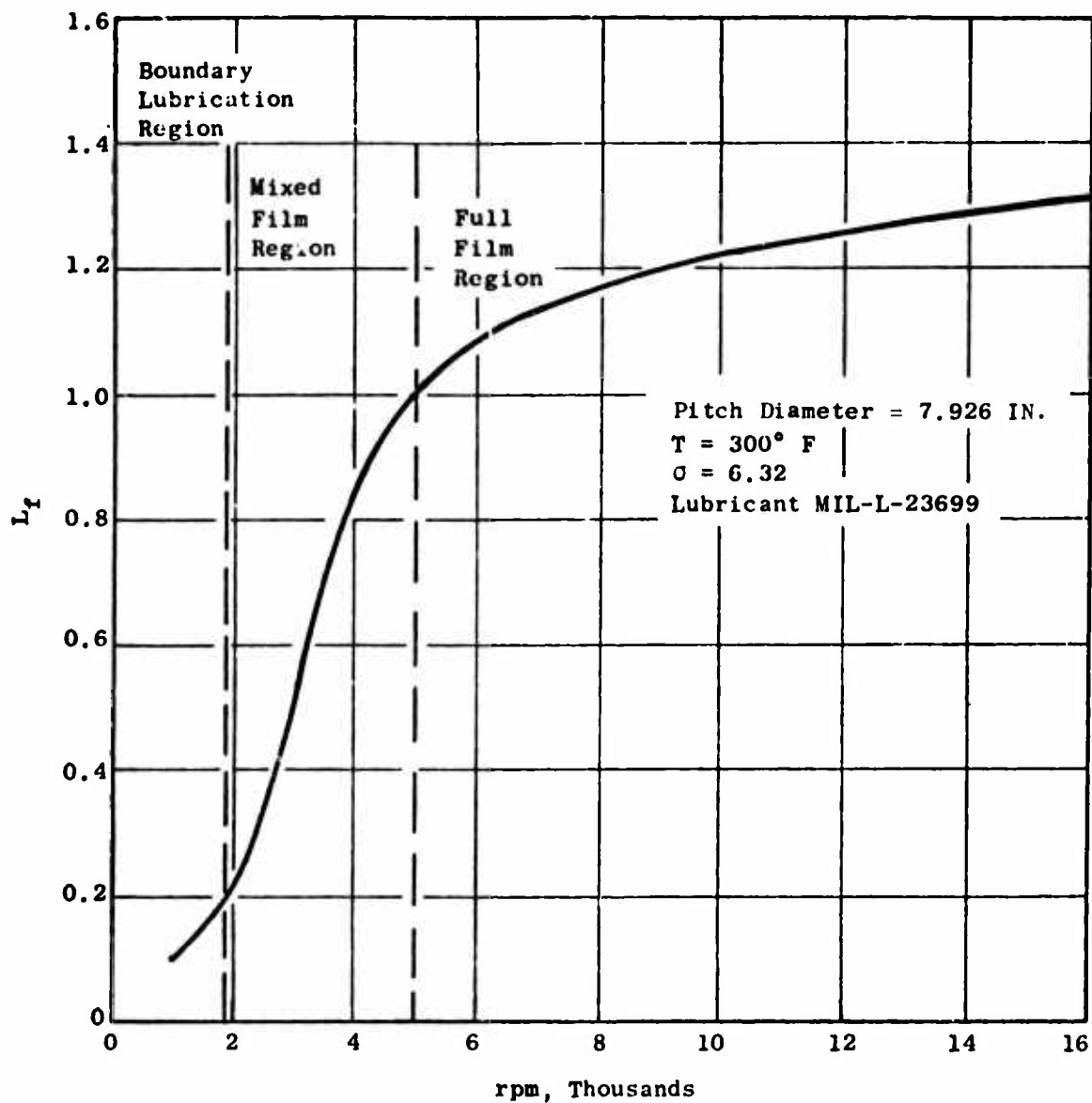for a Main-Shaft Ball Bearing

116

Figure B-3. Lubrication Life Factor Versus Shaft rpm
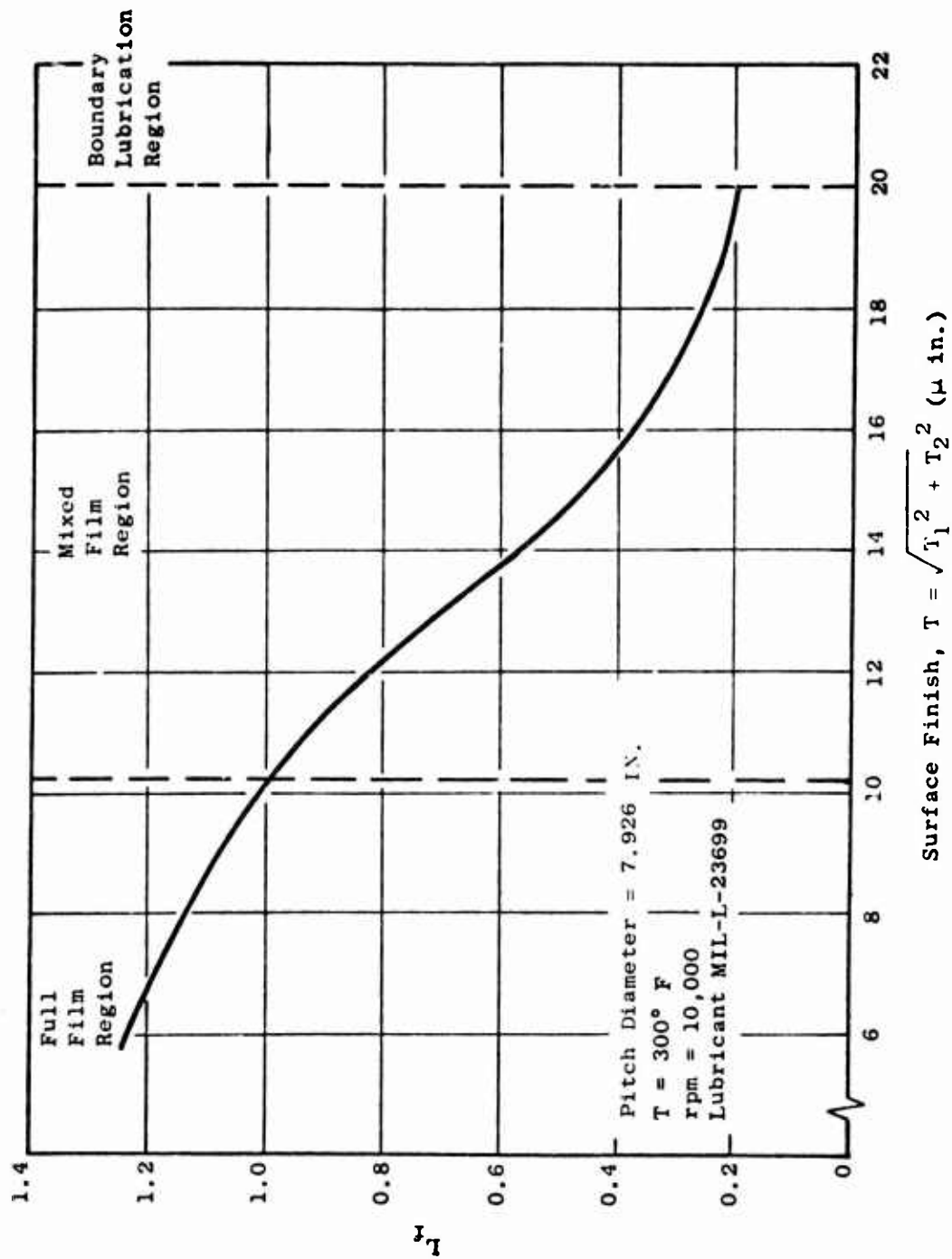for a Main-Shaft Ball Bearing

117

Figure B-4. Lubrication Life Factor Versus Surface Finish Parameter for a Main-Shaft Ball Bearing

that is quite unstable unless extreme care is taken to cool the bearing and not allow temperature variations. As discussed in the previous section, a small change in clearance results in a significant change in operating contact angles. The test bearings with jet lubrication experienced ball speed variations when none were expected. It is concluded that the ball speed was unstable under the cooling conditions being used. Therefore, the balls and cage operate with continuous interference. This cage interference was determined by the fact that the majority of these early failures exhibited heavy cage wear and/or damage. The cage-ball interference causes excessive sliding velocity components in the ball-raceway and ball-cage contacts which produce excessive local heat generation and lubricant film breakdown. The metal-to-metal contact that occurs produces micro-pitting in the balls and raceways that eventually leads to surface initiated fatigue. This type of phenomenon has been observed in engine main shaft bearings, where cage-ball interference and improper ball tracking occurred. Further evidence to substantiate this conclusion in the early control bearing failures stems from the fact that only after a cage redesign to be inner-land riding in connection with under-race cooling did consistent subsurface initiated fatigue failures begin to occur. Implementation of the inner-land riding cages to the remaining control bearings and to the ausformed bearings allowed the remaining testing to be conducted in the full EHD film lubrication region with no further surface-initiated fatigue failures being experienced. The bearings are considered to have minimum margin for the test conditions, however.